

THE STRUCTURES OF HEXAHELICENE
AND OTHER MOLECULES.

A Thesis

submitted to the University of Glasgow
for the degree of Master of Science
in the Faculty of Science,

by

Ian Renton Mackay, B.Sc.

Chemistry Department

December, 1970.

ProQuest Number: 11011949

All rights reserved

INFORMATION TO ALL USERS

The quality of this reproduction is dependent upon the quality of the copy submitted.

In the unlikely event that the author did not send a complete manuscript and there are missing pages, these will be noted. Also, if material had to be removed, a note will indicate the deletion.



ProQuest 11011949

Published by ProQuest LLC (2018). Copyright of the Dissertation is held by the Author.

All rights reserved.

This work is protected against unauthorized copying under Title 17, United States Code
Microform Edition © ProQuest LLC.

ProQuest LLC.
789 East Eisenhower Parkway
P.O. Box 1346
Ann Arbor, MI 48106 – 1346

ACKNOWLEDGEMENTS.

It is with great pleasure that I wish to thank my supervisor, Professor J.M.Robertson, for his guidance and interest throughout the course of the work described in this thesis.

I would also especially like to thank Dr. D.M.Hawley for his unfailing help and critical reading of parts of this manuscript. I wish to express my gratitude for the assistance of Dr. A.F.Cameron in preparing the report on pancuronium bromide, of Professor G.Ferguson who was my co-supervisor during my first few months of study, and of Dr. H.H.Mills and Dr. J.G.Sime in the theoretical and computing aspects of the work undertaken.

I am indebted to Dr. K.H.Overton, who supplied the crystals of the portentol derivative, for his collaboration throughout the course of the analysis, and to Professor M.S.Newman of the Ohio State University for the crystals of the hexahelicene complex.

My thanks are due to friends throughout the chemistry department for their assistance and in particular to Mr. A.L.MacDonald, Mr. R.S.Dunlop and Dr. M.Currie. I would also like to express my gratitude to Dr. R.Kadlec and Dr. A.Barrett of Boston University for their generous

hospitality during my stay with them and their co-operation in the development of the absorption correction routine.

I am obliged to Professor D.W.J.Cruickshank, Drs. K.W.Muir, A.McAdam, W.S.McDonald, D.R.McGregor, W.Oberhänsli, D.R.Pollard, J.G.Sime, and J.G.F.Smith for the use of their KDF9 computer programs.

I am sincerely grateful to the Carnegie Trust for the Universities of Scotland for their award of a scholarship during the period of my studies.

SUMMARY.

The first chapter of this thesis is concerned with an account of the structural analysis by X-ray diffraction methods of a molecular complex containing hexahelicene. The use of a complexing agent which contains a heavy atom has enabled the helical structure of this very interesting polycondensed aromatic hydrocarbon to be established and, although the atomic parameters which are presented are not fully refined, it is apparent that this conformation is achieved with very little distortion of the component benzene rings.

The second chapter deals with the structure of the amino-sterol pancuronium bromide, and the relationship between its molecular geometry and clinical properties is discussed. The structure determination of the novel polyketide lactone portentol is described in the third chapter. This molecule exhibits a fairly high degree of molecular overcrowding and this is shown to result in a considerable distortion of the molecular framework.

Finally, some theoretical and practical aspects of the correction of diffraction data for the effects of absorption of X-radiation by crystalline material are discussed and a description is given of a suite of data-reduction computer programs containing such a correction.

CONTENTS.

	page
ACKNOWLEDGEMENTS.	i
SUMMARY.	iii

CHAPTER 1.THE CRYSTAL AND MOLECULAR STRUCTURE OF A HEXAHELICENE
COMPLEX.

1.1 Introduction.	1
1.2 Crystal Data.	6
1.3 Intensity Data.	7
1.4 Structure Determination and Refinement.	8
1.5 Discussion.	13

CHAPTER 2.THE CRYSTAL AND MOLECULAR STRUCTURE OF PANCURONIUM BROMIDE.

2.1 Introduction.	18
2.2 Crystal Data.	19
2.3 Intensity Data.	20
2.4 Structure Determination and Refinement.	21
2.5 Absolute Configuration.	23
2.6 Discussion.	25

CHAPTER 3.THE CRYSTAL STRUCTURE AND ABSOLUTE STEREOCHEMISTRY OF
A HEAVY-ATOM DERIVATIVE OF PORTENTOL.

	page
3.1 Introduction.	30
3.2 Crystal Data.	32
3.3 Intensity Data.	33
3.4 Structure Determination and Refinement.	34
3.5 Absolute Configuration.	37
3.6 Discussion.	39

CHAPTER 4.

THE EVALUATION OF ABSORPTION EFFECTS IN A DATA-REDUCTION PROGRAM.

4.1 Introduction.	46
4.2 The Absorption Correction.	47
4.3 The Gaussian Integration Method of Absorption Correction.	54
4.4 A Description of the Programs.	60

REFERENCES.	66
-------------	----

APPENDIX 1.

The Gaussian Quadrature Method of Numerical Integration.

APPENDIX 2.

KDF9 ALGOL Listing of the Data-reduction Programs A1 and A2.

CHAPTER 1THE CRYSTAL AND MOLECULAR STRUCTURE OF A
HEXAHELICENE COMPLEX.1.1 Introduction.

The benzologue hydrocarbons (I) to (VIII) form an extremely interesting series of polycondensed aromatic hydrocarbons due to the progressive interaction of the atoms of the terminal rings, which produces an increasing deviation from planarity. This has been shown in the results of the crystal structure determinations carried out on the lower homologues of the series (I, II, III) and it was also found that this non-planar configuration was achieved without effecting significant alterations in the bond lengths and angles. This latter finding was to be expected, as all of these molecules retain typical aromatic properties, and it indicated that the increasing molecular overcrowding would result in a helical structure for the higher benzologues, the helicene series (IV to VIII).

Hexahelicene (IV), first synthesised by Newman and Lednicer in 1956, is considered to be the first true member of this series, as its structure, which is unambiguously established by the method of preparation, corresponds to one complete turn of a helix. The resulting

molecular asymmetry was shown by the resolution of hexahelicene into its two optically-active components, which exhibit the very high specific rotation value ($[\alpha]_D^{24}$ chloroform) of 3640° (Newman, Lutz and Lednicer, 1955). Furthermore, these components are so optically stable, as a result of the intramolecular overcrowding, that even at their melting-point racemisation is not complete.

Because of the unique aspects of its structure, a great deal of interest was provoked by the synthesis of hexahelicene, and many studies have been published of its theoretical, optical, spectroscopical and chemical properties (see under previous reference). Unfortunately, the application of Newman's synthetic method is restricted to hexahelicene and it was not until 1967 that higher members of the series were reported. Professor R.H. Martin's group at the Université Libre in Brussels had been working for some time on the synthesis and n.m.r. investigation of polycyclic aromatic compounds, and in that year they reported an alternative chemical route to hexahelicene. This was rapidly followed by the description of a synthetic method, involving the photo-induced cyclisation of phenanthrene moieties, by the use of which they have since been able to produce heptahelicene (V), octahelicene (VI), nonahelicene (VII), tridecahelicene (VIII) - the first of the multi-layered helicenes, and 4-azahexahelicene (IX),

Table

The Helicene Series and Related Molecules.

- (a) I.U.P.A.C. nomenclature.
- (b) Nomenclature proposed by M.S. Newman, and used by R.H. Martin.
- (c) Principal references.

References.

Structure determination by X-ray diffraction.

1. Trotter (1963).
2. Herbststein and Schmidt (1954).
3. Hirschfeld, Sandler and Schmidt (1963).
4. McIntosh, Robertson and Vand (1952).
5. Mackay, Robertson and Sine (1969).
6. Stulen and Visser (1969).

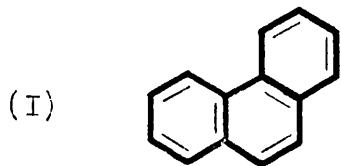
Synthesis and n.m.r. studies.

- 7.* Newman and Lednicer (1956).
8. Martin and Bogaert-Verhooghen (1967).
9. Martin, Flammang-Barbieux and Nasielski (1967).
10. Martin, Flammang-Barbieux, Cosyn and Gelbcke (1968).
11. Martin, Morren and Schurter (1969).
12. Martin and Deblecker (1969).
13. Wynberg and Groen (1968).

Review of n.m.r. studies of the helicenes.

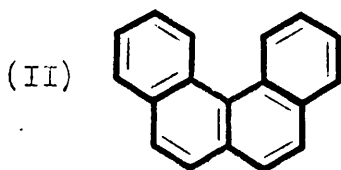
14. Martin, Defay, Figeys, Flammang-Barbieux, Cosyn, Gelbcke and Schurter (1969).

* The n.m.r. analysis reported in this paper has since proved erroneous in the light of the detailed investigations of Martin et al. (reference 14).



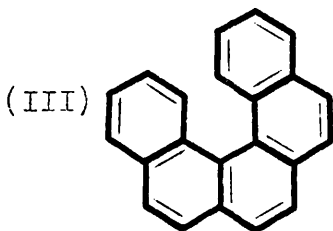
(a) phenanthrene

(c) 1



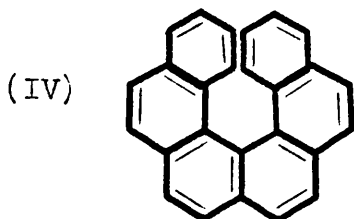
(a) benzo[c]phenanthrene

(c) 2, 3



(a) dibenzo[c,g]phenanthrene

(c) 4



(a) phenanthro[3.4-c]phenanthrene

(b) hexahelicene

(c) 5, 7, 8, 10

Representation of molecules V through VIII after R.H. Martin



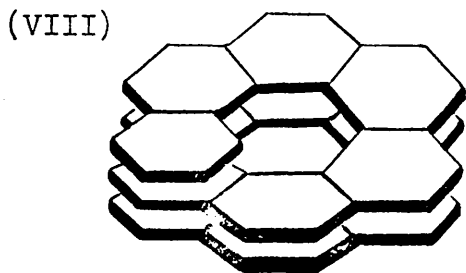
- (a) benzo[c]phenanthro[4.3-g]
phenanthrene
- (b) heptahelicene
- (c) 9, 1C



- (a) naphtho[2.1-c]phenanthro[4.3-g]
phenanthrene
- (b) octahelicene
- (c) 1C

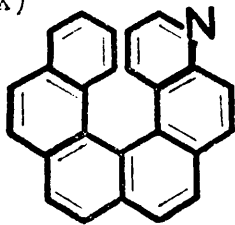


- (a) bisphenanthro[3.4-c;4'.3'-g]
phenanthrene
- (b) nonahelicene
- (c) 1C



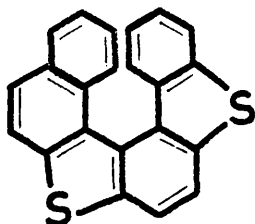
- (b) tridecahelicene
- (c) 11

(IX)



- (a) benzo[c]phenanthro[1.2-f]quinoline
- (b) 4-azahexahelicene
- (c) 12

(X)



- (a) benzo[d]naphtho[1.2-d'],
benzo[1.2-b;4.3-b]dithiophen
- (c) 6, 13

all in very high yields.

With this tremendous advance in the synthesis of such an unusual and extremely interesting range of compounds the precise knowledge of the corresponding molecular dimensions, which could be obtained by X-ray diffraction analyses, would obviously be of great value in the further study of the series. Investigations of the crystals of hexahelicene and heptahelicene have, in fact, been carried out but no structural results have, as yet, been reported. These both crystallise in non-centrosymmetric space groups, hexahelicene in $P2_12_12_1$ (Hahn, 1958) and heptahelicene in $P2_1$ (Martin, 1968) and thus do not lend themselves easily to the application of direct methods. However, it would certainly be expected that, given a good crystalline sample, the rapidly increasing sophistication of non-centrosymmetric direct-methods programs will facilitate the structural analyses of the helicene molecules.

A far simpler approach, at this time, is the use of the heavy-atom method and this has been successfully employed in the structure determination of the heterohelicene (X), which also crystallises in the space group $P2_1$. The application of this technique with respect to the helicenes (IV to VIII) would, however, require the use of a heavy-atom derivative such as the 7-bromohexahelicene reported by Martin and Schurter (1969). Unfortunately,

as the object of a structural study would be concerned with the distortions produced by the molecular overcrowding, the use of a heavy-atom derivative, which would probably introduce further distortions, is not particularly desirable in an accurate structure determination. In the light of this present report, an analysis of optically-active crystals of the latter molecule would still be very much worthwhile, as it would establish the important and eagerly awaited absolute configuration of hexahelicene. However, some difficulty has been encountered in the preparation of suitably crystalline samples of the helicenes and their derivatives (Martin, 1970).

An alternative approach in the application of the heavy-atom method, which has successfully overcome all of these obstacles, is the use of a π - π molecular complex, such as was employed in this analysis. Crystals of these complexes are formed from stacks of alternate donor and acceptor molecules, where an aromatic hydrocarbon is the donor and a benzoquinone or an aromatic nitro compound is the acceptor, and, since the component molecules are separated by almost van der Waals distances, one can assume that the structure of the donor to be studied will be completely undistorted. The bonding in such complexes has been frequently investigated (for a recent and very thorough review see Prout and Wright,

1968) and the classical interpretation of Mulliken (1952) and Nakamoto (1952) is of a charge-transfer process involving the overlap of π -orbitals. However, other important influences, notably dispersion forces, are also known to be involved and a theoretical understanding of the nature of the bonding is still incomplete.

Newman and Blum (1964) prepared 4-bromo-2,5,7-trinitro-fluorenone (BTNF) and this has been found to be an excellent complexing agent which, as a result of the beautiful crystallinity and high stability of the complexes which it forms, is ideally suited for the structure determination of polycyclic aromatics by the heavy-atom method. Complexes of BTNF with anthracene and with 1,12-dimethyl-3,4-benzophenanthrene have been studied (Pollard, 1968) and it was found that the structures obtained for the aromatic hydrocarbons were in excellent agreement with those previously determined for the uncomplexed molecules. A 1:1 complex of BTNF and hexahelicene was therefore prepared by Professor Newman and the subsequent X-ray analysis has revealed the structure of hexahelicene.

1.2 Crystal Data.

Hexahelicene : 4-Bromo-2,5,7-trinitrofluorenone.

$C_{26}H_{16}$: $C_{13}H_4N_3O_7Br$, $M = 722.5$,

Triclinic,

$a = 9.30 \pm 0.02 \text{ \AA}$, $\alpha = 114.9 \pm 0.3^\circ$,

$b = 20.63 \pm 0.03 \text{ \AA}$, $\beta = 93.7 \pm 0.3^\circ$,

$c = 18.90 \pm 0.03 \text{ \AA}$, $\gamma = 98.7 \pm 0.3^\circ$.

Volume of unit cell = 3219 \AA^3 .

$D_m = 1.52$ (by flotation).

$Z = 4$.

$D_c = 1.49$.

$F(CCC) = 1464$.

Linear absorption coefficient ($\lambda = 1.5418 \text{ \AA}$), $\mu = 24.1 \text{ cm}^{-1}$.

Space group $P\bar{1}$ (C_1^1 , No. 2).

The crystals consisted of small dark red prisms and the cell dimensions were determined from rotation and Weissenberg photographs, taken about the a and c axes with $Cu K_\alpha$ radiation, and from precession photographs of the $Ck1$, hCl and hkC nets taken with $Mo K_\alpha$ radiation.

The triclinic cell was indexed, by convention, on the Delaunay-reduced cell (Jeffreys, 1968) such that the direct cell vectors formed a right-handed set of axes in

an obtuse unit cell (i.e. all angles $\geq 90^\circ$). The molecular complex is optically active and, since it crystallises as the racemate, the space group $\bar{P}1$ was indicated and subsequently confirmed in the course of the analysis.

1.3 Intensity Data.

The intensity data were collected using a small crystal ($0.25 \times 0.15 \times 0.15$ mm.) mounted about the a axis and multiple-film equ-inclination Weissenberg photographs (Cu $K\alpha$ radiation) were taken of the $0kl$ to $8kl$ reciprocal lattice nets, using six films per pack (Robertson, 1943). In order to collect all of the unique data, four octants in a triclinic cell, two sets of photographs were required of each layer - the first to record the $hkl/\bar{1}$ quadrant, and the second the $h\bar{k}l/\bar{1}$. In order to enable batch scaling, using the h index as a batch number, the indices of the latter quadrant were converted to the symmetry-related $\bar{h}k\bar{l}/1$. The indexing of the upper-layer photographs was confirmed by comparison of the intensity pattern of the $hk0$ and $h0l$ reflexions with the corresponding reciprocal lattice nets recorded on precession photographs.

The intensities thus obtained were estimated visually by comparison with a calibrated step-wedge

based on a selected Ckl reflexion from the same crystal. Lorentz, polarisation and rotation factors (Tunell, 1939) were applied to give 6269 unique observed structure amplitudes, representing approximately 42% of the data accessible to Cu K_{α} radiation. These were placed on an approximately absolute scale by comparison with the first set of structure factors, using an individual scale factor for each of the seventeen batches, and the final scale factors were determined by least-squares methods. Corrections were not made for absorption or extinction effects and no unobserved reflexions were included in the analysis.

1.4 Structure Determination and Refinement.

The asymmetric unit contains two heavy atoms and, due to the presence of the centre of symmetry, these give rise to four heavy-atom vectors in the three-dimensional Patterson synthesis, having the coordinates,

$$(1) \quad 2x_1 \quad 2y_1 \quad 2z_1,$$

$$(2) \quad 2x_2 \quad 2y_2 \quad 2z_2,$$

$$(3) \quad (x_1 - x_2) \quad (y_1 - y_2) \quad (z_1 - z_2),$$

$$(4) \quad (x_1 + x_2) \quad (y_1 + y_2) \quad (z_1 + z_2).$$

Peaks (3) and (4) are of double weight and the search for these is made easier by the simple mathematical relationship of each of them to peaks (1) and (2). Hence

a consistent set of fractional coordinates for the two bromine atoms was found to be,

Br(1)	0.596	0.087	0.643,
Br(2)	0.578	0.048	0.238.

The first set of structure factors resulted in an R factor of 0.549 and the observed structure amplitudes, taken with the signs associated with the bromine atoms, were then used in a three-dimensional Fourier summation. The resulting electron-density distribution was remarkably clear, revealing the two BTNF and the two hexahelicene molecules in the asymmetric unit, and the positions of 64 of the 100 non-hydrogen atoms were unambiguously determined.

Four further cycles of structure-factor and Fourier calculations led to improved coordinates for all of the atoms and reduced R to 0.240 . Photographs of the electron-density distribution of the two hexahelicene molecules, drawn on a glass stack, are shown in Figures 1.2 and 1.3 .

The least-squares refinement, involving the parameters of the 100 atoms in the asymmetric unit and 6269 data items, posed a very considerable problem in terms of computing power. In order to make the calculations feasible on our KDF9 computer, a subset of

the diffraction data, composed of 2176 randomly selected values, was used to carry out the isotropic refinement. Furthermore, the hexahelicene and BTNF parameters had to be refined alternately in successive cycles, so as to reduce the number of parameters involved in each cycle. By these means a limited refinement of the positional, isotropic vibrational, and scale parameters was enabled. The block-diagonal approximation was used and an overall scale factor was adopted at the beginning of the refinement.

A weighting scheme of the form

$$\sqrt{w} = \left[\frac{[1 - \exp(-p_1 (\sin \vartheta / \lambda)^2)]}{[1 + p_2 |F_o|]} \right]^{\frac{1}{2}},$$

was applied throughout. Initial values of p_1 and p_2 were set at 500 and zero respectively, and these were subsequently modified to obtain constant averages of $w\Delta^2$, for reflexions batched according to $|F_o|$ and $\sin \vartheta / \lambda$. The final values of p_1 and p_2 were 50 and 0.01 respectively.

Seven cycles of isotropic least-squares calculations were required to reach the point of convergence for this data set, and values of

$$R = 0.182 ,$$

$$R' = 0.411 ,$$

$$w\Delta^2 = 63,083 ,$$

were obtained at this point (these terms are defined in

Table 2.1). The fractional coordinates and thermal parameters obtained at this stage are given in Table 1.2, and these were used, with the full data set, in a structure factor calculation to produce the calculated structure factors for all of the data. These are listed in Table 1.1 along with the observed structure amplitudes. The theoretical scattering factors used in all the structure-factor calculations are those given in "International Tables for X-ray Crystallography", Vol.III.

Figure 1.1 shows the numbering scheme adopted for the atoms of the complex and for the hexahelicene rings. Table 1.3 lists the bond lengths, valence angles and relevant inter- and intramolecular non-bonded distances. Throughout the course of the analysis the positioning of the atoms of complex 2 proved considerably more difficult than with those of complex 1, and this is reflected in the larger values obtained for the estimated standard deviations of these atoms and in the resulting bond lengths and angles. Repeated attempts were made, using Fourier and difference Fourier techniques, to improve this situation but the changes effected were only marginal and complex 2 remains less well refined than complex 1. It is felt that a least-squares refinement, involving the full data set, would considerably improve this situation.

The best mean planes through the six benzene rings of both hexahelicene molecules were calculated and the results are given in Table 1.4 .

At this point further refinement of the parameters proved outwith the capabilities of our computer and attempts to transfer the analysis to more powerful computing facilities have, as yet, met with no success.

Table 1.1

Observed structure amplitudes and final calculated structure factors.

Table with multiple columns containing alphanumeric data, organized in a grid-like structure across two pages.

PAGE 7										PAGE 8																																								
L	F	FF	L	F	FC	M	L	F	FC	L	F	FC	M	L	F	FC	L	F	FC	L	F	FC	M	L	F	FC																								
1	2	4	6	8	10	12	14	16	18	20	22	24	26	28	30	32	34	36	38	40	42	44	46	48	50	52	54	56	58	60	62	64	66	68	70	72	74	76	78	80	82	84	86	88	90	92	94	96	98	100
1	2	4	6	8	10	12	14	16	18	20	22	24	26	28	30	32	34	36	38	40	42	44	46	48	50	52	54	56	58	60	62	64	66	68	70	72	74	76	78	80	82	84	86	88	90	92	94	96	98	100

Table 1.2Fractional coordinates and thermal parameters (\AA^2).(a) Complex 1.

	x/a	y/b	z/c	Uiso.
Br	0.590	0.087	0.641	0.076
O(1)	0.991	0.041	0.801	0.097
O(2)	0.903	0.038	0.279	0.084
O(3)	0.260	0.300	0.445	0.073
O(4)	0.735	0.491	0.489	0.084
O(5)	0.912	0.454	0.419	0.067
O(6)	0.843	0.190	0.248	0.082
O(7)	0.637	0.168	0.181	0.076
N(1)	0.024	0.015	0.249	0.065
N(2)	0.792	0.446	0.440	0.065
N(3)	0.729	0.195	0.239	0.038
C(1)	0.734	0.362	0.594	0.033
C(2)	0.867	0.401	0.581	0.037
C(3)	0.966	0.363	0.539	0.040
C(4)	0.925	0.286	0.495	0.051
C(5)	0.797	0.249	0.503	0.033
C(6)	0.741	0.168	0.455	0.059
C(7)	0.613	0.136	0.451	0.046
C(8)	0.519	0.172	0.498	0.050
C(9)	0.367	0.135	0.494	0.070
C(10)	0.270	0.174	0.534	0.044

	x/a	y/b	z/c	Uiso
C(11)	0.313	0.248	0.598	0.054
C(12)	0.209	0.282	0.640	0.060
C(13)	0.261	0.347	0.695	0.057
C(14)	0.413	0.373	0.732	0.035
C(15)	0.456	0.440	0.805	0.042
C(16)	0.595	0.465	0.841	0.053
C(17)	0.699	0.423	0.811	0.040
C(18)	0.841	0.441	0.849	0.046
C(19)	0.946	0.392	0.828	0.057
C(20)	0.891	0.329	0.766	0.042
C(21)	0.759	0.307	0.721	0.041
C(22)	0.659	0.354	0.739	0.029
C(23)	0.510	0.336	0.699	0.031
C(24)	0.470	0.275	0.619	0.037
C(25)	0.560	0.245	0.560	0.040
C(26)	0.698	0.285	0.553	0.036
C(27)	0.403	0.086	0.254	0.057
C(28)	0.285	0.043	0.244	0.065
C(29)	0.154	0.069	0.272	0.023
C(30)	0.164	0.141	0.325	0.059
C(31)	0.296	0.185	0.338	0.052
C(32)	0.335	0.267	0.397	0.054
C(33)	0.479	0.287	0.392	0.048
C(34)	0.564	0.358	0.428	0.045
C(35)	0.704	0.369	0.404	0.058

	x/a	y/b	z/c	Uiso
C(36)	0.764	0.320	0.350	0.042
C(37)	0.666	0.246	0.306	0.041
C(38)	0.530	0.220	0.330	0.036
C(39)	0.419	0.163	0.302	0.044

(b) Complex 2.

Br	0.577	0.049	0.234	0.063
O(1)	0.960	0.035	0.445	0.100
O(2)	0.894	0.033	0.611	0.119
O(3)	0.189	0.297	0.840	0.062
O(4)	0.858	0.422	0.027	0.080
O(5)	0.669	0.470	0.028	0.092
O(6)	0.857	0.181	0.823	0.103
O(7)	0.658	0.114	0.810	0.085
N(1)	0.016	0.018	0.599	0.089
N(2)	0.730	0.424	0.008	0.069
N(3)	0.757	0.164	0.808	0.015
C(1)	0.374	0.280	0.196	0.043
C(2)	0.248	0.258	0.220	0.082
C(3)	0.171	0.309	0.270	0.084
C(4)	0.241	0.376	0.312	0.084
C(5)	0.378	0.401	0.296	0.083
C(6)	0.470	0.479	0.342	0.114
C(7)	0.589	0.489	0.329	0.119
C(8)	0.678	0.455	0.278	0.132

	x/a	y/b	z/c	Uiso
C(9)	0.815	0.470	0.264	0.117
C(10)	0.886	0.425	0.229	0.073
C(11)	0.843	0.349	0.166	0.131
C(12)	0.877	0.287	0.110	0.112
C(13)	0.827	0.238	0.065	0.090
C(14)	0.666	0.215	0.035	0.101
C(15)	0.588	0.149	0.976	0.107
C(16)	0.467	0.139	0.944	0.108
C(17)	0.356	0.195	0.978	0.077
C(18)	0.207	0.197	0.948	0.080
C(19)	0.152	0.249	0.975	0.075
C(20)	0.232	0.326	0.033	0.084
C(21)	0.366	0.321	0.062	0.056
C(22)	0.444	0.264	0.043	0.060
C(23)	0.581	0.268	0.075	0.063
C(24)	0.655	0.329	0.145	0.056
C(25)	0.595	0.377	0.215	0.061
C(26)	0.452	0.353	0.234	0.052
C(27)	0.412	0.104	0.672	0.042
C(28)	0.284	0.060	0.625	0.064
C(29)	0.165	0.072	0.653	0.051
C(30)	0.134	0.142	0.711	0.053
C(31)	0.267	0.185	0.755	0.052
C(32)	0.285	0.262	0.822	0.049

	x/a	y/b	z/c	Uiso
C(33)	0.438	0.281	0.853	0.042
C(34)	0.504	0.350	0.918	0.049
C(35)	0.655	0.351	0.942	0.044
C(36)	0.722	0.298	0.908	0.043
C(37)	0.655	0.232	0.840	0.042
C(38)	0.507	0.227	0.814	0.038
C(39)	0.401	0.170	0.745	0.045

Average estimated standard deviations

Complex 1

hexahelicene	C	± 0.004	± 0.002	± 0.002	± 0.008
BTNF	C	± 0.005	± 0.002	± 0.003	± 0.013
BTNF	N	± 0.004	± 0.002	± 0.002	± 0.010
BTNF	O	± 0.003	± 0.002	± 0.002	± 0.008
BTNF	Br	± 0.0006	± 0.0003	± 0.0003	± 0.001

Complex 2

hexahelicene	C	± 0.005	± 0.003	± 0.003	± 0.012
BTNF	C	± 0.005	± 0.002	± 0.003	± 0.013
BTNF	N	± 0.004	± 0.002	± 0.002	± 0.010
BTNF	O	± 0.003	± 0.002	± 0.002	± 0.008
BTNF	Br	± 0.0006	± 0.0003	± 0.0003	± 0.001

Table 1.3

(a) Bond lengths (Å).

<u>Hexahelicene</u>	Complex 1	Complex 2
C(1) - C(2)	1.47	1.37
C(2) - C(3)	1.38	1.42
C(3) - C(4)	1.42	1.30
C(4) - C(5)	1.37	1.40
C(5) - C(26)	1.41	1.48
C(5) - C(6)	1.50	1.55
C(6) - C(7)	1.25	1.16
C(7) - C(8)	1.36	1.34
C(8) - C(25)	1.44	1.59
C(8) - C(9)	1.49	1.34
C(9) - C(10)	1.35	1.20
C(10) - C(11)	1.46	1.49
C(11) - C(24)	1.44	1.71
C(11) - C(12)	1.38	1.37
C(12) - C(13)	1.29	1.03
C(13) - C(14)	1.45	1.50
C(14) - C(23)	1.30	1.42
C(14) - C(15)	1.46	1.40
C(15) - C(16)	1.34	1.19
C(16) - C(17)	1.39	1.62
C(17) - C(22)	1.47	1.50
C(17) - C(18)	1.38	1.49
C(18) - C(19)	1.46	1.18
C(19) - C(20)	1.32	1.53
C(20) - C(21)	1.34	1.36
C(21) - C(22)	1.40	1.40
C(22) - C(23)	1.44	1.36
C(23) - C(24)	1.49	1.43
C(24) - C(25)	1.42	1.48
C(25) - C(26)	1.46	1.46
C(26) - C(1)	1.42	1.41

Average estimated standard deviation

C - C

±0.05

±0.07

<u>BTNF</u>	Complex 1	Complex 2
Br - C(27)	1.88	1.83
O(1) - N(1)	1.15	1.15
O(2) - N(1)	1.35	1.23
O(3) - C(32)	1.22	1.21
O(4) - N(2)	1.22	1.23
O(5) - N(2)	1.21	1.11
O(6) - N(3)	1.09	0.92
O(7) - N(3)	1.20	1.29
N(1) - C(29)	1.42	1.61
N(2) - C(35)	1.51	1.52
N(3) - C(37)	1.50	1.73
C(27) - C(28)	1.25	1.37
C(28) - C(29)	1.45	1.27
C(29) - C(30)	1.37	1.48
C(30) - C(31)	1.35	1.40
C(31) - C(39)	1.41	1.34
C(31) - C(32)	1.55	1.53
C(32) - C(33)	1.37	1.43
C(33) - C(38)	1.44	1.35
C(33) - C(34)	1.41	1.42
C(34) - C(35)	1.43	1.44
C(35) - C(36)	1.32	1.30
C(36) - C(37)	1.46	1.43
C(37) - C(38)	1.44	1.41
C(38) - C(39)	1.46	1.50
C(39) - C(27)	1.44	1.51

Average estimated standard deviations

Br - C	<u>+0.04</u>	<u>+0.04</u>
O - N	<u>+0.05</u>	<u>+0.05</u>
N - C	<u>+0.06</u>	<u>+0.06</u>
O - C	<u>+0.06</u>	<u>+0.06</u>
C - C	<u>+0.07</u>	<u>+0.07</u>

(b) Valency Angles ($^{\circ}$).

<u>Hexahelicene</u>	Complex 1	Complex 2
C(26) - C(1) - C(2)	118.9	121.6
C(1) - C(2) - C(3)	119.7	121.0
C(2) - C(3) - C(4)	119.5	118.7
C(3) - C(4) - C(5)	120.5	120.9
C(4) - C(5) - C(26)	122.1	122.1
C(4) - C(5) - C(6)	123.6	125.3
C(6) - C(5) - C(26)	114.0	112.5
C(5) - C(6) - C(7)	124.2	117.3
C(6) - C(7) - C(8)	120.3	140.0
C(7) - C(8) - C(25)	124.4	111.4
C(7) - C(8) - C(9)	121.1	138.0
C(9) - C(8) - C(25)	114.3	110.5
C(8) - C(9) - C(10)	120.0	125.5
C(9) - C(10) - C(11)	123.2	132.4
C(10) - C(11) - C(24)	115.2	107.2
C(10) - C(11) - C(12)	119.9	151.9
C(12) - C(11) - C(24)	124.5	100.7
C(11) - C(12) - C(13)	114.2	140.6
C(12) - C(13) - C(14)	124.6	125.1
C(13) - C(14) - C(23)	118.5	114.7
C(13) - C(14) - C(15)	121.2	129.0
C(15) - C(14) - C(23)	120.4	116.2
C(14) - C(15) - C(16)	122.4	125.8
C(15) - C(16) - C(17)	118.6	122.8
C(16) - C(17) - C(22)	120.6	107.9
C(16) - C(17) - C(18)	122.6	133.4
C(18) - C(17) - C(22)	116.7	116.7
C(17) - C(18) - C(19)	124.0	123.7
C(18) - C(19) - C(20)	112.4	125.4
C(19) - C(20) - C(21)	129.3	108.1
C(20) - C(21) - C(22)	119.4	133.2
C(21) - C(22) - C(17)	117.5	111.4
C(21) - C(22) - C(23)	125.0	126.6
C(17) - C(22) - C(23)	116.7	122.0
C(22) - C(23) - C(14)	120.7	121.0
C(22) - C(23) - C(24)	119.8	122.2
C(14) - C(23) - C(24)	119.4	116.3
C(23) - C(24) - C(11)	112.5	120.9
C(23) - C(24) - C(25)	129.8	129.7
C(11) - C(24) - C(25)	117.7	108.6
C(24) - C(25) - C(26)	125.0	121.8
C(24) - C(25) - C(8)	122.4	124.9
C(8) - C(25) - C(26)	112.5	113.2
C(25) - C(26) - C(5)	122.1	124.1
C(5) - C(26) - C(1)	118.3	112.9
C(25) - C(26) - C(1)	119.6	122.9

<u>BTF</u>	Complex 1	Complex 2
O(1) - N(1) - C(29)	124.6	111.6
O(2) - N(1) - C(29)	116.4	122.7
O(1) - N(1) - O(2)	117.5	125.6
O(4) - N(2) - C(35)	114.7	109.8
O(5) - N(2) - C(35)	116.1	118.5
O(4) - N(2) - O(5)	129.1	131.4
O(6) - N(3) - C(37)	118.6	113.8
O(7) - N(3) - C(37)	109.5	95.9
O(6) - N(3) - O(7)	131.8	137.5
Br - C(27) - C(28)	119.7	120.7
Br - C(27) - C(39)	116.7	121.1
C(39) - C(27) - C(28)	120.9	117.9
C(27) - C(28) - C(29)	121.7	117.3
C(28) - C(29) - N(1)	115.5	116.9
C(28) - C(29) - C(30)	119.9	128.4
N(1) - C(29) - C(30)	124.3	111.0
C(29) - C(30) - C(31)	116.2	107.9
C(30) - C(31) - C(39)	124.8	126.7
C(30) - C(31) - C(32)	125.4	125.2
C(39) - C(31) - C(32)	109.8	107.9
C(31) - C(32) - O(3)	126.1	125.6
C(31) - C(32) - C(33)	103.5	104.1
O(3) - C(32) - C(33)	129.3	130.3
C(32) - C(33) - C(38)	111.7	110.7
C(32) - C(33) - C(34)	126.1	123.3
C(38) - C(33) - C(34)	121.0	126.0
C(33) - C(34) - C(35)	116.6	111.4
C(34) - C(35) - N(2)	116.8	113.0
C(34) - C(35) - C(36)	127.5	123.8
N(2) - C(35) - C(36)	115.7	123.1
C(35) - C(36) - C(37)	115.2	123.3
C(36) - C(37) - N(3)	115.1	116.6
C(36) - C(37) - C(38)	121.4	115.6
N(3) - C(37) - C(38)	123.3	127.2
C(37) - C(38) - C(33)	117.5	119.6
C(37) - C(38) - C(39)	133.6	132.4
C(33) - C(38) - C(39)	108.9	107.9
C(38) - C(39) - C(31)	105.1	107.5
C(38) - C(39) - C(27)	139.6	135.5
C(31) - C(39) - C(27)	115.3	116.9

c) Intramolecular non-bonded distances (Å) in the hexahelicene molecules which define the deviation of the molecule from planarity.

	Complex 1	Complex 2
C(1) C(21)	3.06	3.04
C(2) C(20)	4.25	4.24
C(22) . . . C(26)	3.29	3.32

d) Shortest intermolecular contacts between BTNF and hexahelicene molecules.

Complex 1 atom		Complex 2 atom	distance (Å)
C(33)	. . .	C(5)	3.73
C(32)	. . .	C(5)	4.04
C(31)	. . .	C(2)	3.28
C(13)	. . .	C(32)	3.48
C(14)	. . .	C(32)	3.44

Table 1.4

Mean planes through the benzene rings of the hexahelicene molecules.

a) Deviation of individual atoms, and the root mean square deviation of the atoms, from the best mean plane.

Plane	Complex 1	Complex 2
Ring 1		
C(1)	-0.03	0.03
C(2)	0.06	-0.09
C(3)	-0.05	0.09
C(4)	0.02	-0.03
C(5)	0.02	-0.03
C(26)	-0.01	0.03
r.m.s.	0.04	0.06
Ring 2		
C(5)	0.03	-0.02
C(6)	-0.08	0.06
C(7)	0.02	-0.02
C(8)	0.07	-0.05
C(25)	-0.10	0.07
C(26)	0.06	-0.04
r.m.s.	0.06	0.05
Ring 3		
C(8)	0.05	-0.07
C(9)	-0.13	0.18
C(10)	0.07	-0.05
C(11)	0.08	-0.12
C(24)	-0.17	0.20
C(25)	0.10	-0.13
r.m.s.	0.10	0.14
Ring 4		
C(11)	-0.03	0.04
C(12)	-0.11	0.02
C(13)	0.13	-0.04
C(14)	-0.01	-0.01
C(23)	-0.12	0.07
C(24)	0.13	-0.08
r.m.s.	0.10	0.05

Ring 5		
C(14)	-0.02	0.18
C(15)	-0.02	-0.23
C(16)	0.03	0.38
C(17)	0.00	-0.13
C(22)	-0.04	0.19
C(23)	0.05	-0.39
r.m.s.	0.03	0.27

Ring 6		
C(17)	-0.05	-0.20
C(18)	0.02	0.39
C(19)	0.01	-0.18
C(20)	-0.02	0.15
C(21)	-0.01	-0.35
C(22)	0.04	0.19
r.m.s.	0.03	0.26

b) Dihedral angles between the planes ($^{\circ}$).

Planes	Complex 1	Complex 2
1,2	10.6	8.5
2,3	11.8	14.0
3,4	16.7	15.0
4,5	10.0	19.7
5,6	10.7	3.5

c) Equations of the planes.

Plane no.	P	Q	R	S
1	-0.4722	0.1605	-0.8668	-8.8983
	-0.4623	0.2859	-0.8393	-1.1972
2	-0.3820	0.3207	-0.8667	-7.7403
	-0.3795	0.4034	-0.8302	-0.0659
3	-0.2217	0.4503	-0.8649	-6.6487
	-0.1452	0.4356	-0.8884	1.5444
4	0.0576	0.5292	-0.8465	-5.2488
	0.1162	0.4288	-0.8959	3.3558
5	0.2236	0.4787	-0.8491	-4.9475
	-0.5421	-0.8352	-0.0930	-5.6737
6	0.3555	0.3485	-0.8673	-5.1334
	-0.5919	-0.8002	-0.0969	-5.7263

In this table P, Q and R are the direction cosines of the plane normal and S is the plane to origin distance. The plane equation is thus

$$PX + QY + RZ = S$$

where X, Y and Z are orthogonalised coordinates in Å.

The first equation given for each plane refers to complex 1 and the second to complex 2.

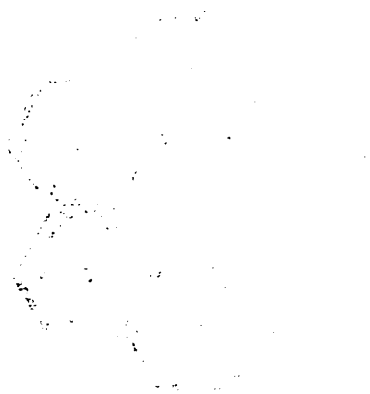
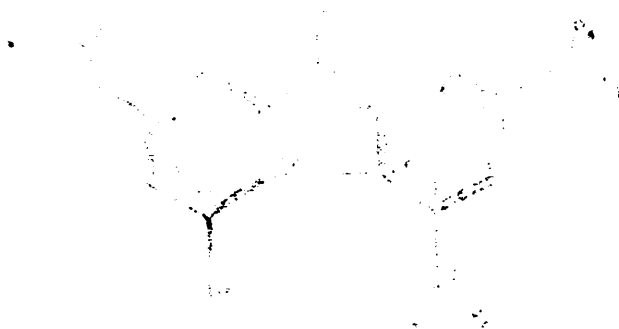


Figure 1.1

The numbering scheme adopted for the atoms
of the complex.



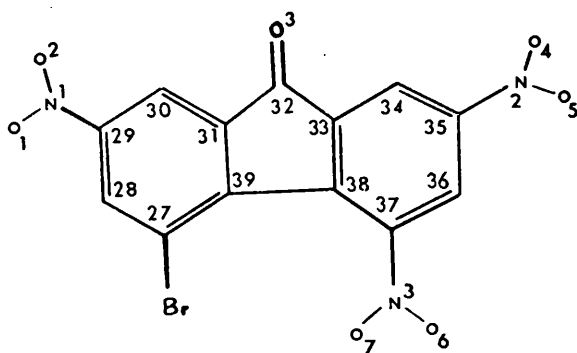
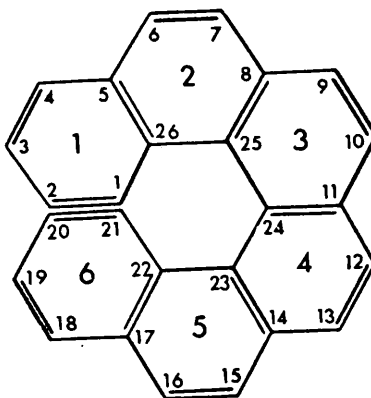


Figure 1.2

The electron-density distribution, at $R = 0.240$, of two symmetry-related hexahelicene molecules.

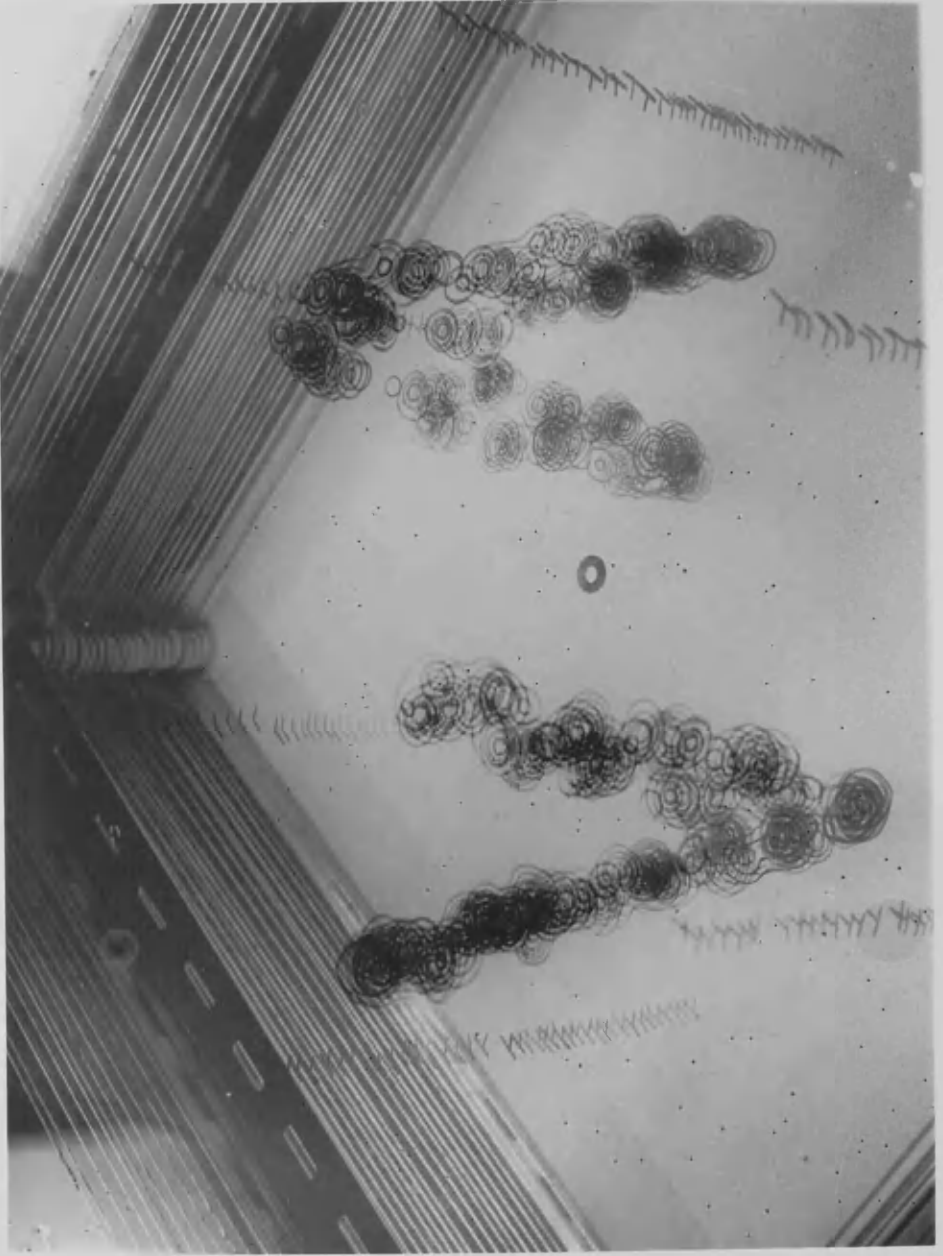
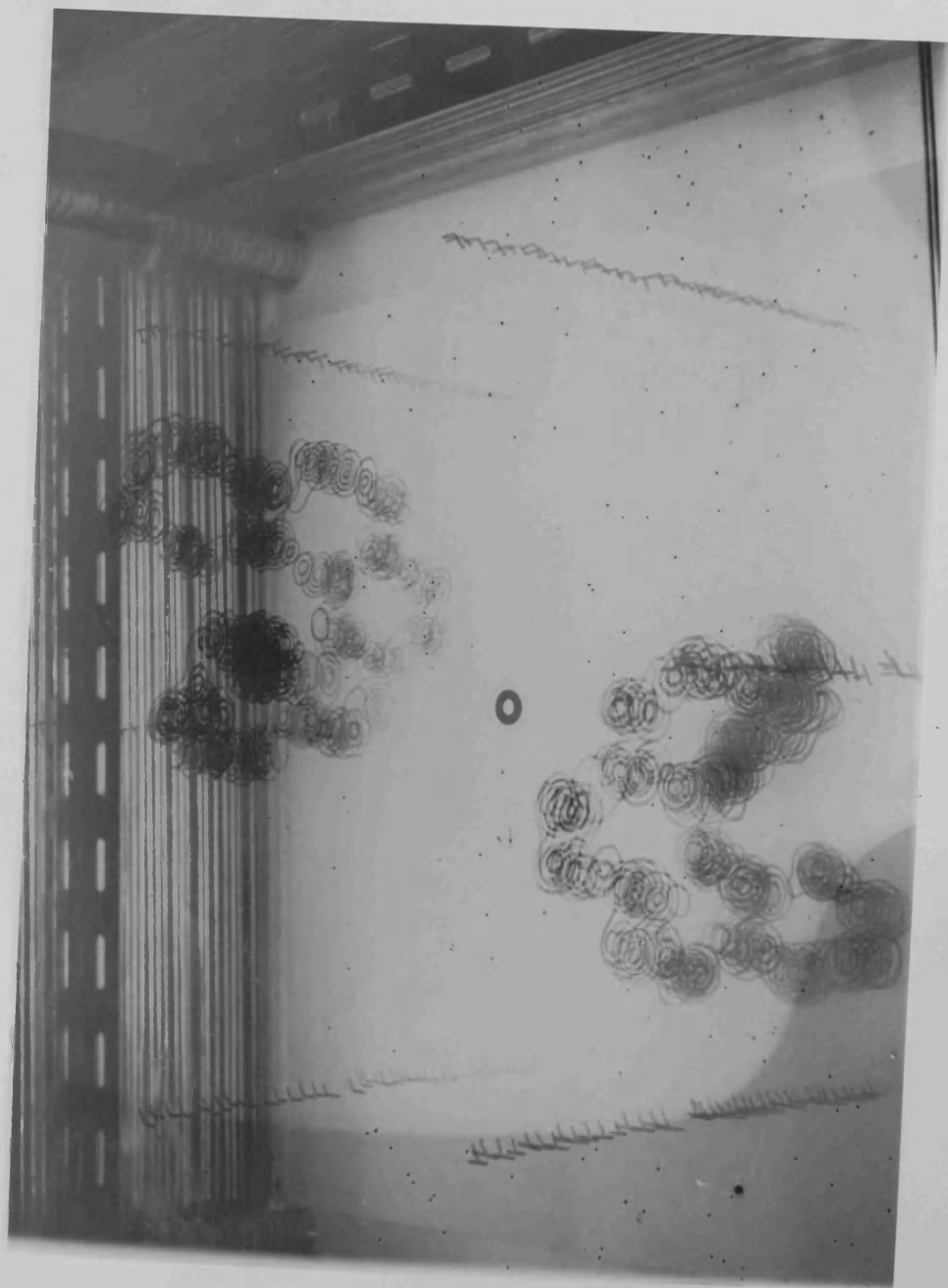


Figure 1.3

The electron-density distribution, at $R = 0.240$, of two symmetry-related hexahelicene molecules.



1.5 Discussion.

The results of the analysis show clearly the helical structure of hexahelicene and, although one is clearly restricted in drawing conclusions at this stage of the refinement, it would appear that this is achieved with very little distortion of the aromatic rings.

The crystal structure of the complex is built up of alternate donor (hexahelicene) and acceptor (BTNF) molecules with the overlap of aromatic rings which is typical of π - π molecular complexes. Each BTNF molecule is sandwiched between two hexahelicene molecules, with three rings of the former compound lying nearly parallel to rings 1, 2, 3 and rings 4, 5, 6 of the two adjacent hexahelicene molecules at approximately van der Waals separation distances (Table 1.3d). This results in the electron density within the unit cell being concentrated on a set of parallel planes, approximating the $15\bar{5}$ planes.

In the unit cell of the complex two of the four hexahelicene molecules are the left-handed enantiomer and two are right-handed, each of the former being related to the latter through the centre of symmetry of the space group.

There are two particularly interesting points about the structure of the hydrocarbon which previous work on

hexahelicene and the lower homologues of the series have indicated.

The first concerns the effect of the distortion from planarity on the bond lengths and angles, particularly at the junction of rings 3 and 4. Rhodes has studied the electronic spectra of hexahelicene (1962) and found a striking resemblance to the spectra of phenanthrene, indicating that the distortion causes the hexahelicene to approximate two weakly conjugated phenanthrene units. With respect to this, it is interesting to note that in the two-dimensional analysis carried out on 3:4-5:6 dibenzophenanthrene (pentahelicene) by M^CIntosh, Robertson and Vand (1954) it was found that the bonds connecting the two naphthalene wings in the molecule were longer than the others in the structure, and these are the bonds which are probably subject to the greatest distortion.

In hexahelicene it would be expected that this effect would be reflected in the values of the bond lengths and angles of rings 3 and 4 (Table 1.3a and b). Inspection of these shows clearly that, in complex 1, there are no significant deviations from the values which would be expected in an undistorted benzenoid ring, with the possible exception of the angle C(23)-C(24)-C(25) which was found to be 129.8°. This angle is the most sensitive of all

the molecular dimensions to any distortion from planarity and hence indicates the comparative ease with which the helical structure is attained. It is somewhat more difficult to draw conclusions about the values found for the bond lengths and angles in complex 2, but the lack of any pattern in the deviations would imply no difference from the results obtained in the better refined complex 1.

A more sensitive indication as to how the non-planarity of the molecule is achieved is obtained by examining the best mean planes through each of the benzene rings (Table 1.4). It is found that the distortion from planarity which is required of the individual rings is not uniformly distributed, and this is clearly shown by the root mean square distance of the atoms from each plane and by the dihedral angles between the planes. As would be expected, these increase from the terminal rings, 1 and 6, where the deviations of the atoms are not significant, to the "bridge" rings, 3 and 4, where the effects of the molecular distortion are most strongly felt, and correspondingly the deviations of the atoms from planarity are greatest. The results obtained for complex 2 correspond well with those of complex 1 for rings 1, 2 and 3. As was mentioned previously, the electron-density distribution over rings 4, 5, and 6 of the second complex proved very

difficult to interpret and this resulted in small errors arising in some of the atomic positions which are reflected in the calculated best mean planes.

The second point of interest, referred to before, is the degree of the distortion of the molecule, i.e. the pitch of the helix. Calculations made by Fitts and Kirkwood (1955) of the optical rotation of hexahelicene assumed that the distance between the nearest pair of non-bonded carbon atoms would be 3.8 Å, which is the packing distance between neighbouring molecules in benzene crystals. However, Coulson (1963) has shown that overcrowded atoms can be much closer than the sum of their van der Waals radii at little cost in energy and the theoretical calculations of Herraes Zarza and Sanchez (1965) to find the minimum displacement potential energy showed this separation distance to be 3.004 Å. This represents the distance between C(1) and C(21) and is in good agreement with the values 3.06 and 3.04 Å observed in this analysis (Table 1.3c). In the recently reported structure of the heterohelicene benzo(d)naphtho(1,2-d')benzo(1,2-b:4,3-b')dithiophen, (Stulen and Visser, 1969, structure X in the Table), the corresponding separation distance was found to be 2.91 Å.

The bond lengths observed in the four molecules do not deviate significantly from accepted values and those

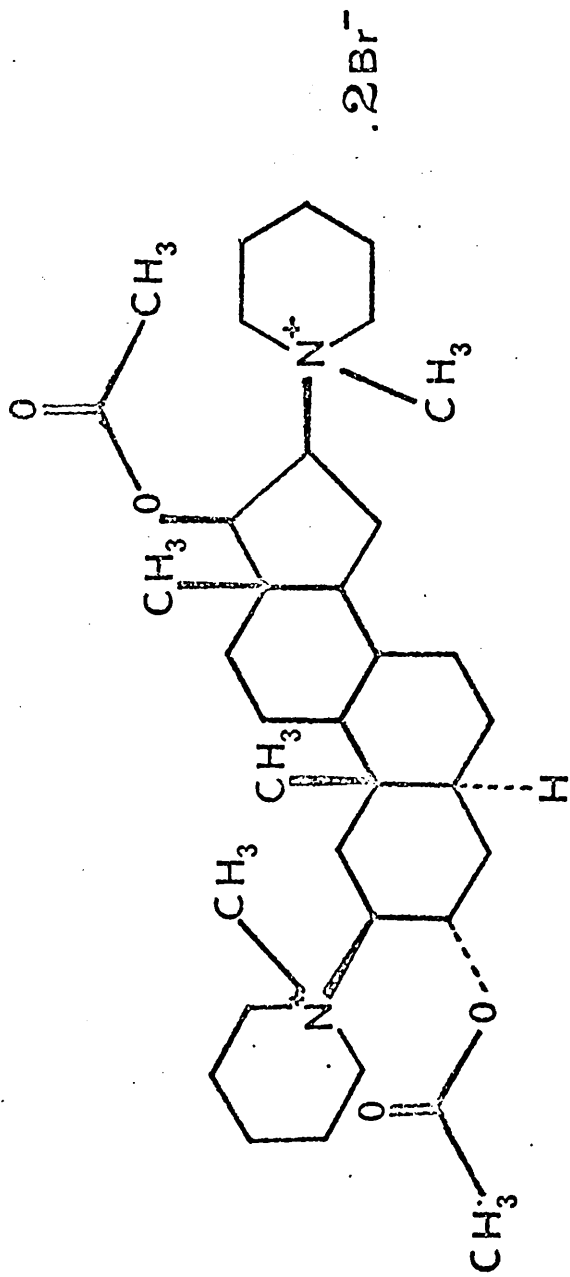
established for the BTNF molecules correspond well, at this stage, with those established previously by Hollard (1968), as do the intermolecular contacts between the two molecules of the complex (Table 1.3d).

In conclusion, the helical structure of hexahelicene has been established and it has been shown that this is achieved without any great change in the bond lengths and angles or severe buckling of the benzene rings.

CHAPTER 2THE CRYSTAL AND MOLECULAR STRUCTURE OF PANCURONIUM BROMIDE.2.1 Introduction.

Pancuronium bromide (I), 3α , 17β - diacetoxy - 2β , 16β - dipiperidino - 5α - androstane dimethobromide, was synthesised (Bucket et al., 1967) in the course of an investigation into the biological activities of derivatives of 5α - androstane, and was found to be of clinical importance as a result of its properties as a neuromuscular blocking agent.

It has been shown (Savage et al., 1970) from n.m.r. evidence that the steric compression resulting from the presence of the two quaternary groups in the amino-sterol locks the rings A and D in specific conformations which are unaffected by acetylation of the hydroxyl groups at the 3- and 17- positions. Thus the structural rigidity, which relates to the potency and specificity of action of the agent, allows one to assume that the solid-state conformation approximates to that of the molecule in a biological system. A structural analysis by X-ray diffraction was thus undertaken, in collaboration with A.F. Cameron, G. Ferguson and C. Hannaway, in order to determine the conformation of the molecule.

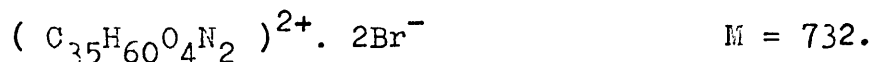


(I) Pancuronium Bromide

2.2 Crystal Data.

The crystalline sample was supplied by Organon Laboratories Ltd., having been recrystallised from an ether/dichloromethane/water mixture and it was found, during the course of the analysis, that one molecule each of dichloromethane and water were present in the asymmetric unit.

Pancuronium bromide



Orthorhombic,

$$\underline{a} = 11.10 \pm 0.03 \text{ \AA},$$

$$\underline{b} = 13.99 \pm 0.04 \text{ \AA},$$

$$\underline{c} = 26.07 \pm 0.06 \text{ \AA}.$$

Volume of unit cell = 4048 \AA^3 .

$D_m = 1.40$ (by flotation in aqueous potassium iodide).

$Z = 4$.

$D_c = 1.35$ (including water and dichloromethane).

$F(000) = 1752$.

Linear absorption coefficient, $\mu = 24.1 \text{ cm}^{-1}$ (Cu $K\alpha$).

Absent spectra : $h00$ when $h = 2n + 1$,

$0k0$ when $k = 2n + 1$,

$00l$ when $l = 2n + 1$.

Space group : $P2_12_12_1$ (D_2^4 , no. 19)

(uniquely determined by systematic absences).

The unit cell parameters were determined from oscillation and Weissenberg photographs (Cu $K\alpha$ radiation, $\lambda = 1.5418 \text{ \AA}$) and from precession photographs (Mo $K\alpha$ radiation, $\lambda = 0.7107 \text{ \AA}$).

2.3 Intensity Data.

The intensity data were recorded on equi-inclination Weissenberg photographs of the $0kl, \dots, 8kl$ reciprocal lattice nets, using Cu $K\alpha$ radiation. As decomposition was found to occur on exposure to X-rays, it was necessary to use a total of four small crystals, coated in collodian, and to restrict the data collection to the minimum of one octant required by orthorhombic symmetry.

In this way some 2113 independent reflexions were observed, and these were visually estimated by comparison with a calibrated intensity scale using the multiple-film technique (Robertson, 1943). Lorentz, polarisation and rotation corrections (Tunell, 1939) were applied to these intensities to give the observed structure amplitudes on a relative scale and an approximately absolute scale was obtained at a later stage by scaling these to the calculated values for each layer. Corrections were not made for the effects of absorption and extinction.

2.4 Structure Determination and Refinement.

The unit cell of the crystal, containing four molecules of pancuronium bromide, has two bromine ions in the asymmetric unit and these, therefore, give rise to two sets of heavy-atom vectors in the three-dimensional Patterson synthesis. The first set of peaks, due to the vectors between each bromine ion in symmetry-related positions, should occur for both ions on the Harker sections $U = \frac{1}{2}$, $V = \frac{1}{2}$ and $W = \frac{1}{2}$. The second set gives rise to general peaks corresponding to the vectors between Br(1) and Br(2) in all equivalent positions. The fractional coordinates of the two bromine ions were obtained from the Harker sections and verified by their prediction of the positions of the general peaks :

Br(1)	0.250	0.134	0.086,
Br(2)	0.888	0.173	0.230.

The electron-density distribution was calculated, phased from structure factors for the bromine ions alone, and this revealed the complete steroidal skeleton. Subsequent Fourier syntheses revealed the entire molecule and also two large unidentified peaks, consistent with the presence of another molecule. Chemical analysis indicated that one molecule each of dichloromethane and water were present in the asymmetric unit, and assigning

the unidentified peaks as the chlorine atoms of dichloromethane revealed the remaining carbon and oxygen atoms. Five cycles of structure factor calculations and Fourier synthesis were required in all, and the R factor was reduced to 0.208.

Positional, vibrational and scale parameters were refined (Table 2.1) by least-squares methods using the block diagonal approximation, a shift factor of 0.75, and a weighting scheme of the form

$$\sqrt{w} = [1 - \exp(-p_1(\sin \theta / \lambda)^2)] / (1 + p_2|F_o| + p_3|F_o|^2)^{\frac{1}{2}}.$$

Unit weighting was initially applied to all reflexions and the parameters p_1 , p_2 and p_3 were subsequently adjusted in order to maintain constant averages of $w\Delta^2$ for reflexions batched according to $|F_o|$ and $\sin \theta / \lambda$; the final values of p_1 , p_2 and p_3 were 100, 0.01 and 0.0001 respectively.

All atoms were refined isotropically and anisotropic temperature factors were applied to the bromine and chlorine atoms after cycle 9. Layer scale factors were employed in the first four cycles, after which an overall scale factor was refined.

The refinement converged after 12 cycles with R at 0.129 and the observed and final calculated structure amplitudes are listed in Table 2.2. The atomic scattering factors used in the structure-factor calculations are

those given in the "International Tables for X-ray Crystallography", Vol. III.

A final ($F_o - F_c$) distribution was calculated and showed no significant errors in the structural model, nor was it possible to locate, from a Fourier synthesis, any further molecules of water which might have been present. Table 2.3 contains the final fractional coordinates and thermal parameters and Table 2.4, the bond lengths, valence angles, intra- and intermolecular non-bonded distances. The corresponding estimated standard deviations given in these tables were derived from the inverse of the least-squares normal-equation matrix.

The numbering scheme which was adopted in the analysis is shown in Fig. 2.1 and the molecular packing diagram, viewed along the a axis, in Fig 2.2.

2.5 Absolute Configuration.

The initial atomic coordinates were chosen to conform to the stereochemistry which had been predicted on the basis of the known absolute configuration of the 5 α -androstande (Klyne, 1965) from which the pancuronium bromide was prepared. Subsequently the method of anomalous scattering (Bijvoet, 1949) was used, when examination of 15 pairs of equivalent reflexions showing

this effect verified that the model obtained from the analysis had, in fact, the correct absolute configuration.

Table 2.1

Progress of Refinement.

Parameters refined	Cycle No.	Final R	Final R'
x,y,z,Uiso for all atoms (non-hydrogen), layer scale factors, unit weights.	1 - 4	0.182	0.0639
x,y,z,Uiso for all atoms, overall scale factor, weighting scheme adjusted.	5 - 8	0.178	0.0562
x,y,z,Uiso for C, O, N, x,y,z,Uij for Br, Cl, overall scale factor, weighting scheme adjusted.	9 - 12	0.129	0.0252

where

$$R = \frac{\sum_{hkl} \left| |F_o| - |F_c| \right|}{\sum_{hkl} |F_o|},$$

$$R' = \frac{\sum_{hkl} w \Delta^2}{\sum_{hkl} w F_o^2},$$

$$\Delta = |F_o| - |F_c|.$$

Main data table containing multiple columns of numerical values and categorical labels. The table is organized in a grid-like structure with repeating column headers.

Continuation of the main data table from the previous section, showing similar columns and numerical data points.

3 2 14	99.19	99.62	99.31	100.35	3.12	1	3 9 18	29.88	29.77	30.27	30.67	-0.39	1	4 4 15	32.86	33.14	-30.31	17.99	0.82
3 2 15	99.26	99.38	99.64	100.34	3.12	1	3 9 19	29.94	29.99	30.27	30.67	-0.39	1	4 4 16	32.90	33.14	-30.31	17.99	0.82
3 2 16	99.31	99.65	99.65	100.03	3.12	1	3 9 20	29.98	29.97	30.27	30.67	-0.39	1	4 4 17	32.94	33.14	-30.31	17.99	0.82
3 2 17	99.33	99.33	99.64	100.03	3.12	1	3 9 21	30.03	29.97	30.27	30.67	-0.39	1	4 4 18	32.98	33.14	-30.31	17.99	0.82
3 2 18	99.35	99.35	99.64	100.03	3.12	1	3 9 22	30.08	29.97	30.27	30.67	-0.39	1	4 4 19	33.02	33.14	-30.31	17.99	0.82
3 2 19	99.37	99.37	99.64	100.03	3.12	1	3 9 23	30.13	29.97	30.27	30.67	-0.39	1	4 4 20	33.06	33.14	-30.31	17.99	0.82
3 2 20	99.39	99.39	99.64	100.03	3.12	1	3 9 24	30.18	29.97	30.27	30.67	-0.39	1	4 4 21	33.10	33.14	-30.31	17.99	0.82
3 2 21	99.41	99.41	99.64	100.03	3.12	1	3 9 25	30.23	29.97	30.27	30.67	-0.39	1	4 4 22	33.14	33.14	-30.31	17.99	0.82
3 2 22	99.43	99.43	99.64	100.03	3.12	1	3 9 26	30.28	29.97	30.27	30.67	-0.39	1	4 4 23	33.18	33.14	-30.31	17.99	0.82
3 2 23	99.45	99.45	99.64	100.03	3.12	1	3 9 27	30.33	29.97	30.27	30.67	-0.39	1	4 4 24	33.22	33.14	-30.31	17.99	0.82
3 2 24	99.47	99.47	99.64	100.03	3.12	1	3 9 28	30.38	29.97	30.27	30.67	-0.39	1	4 4 25	33.26	33.14	-30.31	17.99	0.82
3 2 25	99.49	99.49	99.64	100.03	3.12	1	3 9 29	30.43	29.97	30.27	30.67	-0.39	1	4 4 26	33.30	33.14	-30.31	17.99	0.82
3 2 26	99.51	99.51	99.64	100.03	3.12	1	3 9 30	30.48	29.97	30.27	30.67	-0.39	1	4 4 27	33.34	33.14	-30.31	17.99	0.82
3 2 27	99.53	99.53	99.64	100.03	3.12	1	3 9 31	30.53	29.97	30.27	30.67	-0.39	1	4 4 28	33.38	33.14	-30.31	17.99	0.82
3 2 28	99.55	99.55	99.64	100.03	3.12	1	3 9 32	30.58	29.97	30.27	30.67	-0.39	1	4 4 29	33.42	33.14	-30.31	17.99	0.82
3 2 29	99.57	99.57	99.64	100.03	3.12	1	3 9 33	30.63	29.97	30.27	30.67	-0.39	1	4 4 30	33.46	33.14	-30.31	17.99	0.82
3 2 30	99.59	99.59	99.64	100.03	3.12	1	3 9 34	30.68	29.97	30.27	30.67	-0.39	1	4 4 31	33.50	33.14	-30.31	17.99	0.82
3 2 31	99.61	99.61	99.64	100.03	3.12	1	3 9 35	30.73	29.97	30.27	30.67	-0.39	1	4 4 32	33.54	33.14	-30.31	17.99	0.82
3 2 32	99.63	99.63	99.64	100.03	3.12	1	3 9 36	30.78	29.97	30.27	30.67	-0.39	1	4 4 33	33.58	33.14	-30.31	17.99	0.82
3 2 33	99.65	99.65	99.64	100.03	3.12	1	3 9 37	30.83	29.97	30.27	30.67	-0.39	1	4 4 34	33.62	33.14	-30.31	17.99	0.82
3 2 34	99.67	99.67	99.64	100.03	3.12	1	3 9 38	30.88	29.97	30.27	30.67	-0.39	1	4 4 35	33.66	33.14	-30.31	17.99	0.82
3 2 35	99.69	99.69	99.64	100.03	3.12	1	3 9 39	30.93	29.97	30.27	30.67	-0.39	1	4 4 36	33.70	33.14	-30.31	17.99	0.82
3 2 36	99.71	99.71	99.64	100.03	3.12	1	3 9 40	30.98	29.97	30.27	30.67	-0.39	1	4 4 37	33.74	33.14	-30.31	17.99	0.82
3 2 37	99.73	99.73	99.64	100.03	3.12	1	3 9 41	31.03	29.97	30.27	30.67	-0.39	1	4 4 38	33.78	33.14	-30.31	17.99	0.82
3 2 38	99.75	99.75	99.64	100.03	3.12	1	3 9 42	31.08	29.97	30.27	30.67	-0.39	1	4 4 39	33.82	33.14	-30.31	17.99	0.82
3 2 39	99.77	99.77	99.64	100.03	3.12	1	3 9 43	31.13	29.97	30.27	30.67	-0.39	1	4 4 40	33.86	33.14	-30.31	17.99	0.82
3 2 40	99.79	99.79	99.64	100.03	3.12	1	3 9 44	31.18	29.97	30.27	30.67	-0.39	1	4 4 41	33.90	33.14	-30.31	17.99	0.82
3 2 41	99.81	99.81	99.64	100.03	3.12	1	3 9 45	31.23	29.97	30.27	30.67	-0.39	1	4 4 42	33.94	33.14	-30.31	17.99	0.82
3 2 42	99.83	99.83	99.64	100.03	3.12	1	3 9 46	31.28	29.97	30.27	30.67	-0.39	1	4 4 43	33.98	33.14	-30.31	17.99	0.82
3 2 43	99.85	99.85	99.64	100.03	3.12	1	3 9 47	31.33	29.97	30.27	30.67	-0.39	1	4 4 44	34.02	33.14	-30.31	17.99	0.82
3 2 44	99.87	99.87	99.64	100.03	3.12	1	3 9 48	31.38	29.97	30.27	30.67	-0.39	1	4 4 45	34.06	33.14	-30.31	17.99	0.82
3 2 45	99.89	99.89	99.64	100.03	3.12	1	3 9 49	31.43	29.97	30.27	30.67	-0.39	1	4 4 46	34.10	33.14	-30.31	17.99	0.82
3 2 46	99.91	99.91	99.64	100.03	3.12	1	3 9 50	31.48	29.97	30.27	30.67	-0.39	1	4 4 47	34.14	33.14	-30.31	17.99	0.82
3 2 47	99.93	99.93	99.64	100.03	3.12	1	3 9 51	31.53	29.97	30.27	30.67	-0.39	1	4 4 48	34.18	33.14	-30.31	17.99	0.82
3 2 48	99.95	99.95	99.64	100.03	3.12	1	3 9 52	31.58	29.97	30.27	30.67	-0.39	1	4 4 49	34.22	33.14	-30.31	17.99	0.82
3 2 49	99.97	99.97	99.64	100.03	3.12	1	3 9 53	31.63	29.97	30.27	30.67	-0.39	1	4 4 50	34.26	33.14	-30.31	17.99	0.82
3 2 50	99.99	99.99	99.64	100.03	3.12	1	3 9 54	31.68	29.97	30.27	30.67	-0.39	1	4 4 51	34.30	33.14	-30.31	17.99	0.82
3 2 51	100.01	100.01	99.64	100.03	3.12	1	3 9 55	31.73	29.97	30.27	30.67	-0.39	1	4 4 52	34.34	33.14	-30.31	17.99	0.82
3 2 52	100.03	100.03	99.64	100.03	3.12	1	3 9 56	31.78	29.97	30.27	30.67	-0.39	1	4 4 53	34.38	33.14	-30.31	17.99	0.82
3 2 53	100.05	100.05	99.64	100.03	3.12	1	3 9 57	31.83	29.97	30.27	30.67	-0.39	1	4 4 54	34.42	33.14	-30.31	17.99	0.82
3 2 54	100.07	100.07	99.64	100.03	3.12	1	3 9 58	31.88	29.97	30.27	30.67	-0.39	1	4 4 55	34.46	33.14	-30.31	17.99	0.82
3 2 55	100.09	100.09	99.64	100.03	3.12	1	3 9 59	31.93	29.97	30.27	30.67	-0.39	1	4 4 56	34.50	33.14	-30.31	17.99	0.82
3 2 56	100.11	100.11	99.64	100.03	3.12	1	3 9 60	31.98	29.97	30.27	30.67	-0.39	1	4 4 57	34.54	33.14	-30.31	17.99	0.82
3 2 57	100.13	100.13	99.64	100.03	3.12	1	3 9 61	32.03	29.97	30.27	30.67	-0.39	1	4 4 58	34.58	33.14	-30.31	17.99	0.82
3 2 58	100.15	100.15	99.64	100.03	3.12	1	3 9 62	32.08	29.97	30.27	30.67	-0.39	1	4 4 59	34.62	33.14	-30.31	17.99	0.82
3 2 59	100.17	100.17	99.64	100.03	3.12	1	3 9 63	32.13	29.97	30.27	30.67	-0.39	1	4 4 60	34.66	33.14	-30.31	17.99	0.82
3 2 60	100.19	100.19	99.64	100.03	3.12	1	3 9 64	32.18	29.97	30.27	30.67	-0.39	1	4 4 61	34.70	33.14	-30.31	17.99	0.82
3 2 61	100.21	100.21	99.64	100.03	3.12	1	3 9 65	32.23	29.97	30.27	30.67	-0.39	1	4 4 62	34.74	33.14	-30.31	17.99	0.82
3 2 62	100.23	100.23	99.64	100.03	3.12	1	3 9 66	32.28	29.97	30.27	30.67	-0.39	1	4 4 63	34.78	33.14	-30.31	17.99	0.82
3 2 63	100.25	100.25	99.64	100.03	3.12	1	3 9 67	32.33	29.97	30.27	30.67	-0.39	1	4 4 64	34.82	33.14	-30.31	17.99	0.82
3 2 64	100.27	100.27	99.64	100.03	3.12	1	3 9 68	32.38	29.97	30.27	30.67	-0.39	1	4 4 65	34.86	33.14	-30.31	17.99	0.82
3 2 65	100.29	100.29	99.64	100.03	3.12	1	3 9 69	32.43	29.97	30.27	30.67	-0.39	1	4 4 66	34.90	33.14	-30.31	17.99	0.82
3 2 66	100.31	100.31	99.64	100.03	3.12	1	3 9 70	32.48	29.97	30.27	30.67	-0.39	1	4 4 67	34.94	33.14	-30.31	17.99	0.82
3 2 67	100.33	100.33	99.64	100.03	3.12	1	3 9 71	32.53	29.97	30.27	30.67	-0.39	1	4 4 68	34.98	33.14	-30.31	17.99	0.82
3 2 68	100.35	100.35	99.64	100.03	3.12	1	3 9 72	32.58	29.97	30.27	30.67	-0.39	1	4 4 69	35.02	33.14	-30.31	17.99	0.82
3 2 69	100.37	100.37	99.64	100.03	3.12	1	3 9 73	32.63	29.97	30.27	30.67	-0.39	1	4 4 70	35.06	33.14	-30.31	17.99	

A large grid of numerical data, likely a table with multiple columns and rows of values. The data is organized in a regular grid pattern, with some cells appearing to have multiple values or small sub-indices. The grid is dense and covers most of the page area.

Table 2.3

Fractional co-ordinates and thermal parameters with e.s.d.s.

	x/a	y/b	z/c	U _{iso}
Br(1)	0.2698(3)	0.1318(3)	0.0855(1)	*
Br(2)	0.8878(3)	0.1724(2)	0.2283(1)	*
Cl(1)	0.8265(13)	0.0923(7)	0.3841(4)	*
Cl(2)	1.0636(14)	0.0106(12)	0.3610(5)	*
N(1)	0.6884(19)	0.1836(12)	0.0624(7)	0.0385(45)
N(2)	-0.0240(19)	0.3957(13)	0.3374(7)	0.0355(47)
O(1)	0.0839(15)	0.2779(10)	0.4195(6)	0.0389(36)
O(2)	0.2245(21)	0.3111(14)	0.4772(7)	0.0739(57)
O(3)	0.6182(16)	0.3844(11)	0.0635(6)	0.0429(39)
O(4)	0.4705(24)	0.4465(17)	0.0147(9)	0.0922(71)
O(5)	0.0879(27)	0.2807(18)	0.1509(10)	0.1068(81)
C(1)	0.1874(22)	0.3775(15)	0.2913(8)	0.0326(50)
C(2)	0.0911(23)	0.3314(16)	0.3303(8)	0.0376(53)
C(3)	0.1661(22)	0.3142(15)	0.3802(8)	0.0322(53)
C(4)	0.2521(27)	0.2340(18)	0.3690(9)	0.0482(65)
C(5)	0.2998(23)	0.2322(15)	0.3118(8)	0.0364(56)
C(6)	0.4178(25)	0.1711(18)	0.3093(9)	0.0481(61)
C(7)	0.4564(23)	0.1640(16)	0.2507(8)	0.0391(55)
C(8)	0.4639(21)	0.2622(14)	0.2286(8)	0.0278(48)
C(9)	0.3606(22)	0.3261(15)	0.2350(8)	0.0326(50)
C(10)	0.3120(22)	0.3348(15)	0.2916(8)	0.0313(50)
C(11)	0.3701(24)	0.4243(16)	0.2109(8)	0.0411(58)

C(12)	C.4077(23)	C.4159(15)	C.1528(8)	C.C339(53)
C(13)	C.5106(23)	C.3548(15)	C.1462(8)	C.C358(54)
C(14)	C.4864(20)	C.2546(13)	C.1716(7)	C.C225(46)
C(15)	C.5840(22)	C.1910(14)	C.1516(8)	C.C322(52)
C(16)	C.5752(19)	C.2144(13)	C.C916(7)	C.C251(45)
C(17)	C.5334(22)	C.3234(15)	C.C895(8)	C.C344(50)
C(18)	C.6383(27)	C.3987(18)	C.1680(9)	C.C550(71)
C(19)	C.3970(23)	C.3899(15)	C.3241(8)	C.C352(52)
C(20)	C.C087(26)	C.4815(17)	C.3732(9)	C.C449(63)
C(21)	C.7994(31)	C.2349(22)	C.C831(12)	C.C719(84)
C(22)	-C.1249(28)	C.3342(19)	C.3555(9)	C.C549(67)
C(23)	-C.2459(28)	C.3818(19)	C.3601(10)	C.C561(70)
C(24)	-C.2790(27)	C.4270(18)	C.3058(10)	C.C558(69)
C(25)	-C.1750(27)	C.4926(18)	C.2860(9)	C.C495(66)
C(26)	-C.C607(25)	C.4373(17)	C.2846(9)	C.C439(62)
C(27)	C.7116(24)	C.C772(16)	C.C710(8)	C.C402(59)
C(28)	C.6012(26)	C.C183(17)	C.C505(9)	C.C442(60)
C(29)	C.5848(35)	C.C341(24)	-C.C075(13)	C.C819(98)
C(30)	C.5719(28)	C.1475(19)	-C.C158(10)	C.C583(74)
C(31)	C.6704(26)	C.C036(17)	C.C042(10)	C.C514(66)
C(32)	C.1308(27)	C.2787(18)	C.4686(9)	C.C511(67)
C(33)	C.C381(31)	C.2396(24)	C.5051(12)	C.C674(84)
C(34)	C.5601(32)	C.4499(11)	C.C303(11)	C.C691(86)
C(35)	C.6659(32)	C.5176(22)	C.C158(12)	C.C714(86)
C(36)	C.9148(45)	C.C166(30)	C.3466(16)	C.1046(130)

* Anisotropic thermal parameters for halogen atoms with e.s.d.s.

	U_{11}	U_{22}	U_{33}	$2U_{23}$	$2U_{31}$	$2U_{12}$
Br(1)	C.0679 24	C.0897 20	C.0666 17	C.0249 35	C.0229 35	C.0591 38
Br(2)	C.0840 26	C.0700 17	C.0605 15	-C.0042 33	C.0053 35	-C.0474 38
Cl(1)	C.1601 114	C.0777 59	C.1063 70	C.0535 112	C.0193 149	C.0408 141
Cl(2)	C.1118 117	C.2047 134	C.1249 94	-C.0395 194	C.0275 164	C.1279 208

where U_{ij} ($i, j = 1, 2, 3$) are the anisotropic thermal parameters (\AA^2) in the general temperature factor expression

$$\exp(-2\pi^2(U_{11}h^2a^{*2} + U_{22}k^2b^{*2} + U_{33}l^2c^{*2} + 2U_{23}klb^*c^* + 2U_{31}lhc^*a^* + 2U_{12}hka^*b^*)) .$$

Table 2.4

(a) Bond lengths and e.s.d.s (Å).

C(1)-C(2)	1.61(3)	C(16)-N(1)	1.53(3)
C(1)-C(1C)	1.51(3)	C(17)-O(3)	1.44(3)
C(2)-C(3)	1.56(3)	C(20)-N(2)	1.56(3)
C(2)-N(2)	1.57(3)	C(21)-N(1)	1.52(4)
C(3)-C(4)	1.50(3)	C(22)-N(2)	1.49(3)
C(3)-O(1)	1.46(3)	C(22)-C(23)	1.50(4)
C(4)-C(5)	1.58(3)	C(23)-C(24)	1.59(4)
C(5)-C(6)	1.56(4)	C(24)-C(25)	1.56(4)
C(5)-C(1C)	1.54(3)	C(23)-C(26)	1.49(3)
C(6)-C(7)	1.59(3)	C(26)-N(2)	1.55(3)
C(7)-C(8)	1.49(3)	C(27)-N(1)	1.53(3)
C(8)-C(9)	1.46(3)	C(27)-C(28)	1.57(4)
C(8)-C(14)	1.57(3)	C(28)-C(29)	1.54(4)
C(9)-C(1C)	1.58(3)	C(29)-C(3C)	1.61(4)
C(9)-C(11)	1.51(3)	C(3C)-C(31)	1.44(4)
C(1C)-C(19)	1.48(3)	C(31)-N(1)	1.56(3)
C(11)-C(12)	1.58(3)	C(32)-C(33)	1.51(4)
C(12)-C(13)	1.44(4)	C(32)-O(1)	1.38(3)
C(13)-C(14)	1.58(3)	C(32)-O(2)	1.16(4)
C(13)-C(17)	1.56(3)	C(34)-C(35)	1.56(4)
C(13)-C(18)	1.64(4)	C(34)-O(3)	1.42(3)
C(14)-C(15)	1.50(3)	C(34)-O(4)	1.08(4)

C(15)-C(16)	1.60(3)	C(36)-C1(1)	1.74(5)
C(16)-C(17)	1.59(3)	C(36)-C1(2)	1.70(5)

(b) Valency angles and e.s.d.s ($^{\circ}$).

C(2) C(1) C(10)	116.6(1.7)	C(15)C(16)C(17)	104.3(1.5)
C(1) C(2) C(3)	103.6(1.8)	C(15)C(16)N(1)	112.3(1.7)
C(1) C(2) N(2)	112.7(1.7)	C(17)C(16)N(1)	119.4(1.6)
C(3) C(2) N(2)	114.9(1.7)	C(16)C(17)C(13)	106.5(1.6)
C(2) C(3) C(4)	107.0(1.8)	C(16)C(17)O(3)	113.1(1.8)
C(2) C(3) O(1)	107.8(1.8)	C(13)C(17)O(3)	112.6(1.7)
C(4) C(3) O(1)	105.8(1.7)	C(23)C(22)N(2)	116.2(2.1)
C(3) C(4) C(5)	114.0(1.9)	C(22)C(23)C(24)	108.2(2.1)
C(4) C(5) C(6)	109.1(1.9)	C(23)C(24)C(25)	110.8(2.3)
C(4) C(5) C(10)	109.7(1.7)	C(24)C(25)C(26)	109.5(2.1)
C(6) C(5) C(10)	115.0(2.0)	C(25)C(26)N(2)	113.4(2.0)
C(5) C(6) C(7)	107.4(1.8)	C(28)C(27)N(1)	109.2(1.9)
C(6) C(7) C(8)	109.1(1.8)	C(27)C(28)C(29)	110.6(2.2)
C(7) C(8) C(9)	118.5(2.0)	C(28)C(29)C(30)	106.5(2.3)
C(7) C(8) C(14)	108.8(1.6)	C(29)C(30)C(31)	114.9(2.5)
C(9) C(8) C(14)	106.4(1.7)	C(30)C(31)N(1)	110.5(2.1)
C(8) C(9) C(10)	114.8(1.7)	C(33)C(32)O(1)	108.9(2.4)
C(8) C(9) C(11)	117.0(2.0)	C(33)C(32)O(2)	129.4(2.5)
C(10)C(9) C(11)	110.0(1.7)	O(1) C(32)O(2)	121.5(2.4)
C(1) C(10)C(5)	106.9(1.9)	C(35)C(34)O(3)	101.5(2.5)
C(1) C(10)C(9)	109.8(1.7)	C(35)C(34)O(4)	129.3(3.0)
C(1) C(10)C(19)	112.5(1.8)	O(3) C(34)O(4)	128.5(3.0)
C(5) C(10)C(9)	106.2(1.7)	O(1)C(36)O(2)	116.9(2.5)

C(5) C(10)C(19)	110.3(1.8)	C(3) D(1) C(32)	114.3(1.8)
C(9) C(10)C(19)	110.9(1.9)	C(17)D(3) C(34)	112.0(2.0)
C(9) C(11)C(12)	110.5(1.7)	C(16)N(1) C(21)	110.7(1.8)
C(11)C(12)C(13)	111.8(1.8)	C(16)N(1) C(27)	109.9(1.6)
C(12)C(13)C(14)	110.1(1.9)	C(16)N(1) C(31)	109.2(1.8)
C(12)C(13)C(17)	114.2(1.8)	C(21)N(1) C(27)	105.7(1.9)
C(12)C(13)C(18)	114.9(1.9)	C(21)N(1) C(31)	114.4(1.9)
C(14)C(13)C(17)	100.1(1.6)	C(27)N(1) C(31)	109.9(1.6)
C(14)C(13)C(18)	109.5(1.8)	C(2) N(2) C(20)	108.7(1.8)
C(17)C(13)C(18)	106.9(1.9)	C(2) N(2) C(22)	108.5(1.7)
C(8) C(14)C(13)	112.3(1.6)	C(2) N(2) C(26)	108.9(1.6)
C(8) C(14)C(15)	120.3(1.7)	C(20)N(2) C(22)	115.4(1.8)
C(13)C(14)C(15)	105.0(1.7)	C(20)N(2) C(26)	107.7(1.6)
C(14)C(15)C(16)	100.1(1.6)	C(22)N(2) C(26)	107.5(1.9)

(c) Some relevant intramolecular non-bonded distances (Å).

O(1)....C(20)	3.20(3)
O(1)....C(22)	2.96(3)
O(1)....N(2)	2.96(3)
O(2)....C(4)	3.04(4)
O(3)....C(21)	2.95(4)
O(3)....C(31)	3.02(3)
O(3)....N(1)	2.92(2)
C(3)....C(22)	3.31(3)
C(1)....C(26)	2.88(3)
C(15)...C(27)	2.99(3)
C(17)...C(31)	3.17(3)

(d) Intermolecular distances (\AA) $< 3.60 \text{ \AA}$.

Br(1)...C(31)	I	3.46
Br(1)...C(35)	I	3.56
Br(2)...O(5)	II	3.36
C(22)...Cl(1)	III	3.51
C(29)...Cl(1)	IV	3.48
C(36)...O(5)	V	3.30
O(2)...C(28)	VI	3.56

Roman numerals refer to the following equivalent positions which should be applied to the coordinates of the second atom :-

I	$1/2 + x$	$1/2 - y$	z
II	$-1 + x$	y	z
III	$1 + x$	y	z
IV	$1/2 - x$	$-y$	$-1 + z$
V	$1 - x$	$-1/2 + y$	$1/2 - z$
VI	$1 - x$	$1/2 + y$	$1/2 - z$

Figure 2.1

View of the molecule along the a axis, showing the numbering scheme adopted in the analysis.

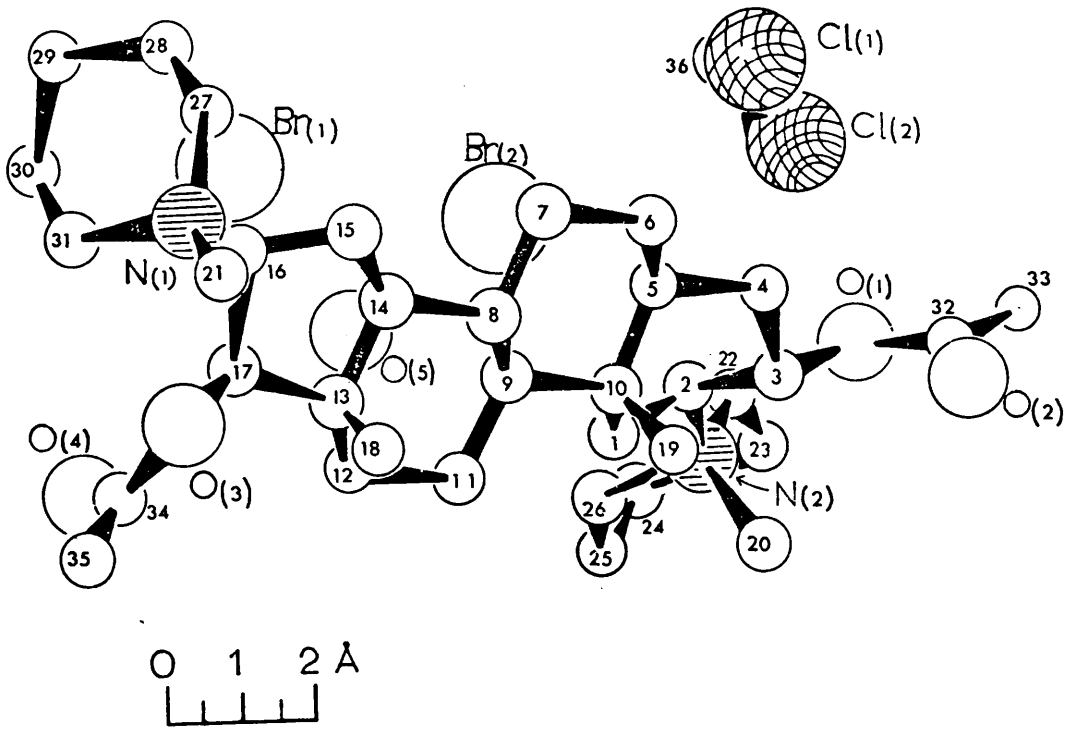
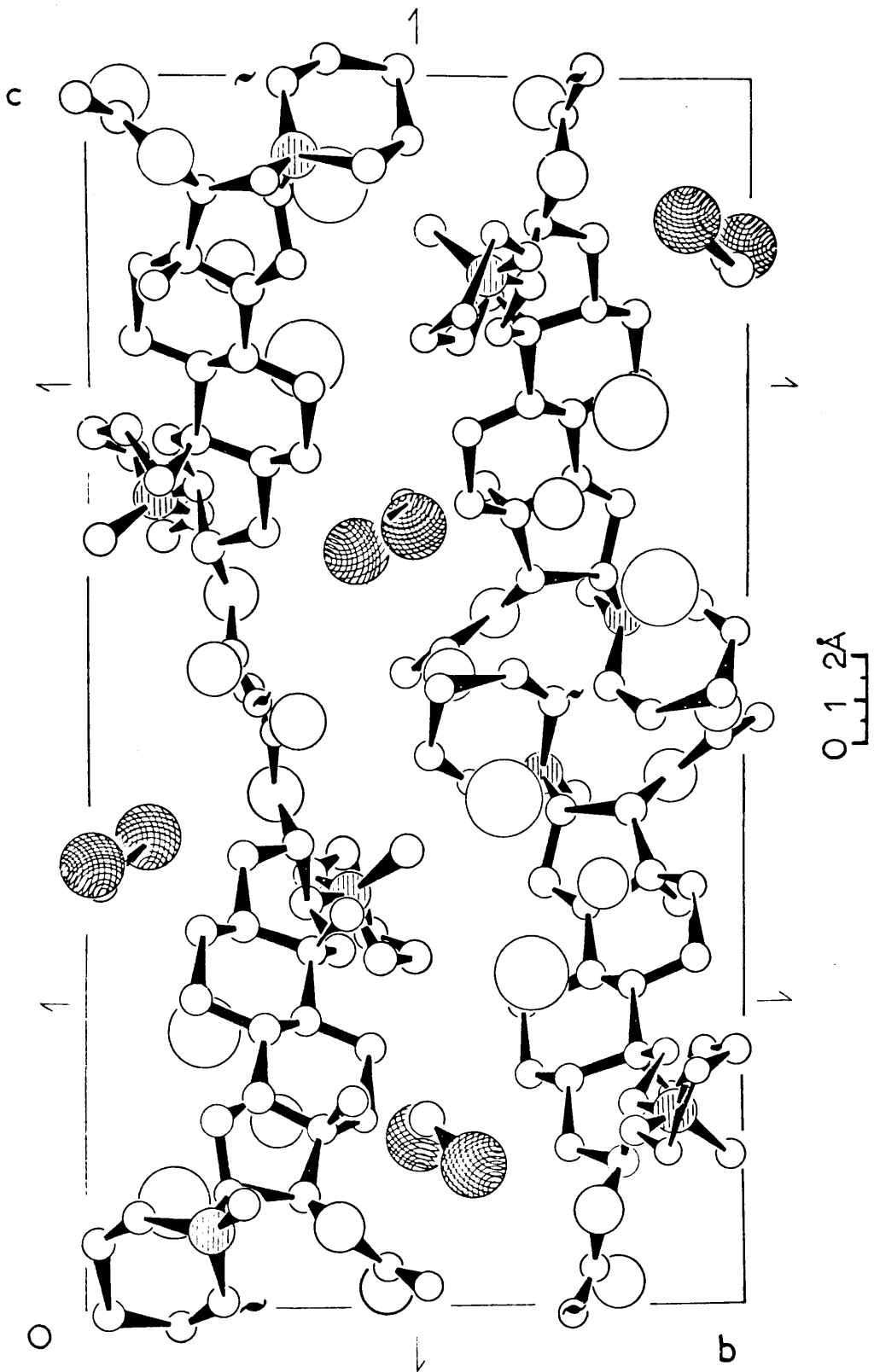


Figure 2.2

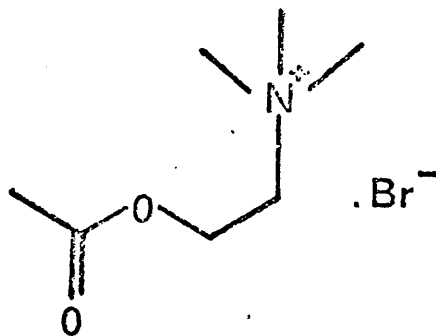
The crystal structure as viewed along the a axis.



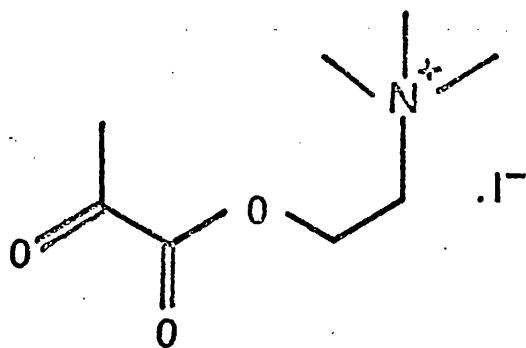
2.6 Discussion.

The clinical importance of pancuronium bromide (I) arises from its effect in cholinergic transmission systems, which is similar to that observed with acetylcholine bromide (II) and lactoylcholine iodide (III). Since pancuronium bromide was synthesised by the incorporation of acetylcholine-like fragments in 5α -androstane (Buckett et al., 1967) it would therefore be of interest to compare the results of this analysis with the previously reported X-ray studies of these latter molecules.

Examination of the interatomic non-bonded distances in pancuronium bromide (I) shows the possibility of hydrogen bonding in the ring A and ring D fragments. Considering the ring A fragment first, it was found that the alcoholic oxygen, O(1), is separated by 3.20 Å and 2.96 Å from the N-carbon atoms C(20) and C(22), respectively, which would indicate the existence of an O(1)...H—C(22) hydrogen bond. The presence of this bond has been previously postulated on the basis of the results obtained for acetylcholine bromide (Canepa, Pauling and Sorum, 1966) and lactoylcholine iodide (Chothia and Pauling, 1968), where the corresponding N-carbon—H...O distances were found to be 3.02 and 2.97 Å respectively.



(II) Acetylcholine bromide



(III) Lactoylcholine iodide

The ring D fragment also exhibits hydrogen bonding but this differs markedly from that observed in the ring A fragment. In this case the alcoholic oxygen, O(3), and the N-carbon atoms, C(31) and C(21), were found to be separated by 3.02 and 2.95 Å, respectively. This would therefore appear to show the presence of two hydrogen bonds of similar strengths to those observed in the ring A fragment and in acetylcholine and lactoylcholine.

Furthermore, it can be seen that such hydrogen bonding, in both ring fragments, will effectively lead to the formation of hetero six-membered rings. For example, in the ring A fragment (and similarly in acetylcholine and lactoylcholine) the involvement of O(1) in a single hydrogen bond results in the formation of such a ring, comprising the atoms O(1)-C(3)-C(2)-N(2)-C(22)-H. Correspondingly, since O(3) is involved in two hydrogen bonds, then two rings may be postulated, involving the atoms O(3)-C(17)-C(16)-N(1)-C(21)-H and O(3)-C(17)-C(16)-N(1)-C(31)-H.

Further evidence to support the existence of these three quasi six-membered rings can be obtained from an examination of the infrared spectrum. Henbest and Lovell (1957), in a study of the infrared spectra of diaxial 3-acetoxy-5-hydroxycholestanes, showed that the hydrogen bonding which takes place between the 5-hydroxyl

group and the alcoholic oxygen of the 3-acetate function, and which results in the formation of quasi six-membered rings, caused an increase of approximately 12cm^{-1} in the stretching frequency of the ester-carbonyl.

In the light of these results, it was therefore expected that a similar effect would be observed in the infrared spectrum of pancuronium bromide. As only quaternary salts would be expected to exhibit this type of hydrogen bonding, and hence the resultant shift in the infrared spectrum, a comparative study of the carbonyl stretching frequencies of the acetoxy groups in a series of quaternised and non-quaternised derivatives of pancuronium bromide was carried out by Savage (1970). The results of this investigation fully confirm the involvement of O(1) and O(3) in hydrogen bonds and, hence, in the proposed quasi six-membered rings. Furthermore, it was found that the shifts observed in the 17-acetoxy frequencies were approximately 30 cm^{-1} while those of the 3-acetoxy group were of the order of 20 cm^{-1} . This would appear to confirm that C(17) is involved in two of the proposed hetero rings whereas the O(1)...C(20) distance does not, in this case, lead to appreciable hydrogen bonding.

A second particular point of interest with regard

to this structural analysis arises as a result of the inclusion of molecules of crystallisation within the crystal structure. The intermolecular non-bonded distances (Table 2.4(d)) indicate that there is a network of hydrogen bonding, involving the bromide ions and the water and dichloromethane molecules, which extends throughout the lattice. Each water molecule is hydrogen-bonded to two bromide ions ($O(5)\dots Br(1) = 3.40 \text{ \AA}$, $O(5)\dots Br(2) = 3.36 \text{ \AA}$) and to a hydrogen of dichloromethane ($O(5)\dots C(36) = 3.30 \text{ \AA}$). There is also the possibility of hydrogen bonding between the dichloromethane and the pancuronium cation ($Cl(1)\dots C(22) = 3.51 \text{ \AA}$, $Cl(1)\dots C(29) = 3.48 \text{ \AA}$).

Much difficulty was experienced in attempting to prepare crystals of pancuronium bromide which did not contain molecules of crystallisation and this involvement, through hydrogen bonding, of such molecules in the crystal structure would obviously provide the explanation for this.

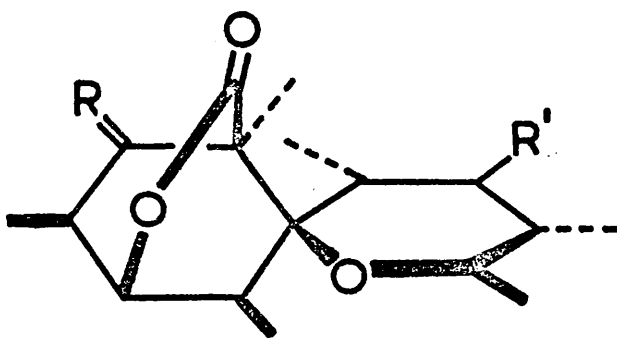
The results of this analysis have shown (*ibid.*) that the clinical potency and specificity of action of pancuronium bromide as a neuromuscular blocking agent are associated with the rigidity of the molecule and, in particular, with the geometries of the two

acetylcholine-like fragments. The ability to form the quasi six-membered rings which have been postulated, both for this molecule and for acetylcholine bromide and lactoylcholine iodide, is obviously of importance with respect to the effects of these molecules in cholinergic transmission systems.

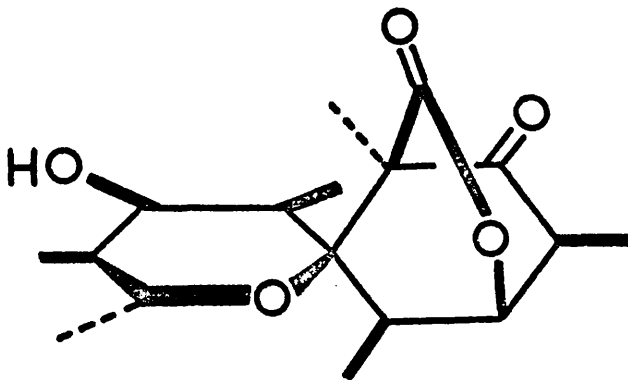
CHAPTER 3THE CRYSTAL STRUCTURE AND ABSOLUTE STEREOCHEMISTRY
OF A HEAVY-ATOM DERIVATIVE OF PORTENTOL.3.1 Introduction.

Portentol is a novel polyketide lactone which has been isolated from *Roccella portentosa* and related lichens by Aberhart, Overton and Huneck (1969, 1970). On the basis of chemical and spectroscopic evidence the optically active molecule was formulated as having the spiro-(2-oxabicyclo-[2,2,2]octane-5,2'-1'-oxacyclohexane) structure (I - I.U.P.A.C. ring numbering convention), with the configurational alternative (V). They also observed a strongly positive ($[\phi]_{227\text{nm.}} +4060^\circ$) Cotton Effect with the dihydroxylactone (III) which, from studies of o.r.d. effects in lactones (Jennings, Klyne and Scopes, 1965), would indicate (I) as being the correct stereochemistry.

Portentol is formally a polypropionate, formed through a polyketide intermediate, whereas previous polypropionates observed in Nature have all been macrolide antibiotics or long chain fatty acids. Furthermore, an investigation of the biosynthesis of portentol acetate (Aberhart, Corbella and Overton, 1970) has revealed that the mechanism by which the polyketide chain is assembled differs in certain important respects from that



- (I) $R = O$ $R' = \alpha CH$
 (II) $R = CH, H$ $R' = \alpha CAc$
 (III) $R = CH, H$ $R' = \alpha CH$
 (IV) $R = p\text{-Br}\cdot C_6H_4\cdot CO\cdot O\text{-}, H$
 $R' = \alpha CAc, H$



(V)

of those previously studied, and hence, in order to put this biosynthetic work on a firm basis, an X-ray analysis of the p-bromobenzoate of the alcohol (II) was undertaken. The results of this study (Ferguson and Mackay, 1970) fully confirmed the constitution and absolute configuration of portentol and established the previously unsupported configuration at C(3).

3.2 Crystal Data.

The crystals were clear-coloured triangular prisms, elongated along the a axis.

$C_{26}H_{33}O_7Br$ $M = 536.9$
 Orthorhombic $a = 8.704 \pm 0.006 \text{ \AA}$,
 $b = 11.065 \pm 0.008 \text{ \AA}$,
 $c = 26.932 \pm 0.018 \text{ \AA}$.

Volume of unit cell = 2593 \AA^3 .

$D_m = 1.34$ (by flotation).

$Z = 4$.

$D_c = 1.38$.

$F(000) = 1120$.

Linear absorption coefficient ($\lambda = 0.71069 \text{ \AA}$), $\mu = 17.3 \text{ cm}^{-1}$.

Absent Spectra : $h00$ when $h = 2n + 1$,
 $0k0$ when $k = 2n + 1$,
 $00l$ when $l = 2n + 1$.

Space Group : $P2_12_12_1$ (D_2^4 , No. 19).

(uniquely determined by systematic absences).

The unit cell parameters were initially established by photographic methods and more accurate values were calculated from the Bragg angles of a number of reflexions, observed on the four-circle diffractometer, using the least-squares orientation matrix program of Dobler and Duerr. The estimated standard deviations were calculated by the same method, using a program written by A. McAdam.

3.3 Intensity Data.

The intensity data were collected on a computer-controlled Hilger and Watts four-circle diffractometer using a small crystal mounted about the a axis on a eucentric goniometer head. The least-squares procedure of Dobler and Duerr was applied to a number of reflexions, whose angular coordinates had previously been refined, in order to obtain the best orientation matrix and cell constants which were consistent with these. The results obtained were then used to calculate the four circle settings for reflexions during the automatic data collection. The integrated intensity of each diffracted beam was measured using an $\omega/2\theta$ scan of 50, 0.01° , steps and a counting time of two seconds at each step. A ten second count at the beginning and end of the scan recorded the background radiation intensity.

A total of 2252 intensity data were collected in the hkl and $hk\bar{l}$ octants of the $Ckl, \dots, 6kl$ reciprocal lattice nets, using $Mo-K\alpha$ radiation ($\lambda = 0.71069 \text{ \AA}$). The equivalent reflexions in the two octants were averaged and Lorentz and polarisation factors applied to give 1327 unique structure amplitudes, 34 of which were unobserved (excluding systematic absences). No corrections were made during the course of the analysis for absorption and extinction effects. The data were

initially put on an approximately absolute scale by making $k\sum|Fo| = \sum|Fc|$, and the scale factor, k , was subsequently refined in the least squares calculations.

3.4 Structure Determination and Refinement.

A three-dimensional Patterson synthesis was computed and, from the positions of the peaks on the Harker sections $U = 1/2$, $V = 1/2$ and $W = 1/2$, which correspond to the vectors between the bromine atoms of the unit cell, the fractional coordinates of the bromine atom were determined :

Br C.000 C.187 C.185

Structure factors were calculated, phased solely on the heavy atom, and an R factor of 0.63 was obtained for the observed reflexions. A Fourier synthesis showed that, as a result of the special position of the bromine atom, the electron-density exhibited perfect pseudo-symmetry in the form of mirror planes at $x = 0$ and $x = 0.5$. No part of the molecule could be identified from this map. Structure factors were then re-calculated, using the improved bromine position obtained in the Fourier, and modified by the use of a weighting function (Sim, 1961) such that the error inherent in the use of the heavy atom phase angles is reduced and the resolution

of the light atoms consequently increased. While the pseudo-symmetry remained, the resolution of the electron-density distribution was sufficiently improved for a set of peaks to be identified as the six carbon atoms of the benzene ring. A structure factor calculation, phased on these seven atoms, reduced the R factor to 0.56 and the resulting electron-density distribution showed a reduction in pseudo-symmetry which allowed a further fourteen atoms of the molecule to be identified.

Seven further cycles of structure factor and Fourier calculations were required before the problems of poor resolution and spurious peaks were overcome and an unambiguous, chemically sensible set of coordinates were derived for the 34 atoms of the asymmetric unit. The R factor at the end of the Fourier refinement stood at 0.25.

Twelve cycles of least-squares calculations were carried out, as detailed in Table 3.1, and Table 3.2 shows the observed and final calculated structure amplitudes and the phase angles. The weighting scheme used was such that

$$\sqrt{w} = \left[\frac{1 - \exp(-p_1 (\sin \vartheta / \lambda)^2)}{1 + p_2 |F_o|} \right]^{1/2}.$$

Unit weights were initially applied, the weighting scheme analysis was examined after each cycle, and the parameters were then adjusted to give constant averages of $w\Delta^2$ for reflexions batched by $|F_o|$ and $\sin \vartheta / \lambda$. The final values of p_1 and p_2 were 50 and 0.01 respectively. The values of the

atomic scattering-factors used in the structure-factor calculations were taken from 'International Tables of Crystallography', Vol. III. Using the final values of the atomic parameters, a three-dimensional difference synthesis was computed and this revealed no errors in the structural model.

Table 3.3(a) lists these final values for the fractional coordinates with their estimated standard deviations and Table 3.3(b) contains the values of U_{ij} , the anisotropic thermal parameters in the general temperature factor expression

$$\exp[-2\pi^2(U_{11}h^2a^{*2} + U_{22}k^2b^{*2} + U_{33}l^2c^{*2} + 2U_{23}klb^*c^* + 2U_{31}lhc^*a^* + 2U_{12}hka^*b^*)].$$

Bond lengths and angles, with their estimated standard deviations in parenthesis, are presented in Table 3.4 along with some relevant intramolecular non-bonded distances and all the intermolecular contacts less than 3.8 Å. Where quoted, standard deviations are in units of the last decimal place. Table 3.5 contains a description of the best mean planes which were calculated, the equations of these planes, and the displacements of selected atoms from them.

Fig. 3.1 was drawn using the Glasgow plotter program and presents the view of the molecule observed down the b axis. The numbering system adopted in the analysis is

indicated in this diagram. The arrangement of the molecules in the unit cell, when viewed down the short a axis, is shown in Fig. 3.2, and Fig. 3.3 is a thermal ellipsoid diagram, drawn by the A.E.R.E. Harwell version of Johnson's ORTEP program. Fig. 3.4 is a representation of the molecule which, it is hoped, will enable an appreciation of the conformational adjustments to be described in section 3.6.

3.5 Absolute Configuration.

The absolute configuration of portental is the same as for the derivative which was used in the analysis and this was determined by the anomalous dispersion method (Bijvoet, 1949). The data were collected in the symmetry-equivalent hkl and $hk\bar{l}$ octants, indexed with respect to a right-handed set of axes (Peerdeman and Bijvoet, 1956). However, since the bromine atom scatters X-radiation anomalously, Freidel's Law will no longer hold and $I(hkl) \neq I(hk\bar{l})$.

Structure factors were calculated for the complete data set, using the complex scattering-curve for bromine ('International Tables of Crystallography', Vol III), and the ratio of the observed intensities was compared with that of the squares of the corresponding calculated

structure factors for each pair of reflexions. This showed that where the former ratio was greater than unity then the latter was consistently less than unity, and vice-versa, indicating that the model which had been used in the analysis, (V), had the wrong configuration. The correct absolute configuration is thus (I), as predicted (Aberhart, Overton and Huneck, 1969 and 1970), and this is shown in Table 3.3 and all drawings of the molecule.

Table 3.1

Progress of Refinement.

Parameters refined	Cycle No.	Final R	Final $w\Delta^2 \times 10^{-4}$	Final R'
x,y,z,Uiso for all atoms (non-hydrogen), full-matrix, unit weights.	1-2	0.210	8.23	0.038
x,y,z,Uiso for all atoms (non-hydrogen), using block-diagonal approximation and weighting scheme.	3-5	0.200	5.42	0.047
x,y,z,with Uij (i,j=1,2,3) for bromine atom and Uiso for other atoms, block-diagonal.	6-11	0.109	1.10	0.015
x,y,z,Uij(i,j=1,2,3) for all atoms (non-hydrogen), block-diagonal.	12-14	0.101	0.96	0.013

where

$$R = \frac{\sum_{hkl} ||F_o| - |F_c||}{\sum_{hkl} |F_o|},$$

$$\Delta = |F_o| - |F_c|,$$

$$R' = \frac{\sum_{hkl} w \Delta^2}{\sum_{hkl} w F_o^2}.$$

Table 3.2

Observed and final calculated values of the structure amplitudes, and the phase angles.

FO				FC				AL				FO				FC				AL							
K	L	F	O	K	L	F	O	K	L	F	O	K	L	F	O	K	L	F	O	K	L	F	O	K	L	F	O
6	7	0	7.6	8.2	20.9	8	0	4	11.7	13.6	18.0	5	2	1	17.0	19.6	30.5	4	5	0	3.9	1.0	0				
6	7	5	7.9	9.3	20.8	8	0	3	14.1	2.5	27.0	5	2	0	11.9	10.7	9.0	4	4	20	15.0	15.0	25.0				
6	7	4	7.0	1.2	19	6	0	2	7.0	3.9	0	5	1	20	12.1	12.7	28.3	4	4	19	1.3	9.9	24.9				
6	7	2	15.1	16.1	19.8	6	0	1	13.0	13.9	9.0	5	1	19	10.1	11.0	9.0	4	4	18	7.9	15.0	51				
6	7	7	8.8	11.1	7.9	5	8	0	10.2	10.8	0	5	1	18	9.2	15.9	25.8	4	4	17	10.2	10.2	23				
6	7	1	9.0	17.3	18.4	5	8	7	3.1	4.8	24.7	5	1	17	13.7	14.9	27.3	4	4	16	10.2	7.0	11.5				
6	7	0	8.5	8.8	18.0	5	8	6	11.7	12.9	2.5	5	1	16	14.3	16.2	5.1	4	4	15	16.2	18.9	16.3				
6	6	10	14.3	11.7	16.9	5	8	5	11.7	11.0	5	5	1	15	12.2	13.1	6.9	4	4	14	11.5	11.0	26.0				
6	6	9	9.1	4.3	15.1	5	8	4	5.8	4.9	7.9	5	1	14	18.6	17.9	25.0	4	4	13	19.2	17.4	8				
6	6	8	1.40	7.8	28.4	5	8	3	4.3	3.0	17.6	5	1	13	13.9	17.1	13.9	4	4	12	21.0	27.3	8.0				
6	6	7	9.0	7.7	25.0	5	8	2	7.8	9.3	35.0	5	1	12	2.6	6.9	31.7	4	4	11	8.4	5.9	39.4				
6	6	6	14.4	13.3	34.3	5	8	1	1.40	5.3	29.3	5	1	11	22.5	24.0	23.2	4	4	10	10.6	13.0	31.1				
6	6	5	8.0	5.9	11.9	5	8	0	1.40	4.2	27.0	5	1	10	29.1	29.8	35.5	4	4	9	14.6	12.0	17.2				
6	6	4	8.2	7.9	35.1	5	7	11	13.5	14.6	22.9	5	1	9	14.1	18.1	6.4	4	4	8	9.7	10.2	1.95				
6	6	3	7.9	8.2	12.7	5	7	10	9.0	7.2	28.6	5	1	8	18.5	15.1	19.8	4	4	7	21.3	23.6	3.6				
6	6	2	11.2	11.9	25.9	5	7	9	1.30	2.0	33.2	5	1	7	8.0	10.0	31.9	4	4	6	14.4	17.4	7.3				
6	6	1	1.9	8.2	32.7	5	7	8	5.2	4.1	24.5	5	1	6	27.4	28.0	11.4	4	4	5	9.1	21.2	18.0	14.3			
6	6	0	9.6	9.1	18.0	5	7	7	17.6	17.2	24.0	5	1	5	11.4	11.4	11.8	4	4	4	20.9	33.0	27.4				
6	5	13	1.40	6.3	10.7	5	7	6	7.9	6.6	27.4	5	1	4	7.7	6.4	26.7	4	4	3	8.8	9.4	31.9				
6	5	12	14.4	9.7	8.2	5	7	5	16.5	14.7	15.7	5	1	3	20.0	20.2	17.8	4	4	2	24.6	28.2	2.1				
6	5	11	11.2	11.7	18.7	5	7	4	10.6	10.1	1.9	5	1	2	39.6	40.7	24.2	4	4	1	32.0	36.2	27				
6	5	10	19.4	19.5	26.9	5	7	3	15.3	16.3	9.2	5	1	1	19.1	21.4	22.0	4	4	0	21.1	23.0	0				
6	5	9	6.8	7.3	5.3	5	7	2	1.30	1.9	3.5	5	1	0	13.1	11.0	9.0	4	3	21	6.4	5.1	19.4				
6	5	8	13.4	10.5	24.7	5	7	1	17.1	15.2	32.2	5	0	20	15.8	13.7	0	4	3	20	19.3	22.7	1.9				
6	5	7	7.0	6.7	14.9	5	7	0	1.30	1.8	27.0	5	0	19	1.30	2.5	9.0	4	3	19	14.6	15.8	17.9				
6	5	6	3.7	6.0	21.9	5	6	14	11.3	11.9	33.0	5	0	18	10.3	9.1	0	4	3	18	10.9	10.0	21.7				
6	5	5	5.6	5.8	3.6	5	6	13	14.4	2.0	5.1	5	0	17	6.0	1.8	27.0	4	3	17	8.2	10.7	35.1				
6	5	4	9.0	5.9	23.8	5	6	12	6.4	9.0	20.7	5	0	16	13.1	12.5	18.0	4	3	16	31.0	30.0	11.0				
6	5	3	10.0	4.8	26.2	5	6	11	18.2	15.4	20.9	5	0	15	19.6	17.9	18.0	4	3	15	13.9	13.0	13.9				
6	5	2	19.2	17.9	8.2	5	6	10	9.7	7.0	11.9	5	0	14	12.0	15.9	0	4	3	14	11.6	15.8	12.4				
6	5	1	21.3	25.4	22.9	5	6	9	9.1	7.7	23.9	5	0	13	27.9	30.9	9.0	4	3	13	6.5	6.5	9.9				
6	4	15	21.0	9	14.3	5	6	8	16.8	15.9	35.5	5	0	12	6.3	0.8	0	4	3	12	24.1	24.9	25.1				
6	4	14	10.2	6.4	30.5	5	6	7	15.6	17.1	3.8	5	0	11	20.8	24.1	9.0	4	3	11	17.5	18.9	25.6				
6	4	13	9.5	11.4	13.8	5	6	6	5.5	7.4	7	5	0	10	17.2	20.9	9	4	3	10	28.4	41.3	8.1				
6	4	12	8.8	4.7	12.8	5	6	5	10.0	13.8	30.0	5	0	9	3.5	2.0	27.0	4	3	9	31.6	31.1	18.0				
6	4	11	6.4	6.5	19.8	5	6	4	4.3	5.3	11	5	0	8	32.4	38.0	0	4	3	8	8.1	8.7	32.4				
6	4	10	17.3	18.3	23.0	5	6	3	15.7	13.0	29.2	5	0	7	20.3	20.7	9.0	4	3	7	7.6	7.4	2.91				
6	4	9	3.4	6.2	3.4	5	6	2	5.6	9.0	8.4	5	0	6	16.7	15.9	18.0	4	3	6	30.7	32.1	23.4				
6	4	8	5.5	4.1	5.8	5	6	1	8.4	5.6	8.3	5	0	5	11.9	11.3	27.0	4	3	5	17.0	19.7	23.8				
6	4	7	13.6	6.9	2.4	5	6	0	9.1	17.0	9.0	5	0	4	16.6	18.4	18.0	4	3	4	23.7	29.9	1.21				
6	4	6	15.3	16.3	7.6	5	5	16	3.1	8.6	10.0	5	0	3	7.1	8.5	27.0	4	3	3	18.3	21.1	13.2				
6	4	5	10.1	13.5	18.0	5	5	15	10.7	11.1	17.0	5	0	2	9.5	6.2	18.0	4	3	2	11.2	12.0	22.6				
6	4	4	19.1	22.0	33.5	5	5	14	1.3	5.0	25.4	5	0	1	4.6	1.8	9.0	4	3	1	29.7	31.2	4.7				
6	4	3	18.3	11.8	11.8	5	5	13	13.3	2.5	15.9	4	9	6	3.9	5.3	0	4	3	0	13.8	13.1	0				
6	4	2	9.9	11.8	6.2	5	5	12	11.7	14.5	32.1	4	9	5	14.1	13.3	25.1	4	2	22	19.0	19.4	24.3				
6	4	1	4.7	2.3	4	5	5	11	8.2	5.8	4.4	4	9	4	12.6	9.1	11.3	4	2	21	18.1	19.7	35.3				
6	3	16	6.5	4.9	36.0	5	5	10	8.3	8.5	16.7	4	9	3	5.8	1.3	30.9	4	2	20	17.2	14.8	5				
6	3	15	19.7	18.4	11.9	5	5	9	12.9	11.1	20.9	4	9	2	15.9	11.1	20.4	4	2	19	23.0	20.0	12.4				
6	3	14	10.6	5.2	30.8	5	5	8	20.4	24.1	28.0	4	9	1	12.0	14.0	5.0	4	2	18	26.1	27.7	1.9				
6	3	13	7.6	4.9	16.9	5	5	7	8.5	6.1	32.3	4	9	0	6.4	6.0	0	4	2	17	19.2	20.6	15.6				
6	3	12	4.7	3.4	5.3	5	5	6	15.8	16.9	4.8	4	8	11	1.40	7.2	32.9	4	2	16	10.1	13.9	11.9				
6	3	11	13.0	10.3	28.3	5	5	5	7.0	4.4	32.4	4	8	10	10.0	11.9	4.6	4	2	15	8.6	10.4	28.8				
6	3	10	16.1	17.8	4.9	5	5	4	3.4	4.2	17.3	4	8	9	10.6	9.8	1.6	4	2	14	13.5	13.2	8.9				
6	3	9	15.6	12.6	17.0	5	5	3	10.0	7.9	18.6	4	8	8	16.2	16.8	1.8	4	2	13	20.9	21.3	9.7				
6	3	8	3.3	7.7	25.8	5	5	2	20.6	20.2	31.0	4	8	7	6.7	8.8	10.9	4	2	12	20.0	28.9	20.1				
6	3	7	9.7	9.0	6.9	5	5	1	6.3	7.0	24.0	4	8	6	9.0	8.5	17.9	4	2	11	14.2	13.4	22.7				
6	3	6	20.9	21.4	23.1	5	4	15	13.7	13.8	2.5	4	8	5	7.1	4.7	24.7	4	2	10	6.8	5.8	13.0				
6	3	5	6.5	5.9	8.1	5	4	17	5.6	4.7	34.1	4	8	4	3	14.9	12.7	4.2	4	2	9	8.1	10.8	11.8			
6	3	4	11.0	14.2	18.0	5	4	16	19.5	21.8	29.8	4	8	3	7.5	5.2	28.2	4	2	8	31.6	33.0	12.8				
6	3	3	9.6	9.5	20.6	5	4	15	16.8	19.9	31.8	4	8	2	7.7	7.7	4.8	4	2	7	32.3	35.9	27.8				
6	3	2	2.6	2.3	28.1	5	4	14	9.5	6.0	17.9	4	8	1	22.0	20.8	18.0	4	2	6	40.2	44.1	33.0				
6	3	1	11.2	19.2	25.0	5	4	13	18.4	21.8	17.1	4	7	15	5.2	9.8	20.1	4	2	5	18.0	17.7	4.2				
6	2	10	10.3	5.3	36.0	5	4	12	9.2	6.4	15.6	4	7	14	12.0	12.1	30.2	4	2	4	14.9	14.6	12.9				
6	2	9	11.2	11.3	10	5	4	11	6.8	7.0	35.4	4	7	13	19.3	18.9	22.6	4	2	3	3.9	11.9	11.9				
6	2	8	8.2	10.6	21.2	5	4	10	5.6	5.1	10.0	4	7	12	12.3	13.3	29.7	4	2	2	21.5	23.7	19.8				
6	2	7	8.5	9.0	2.8</																						

Table with multiple columns and rows containing numerical data. The table is organized into several sections, likely representing different categories or time periods. The columns contain various numerical values, and the rows are indexed from 1 to 42.

M	R	L	FO	FC	AL	M	R	L	FO	FC	AL	M	R	L	FO	FC	AL	M	R	L	FO	FC	AL	
1	5	16.3	19.2	131		1	3	17	21.0	23.0	156	0	9	12	10.0	10.0	270	0	4	19	52.1	61.9	180	
1	5	15.4	9.4	171		1	3	16	9.4	12.4	248	0	9	11	28.8	29.6	270	0	4	14	11.7	11.1	0	
1	5	15.4	15.5	271		1	3	15	15.3	16.9	230	0	9	10	1.3	3.1	90	0	4	13	6.8	6.3	0	
1	5	2	3.7	6.7	322		1	3	14	24.0	25.4	227	0	9	9	22.1	21.8	90	0	4	12	2.3	2.4	360
1	5	25.6	25.9	264		1	3	13	35.9	38.6	23	0	9	8	9.1	5.2	270	0	4	11	19.3	21.9	0	
1	5	12.6	12.9	270		1	3	12	37.3	38.2	17	0	9	7	14.3	18.6	90	0	4	10	19.9	19.3	0	
1	7	19	11.8	11.4	70		1	3	11	65.0	91.6	173	0	9	6	5.3	2.2	90	0	4	9	19.8	24.9	180
1	7	18	11.5	14.0	140		1	3	10	60.0	64.3	169	0	9	5	36.1	36.7	270	0	4	8	2.7	4.0	180
1	7	14	5.7	9.6	165		1	3	9	31.7	31.8	331	0	9	4	13.3	13.4	90	0	4	7	113.1	120.9	0
1	7	16	12.9	10.3	320		1	3	8	21.5	21.6	264	0	9	3	20.3	18.0	90	0	4	6	49.3	51.8	0
1	7	15	8.8	11.7	149		1	3	7	34.2	32.9	52	0	9	2	29.0	21.1	270	0	4	5	84.0	83.9	180
1	7	14	15.8	16.7	314		1	3	6	67.5	71.9	390	0	9	1	11.6	12.7	270	0	4	4	23.1	21.6	0
1	7	13	9.3	14.0	0		1	3	5	108.0	112.0	188	0	8	17	12.0	10.2	180	0	4	3	81.9	85.7	180
1	7	12	26.9	30.0	175		1	3	4	91.5	47.8	166	0	8	16	24.9	23.3	180	0	4	2	23.6	29.3	0
1	7	11	14.9	12.6	194		1	3	3	88.1	92.2	316	0	8	15	1.3	5.2	180	0	4	1	95.1	99.4	0
1	7	10	25.2	24.7	325		1	3	2	76.6	79.2	6	0	8	14	4.6	1.2	360	0	4	0	9.2	14.6	0
1	7	9	11.6	9.9	55		1	3	1	70.8	75.9	156	0	8	13	10.3	7.5	360	0	3	24	9.3	7.5	270
1	7	8	14.3	15.9	197		1	3	0	82.2	82.3	270	0	8	12	9.5	7.9	0	0	3	23	8.9	3.8	270
1	7	7	7.6	14.4	9		1	2	24	25.2	23.9	261	0	8	11	21.2	20.3	0	0	3	22	8.7	6.2	270
1	7	6	27.3	30.6	149		1	2	23	18.0	19.8	311	0	8	10	21.9	24.0	180	0	3	21	22.9	25.0	270
1	7	5	31.1	38.5	177		1	2	22	17.2	20.2	11	0	8	9	1.2	3.1	360	0	3	20	44.5	44.2	90
1	7	4	49.6	55.5	10		1	2	21	8.8	9.5	150	0	8	8	46.7	46.5	0	0	3	19	10.5	9.0	270
1	7	3	12.3	18.0	13		1	2	20	4.9	5.2	167	0	8	7	29.2	27.5	180	0	3	18	16.1	20.4	270
1	7	2	26.3	31.7	234		1	2	19	9.1	8.9	278	0	8	6	1.2	1.8	180	0	3	17	4.8	9.5	270
1	7	1	11.1	11.2	241		1	2	18	27.7	29.5	316	0	8	5	18.3	18.6	180	0	3	16	16.1	22.6	90
1	7	0	30.4	30.7	270		1	2	17	36.8	46.4	279	0	8	4	5.1	5.3	0	0	3	15	23.6	25.6	90
1	6	21	20.7	19.4	281		1	2	16	41.0	44.4	83	0	8	3	9.3	3.1	180	0	3	14	31.1	31.7	90
1	6	20	17.9	15.0	284		1	2	15	29.4	29.8	76	0	8	2	20.4	19.7	0	0	3	13	47.4	50.0	90
1	6	19	12.6	13.5	316		1	2	14	51.2	56.6	263	0	8	1	4.5	3.9	180	0	3	12	85.4	86.8	270
1	6	18	19.0	20.2	267		1	2	13	18.6	19.5	258	0	8	0	29.7	27.1	180	0	3	11	33.8	32.4	270
1	6	17	24.1	24.5	79		1	2	12	19.4	20.9	237	0	7	19	1.4	3.1	90	0	3	10	45.4	46.0	90
1	6	16	23.5	26.0	124		1	2	11	55.3	53.6	211	0	7	18	6.3	6.2	270	0	3	9	43.4	47.2	270
1	6	15	31.2	33.2	258		1	2	10	79.8	76.8	139	0	7	17	20.8	20.6	90	0	3	8	26.7	25.8	270
1	6	14	25.8	23.9	297		1	2	9	19.2	25.4	90	0	7	16	19.9	14.5	90	0	3	7	24.7	31.7	270
1	6	13	16.5	20.5	9		1	2	8	69.4	69.1	247	0	7	15	9.9	2.3	270	0	3	6	18.8	22.8	270
1	6	12	6.0	7.9	380		1	2	7	85.2	87.7	390	0	7	14	1.3	2.5	90	0	3	5	32.5	27.0	270
1	6	11	4.9	8.0	140		1	2	6	69.3	75.9	58	0	7	13	27.6	27.4	270	0	3	4	176.0	184.0	90
1	6	10	27.3	32.0	192		1	2	5	5.6	8.3	133	0	7	12	1.2	4.3	270	0	3	3	30.9	27.4	90
1	6	9	38.2	43.8	253		1	2	4	29.6	20.9	65	0	7	11	29.4	30.5	90	0	3	2	100.7	107.1	270
1	6	8	18.5	20.0	256		1	2	3	71.2	68.5	0	0	7	10	31.3	33.9	90	0	3	1	119.8	109.4	90
1	6	7	34.1	37.8	98		1	2	2	46.0	56.4	292	0	7	9	20.7	20.9	270	0	2	24	11.7	9.6	0
1	6	6	37.2	40.7	74		1	2	1	66.7	100.0	236	0	7	8	20.3	20.2	90	0	2	23	35.8	36.8	180
1	6	5	41.6	45.0	209		1	2	0	95.1	110.8	90	0	7	7	12.7	12.0	270	0	2	22	1.3	2.4	180
1	6	4	27.4	30.6	317		1	1	24	9.2	10.3	120	0	7	6	21.9	23.9	270	0	2	21	8.7	8.3	0
1	6	3	25.1	23.7	233		1	1	23	13.2	11.4	234	0	7	5	32.7	37.1	90	0	2	20	9.3	12.7	0
1	6	2	40.9	42.0	249		1	1	22	24.7	25.7	167	0	7	4	5.7	9.4	270	0	2	19	19.0	16.5	0
1	6	1	51.5	56.2	52		1	1	21	6.6	8.6	2	0	7	3	40.4	44.8	270	0	2	18	22.3	25.6	0
1	6	0	58.2	57.9	90		1	1	20	36.0	37.2	353	0	7	2	3.3	4.8	90	0	2	17	28.1	31.6	180
1	5	22	10.3	8.8	30		1	1	19	19.2	19.8	129	0	7	1	20.2	21.0	90	0	2	16	18.6	18.6	180
1	5	21	23.5	25.0	9		1	1	18	26.8	30.8	228	0	6	21	19.8	19.3	0	0	2	15	10.3	13.4	0
1	5	20	17.7	13.8	147		1	1	17	9.8	12.1	85	0	6	20	4.9	3.3	180	0	2	14	19.2	18.7	360
1	5	19	15.6	16.1	179		1	1	16	7.2	6.8	59	0	6	19	7.6	5.3	180	0	2	13	4.9	2.5	180
1	5	18	12.6	12.6	30		1	1	15	26.1	26.1	179	0	6	18	2.6	1.3	180	0	2	12	13.8	14.8	0
1	5	17	16.5	12.9	67		1	1	14	31.0	35.7	12	0	6	17	40.9	42.9	180	0	2	11	30.1	28.1	180
1	5	16	12.4	12.3	356		1	1	13	88.9	51.7	176	0	6	16	30.5	31.4	0	0	2	10	22.7	23.8	360
1	5	15	10.7	12.9	54		1	1	12	64.9	66.0	155	0	6	15	16.9	21.6	0	0	2	9	57.2	54.9	0
1	5	14	12.9	15.6	264		1	1	11	35.7	36.3	334	0	6	14	11.4	7.3	180	0	2	8	41.6	42.0	0
1	5	13	30.3	32.9	186		1	1	10	79.5	83.0	359	0	6	13	29.6	28.1	180	0	2	7	8.3	8.2	0
1	5	12	30.4	34.0	356		1	1	9	42.4	47.0	233	0	6	12	4.9	3.7	0	0	2	6	96.4	90.8	180
1	5	11	35.1	40.9	14		1	1	8	50.0	42.0	346	0	6	11	8.6	8.1	180	0	2	5	8.7	8.8	90
1	5	10	9.2	11.1	197		1	1	7	56.4	51.1	255	0	6	10	8.4	5.6	360	0	2	4	4.1	10.4	360
1	5	9	31.4	30.4	172		1	1	6	55.7	64.7	166	0	6	9	21.1	19.3	0	0	2	3	124.0	136.4	180
1	5	8	26.4	35.4	266		1	1	5	142.1	154.0	35	0	6	8	19.6	13.5	180	0	2	2	120.4	123.8	0
1	5	7	54.8	59.4	151		1	1	4	108.5	112.4	338	0	6	7	17.4	59.5	180	0	2	1	132.2	157.3	180
1	5	6	45.6	45.3	54		1	1	3	82.2	89.2	167	0	6	6	57.9	61.1	0	0	2	0	94.1	94.8	0
1	5	5	24.2	32.7	339		1	1	2	99.4	104.3	208	0	6	5	20.0	19.4	0	0	1	24	5.9	8.4	270
1	5	4	12.7	14.3	197		1	1																

Table 3.3

(a) Fractional co-ordinates with e.s.d.s.

	x/a	y/b	z/c
Br(1)	-c.47c7(4)	-c.188c(2)	c.6865(1)
O(1)	-c.cC22(14)	c.2c9c(1c)	c.3726(4)
O(2)	-c.2287(14)	c.cC35(11)	c.3224(4)
O(3)	-c.4542(2c)	-c.c9c6(17)	c.319c(6)
O(4)	c.3365(14)	c.1c39(12)	c.4cC1(4)
O(5)	c.2953(17)	c.2863(11)	c.4278(5)
O(6)	c.c368(15)	-c.cC72(11)	c.5c92(4)
O(7)	c.2c77(21)	-c.c367(18)	c.5716(6)
C(1)	c.1cC9(2c)	c.1348(15)	c.4449(6)
C(2)	c.1671(23)	c.c362(16)	c.479c(6)
C(3)	c.2356(22)	-c.c685(17)	c.4483(7)
C(4)	c.26c4(25)	-c.c14c(19)	c.3953(7)
C(5)	c.1c93(21)	c.cC55(16)	c.3679(6)
C(6)	c.c118(2c)	c.c951(14)	c.3978(6)
C(7)	-c.1563(22)	c.c458(15)	c.4c9c(6)
C(8)	-c.2755(2c)	c.c726(15)	c.3694(6)
C(9)	-c.277c(24)	c.2c22(19)	c.3545(7)
C(10)	-c.1224(25)	c.2393(19)	c.3364(7)
C(11)	-c.1c2c(24)	c.3782(18)	c.3295(7)
C(12)	-c.3997(27)	c.2314(2c)	c.3158(8)

C(13)	-C.3337(25)	-C.C711(19)	C.3024(7)
C(14)	-C.2660(25)	-C.1243(19)	C.2548(7)
C(15)	-C.1705(23)	-C.C934(17)	C.4236(7)
C(16)	C.1478(24)	C.C453(17)	C.3123(7)
C(17)	C.3934(27)	-C.1044(21)	C.4712(8)
C(18)	C.2486(23)	C.1863(18)	C.4235(7)
C(19)	C.C192(25)	C.2344(17)	C.4757(7)
C(20)	C.C766(27)	-C.C376(20)	C.5582(8)
C(21)	-C.C655(24)	-C.C775(18)	C.5839(7)
C(22)	-C.C363(30)	-C.1293(21)	C.6337(8)
C(23)	-C.1669(29)	-C.1622(21)	C.6599(8)
C(24)	-C.3086(27)	-C.1447(20)	C.6452(8)
C(25)	-C.3358(27)	-C.C929(21)	C.5985(8)
C(26)	-C.2102(25)	-C.C616(19)	C.5696(7)

(b) Anisotropic thermal parameters and e.s.d.s (\AA^2).

	U_{11}	U_{22}	U_{33}	$2U_{23}$	$2U_{31}$	$2U_{12}$
Br(1)	0.215 3	0.082 1	0.072 1	0.000 3	0.119 4	0.023 4
O(1)	0.064 8	0.075 8	0.038 6	0.004 11	-0.006 12	0.000 16
O(2)	0.060 8	0.067 7	0.049 6	0.009 12	0.006 12	-0.012 14
O(3)	0.112 13	0.145 14	0.108 11	0.095 22	-0.043 22	-0.106 26
O(4)	0.051 8	0.082 9	0.069 8	0.008 14	0.006 14	0.016 15
O(5)	0.092 11	0.052 8	0.092 9	0.002 15	-0.012 16	0.026 16
O(6)	0.068 9	0.085 8	0.037 6	0.000 12	0.005 13	-0.023 16
O(7)	0.113 14	0.178 17	0.082 10	-0.036 24	-0.027 20	0.011 27
C(1)	0.052 12	0.052 10	0.045 10	-0.006 17	-0.001 18	-0.014 19
C(2)	0.055 13	0.068 11	0.058 11	0.018 19	-0.014 21	-0.008 22
C(3)	0.059 14	0.060 11	0.067 11	-0.015 20	0.008 21	0.004 23
C(4)	0.059 14	0.079 12	0.067 12	0.019 21	-0.002 23	-0.002 23
C(5)	0.059 14	0.066 11	0.051 11	-0.016 19	-0.012 19	-0.006 22
C(6)	0.043 12	0.057 10	0.048 9	0.006 16	-0.009 19	0.023 20
C(7)	0.036 13	0.079 11	0.044 10	0.018 18	0.003 20	0.004 20

C(8)	C.C44 12	C.C7C 1C	C.C38 1C	-C.CC3 17	C.C1C 18	C.CC6 2C
C(9)	C.C79 15	C.C85 13	C.C65 13	C.C12 24	C.CC4 23	-C.C18 27
C(10)	C.C83 16	C.C73 13	C.C73 13	C.C41 22	C.C27 23	C.C19 25
C(11)	C.C84 15	C.C71 12	C.C6C 12	C.C37 21	-C.CC9 22	-C.CC8 24
C(12)	C.C56 17	C.113 15	C.C89 14	C.C85 26	C.C36 27	-C.C32 27
C(13)	C.C78 15	C.C86 13	C.C7C 13	-C.C11 24	C.CC2 25	C.C16 26
C(14)	C.C71 15	C.C87 13	C.C63 13	C.C35 22	C.C26 24	C.C16 24
C(15)	C.C59 13	C.C63 11	C.C62 11	C.CC5 2C	-C.CC9 21	-C.C12 23
C(16)	C.C77 15	C.C85 12	C.C52 12	-C.C42 22	-C.C28 24	-C.CC3 23
C(17)	C.C9C 18	C.C89 16	C.C91 15	-C.C14 26	C.C36 27	C.C55 3C
C(18)	C.C74 14	C.C68 12	C.C65 12	C.CC6 23	C.C14 21	C.CC3 24
C(19)	C.C98 15	C.C68 12	C.C51 11	-C.C12 2C	C.C11 22	-C.CC8 25
C(20)	C.C96 17	C.C85 14	C.C76 14	-C.C11 24	-C.CC8 26	C.CC8 27
C(21)	C.C67 14	C.C74 12	C.C67 12	-C.C1C 21	-C.CC7 22	-C.CC2 25
C(22)	C.C99 18	C.1C6 16	C.C88 16	-C.C37 27	-C.C1C 3C	-C.C13 31
C(23)	C.114 17	C.1C1 16	C.C69 15	C.CC9 27	C.C39 28	-C.C1C 31
C(24)	C.12C 17	C.C66 15	C.C82 15	-C.C15 26	C.C33 27	-C.C17 29

c(25)	c.109 17	c.c79 15	c.c77 14	-c.c07 25	c.c43 28	c.c04 29
c(26)	c.c66 16	c.c92 13	c.c68 13	c.c32 24	c.c17 24	c.c02 26

Table 3.4

(a) Bond lengths and e.s.d.s (Å).

Br(1)-C(24)	1.86(2)	C(4)-C(5)	1.52(3)
O(1)-C(6)	1.44(2)	C(5)-C(6)	1.53(2)
O(1)-C(1C)	1.47(2)	C(5)-C(16)	1.59(3)
O(2)-C(13)	1.34(2)	C(6)-C(7)	1.59(3)
O(2)-C(8)	1.53(2)	C(7)-C(8)	1.52(2)
O(3)-C(13)	1.16(3)	C(7)-C(15)	1.59(2)
O(4)-C(18)	1.35(2)	C(8)-C(9)	1.49(3)
O(4)-C(4)	1.47(2)	C(9)-C(1C)	1.49(3)
O(5)-C(18)	1.18(2)	C(9)-C(12)	1.53(3)
O(6)-C(2C)	1.41(2)	C(1C)-C(11)	1.56(3)
O(6)-C(2)	1.48(2)	C(13)-C(14)	1.53(3)
O(7)-C(2C)	1.2C(3)	C(2C)-C(21)	1.49(3)
C(1)-C(18)	1.52(3)	C(21)-C(26)	1.33(3)
C(1)-C(2)	1.54(2)	C(21)-C(22)	1.48(3)
C(1)-C(19)	1.55(3)	C(22)-C(23)	1.39(3)
C(1)-C(6)	1.55(2)	C(23)-C(24)	1.31(3)
C(2)-C(3)	1.54(3)	C(24)-C(25)	1.4C(3)
C(3)-C(17)	1.56(3)	C(25)-C(26)	1.39(3)
C(3)-C(4)	1.56(3)		

(b) Bond angles and e.s.d.s ($^{\circ}$).

C(6) O(1) C(1C)	125.1(1.3)	C(6) C(7) C(15)	116.7(1.5)
C(13)O(2) C(8)	117.2(1.4)	C(9) C(8) C(7)	112.6(1.5)
C(18)O(4) C(4)	112.7(1.5)	C(9) C(8) O(2)	105.1(1.3)
C(2C)O(6) C(2)	113.9(1.5)	C(7) C(8) O(2)	107.6(1.3)
C(18)C(1) C(2)	100.2(1.4)	C(8) C(9) C(1C)	110.2(1.7)
C(18)C(1) C(19)	109.0(1.5)	C(8) C(9) C(12)	113.2(1.7)
C(18)C(1) C(6)	102.5(1.3)	C(1C)C(9) C(12)	110.6(1.7)
C(2) C(1) C(19)	111.0(1.4)	O(1) C(1C)C(9)	111.3(1.5)
C(2) C(1) C(6)	118.3(1.4)	O(1) C(1C)C(11)	102.9(1.5)
C(19)C(1) C(6)	114.2(1.4)	C(9) C(1C)C(11)	114.5(1.8)
O(6) C(2) C(1)	105.8(1.4)	O(3) C(13)O(2)	125.0(1.9)
O(6) C(2) C(3)	110.4(1.4)	O(3) C(13)C(14)	126.9(2.0)
C(1) C(2) C(3)	111.0(1.4)	O(2) C(13)C(14)	108.1(1.7)
C(2) C(3) C(17)	108.6(1.5)	O(5) C(18)O(4)	118.9(1.8)
C(2) C(3) C(4)	104.7(1.5)	O(5) C(18)C(1)	127.1(1.8)
C(17)C(3) C(4)	109.8(1.6)	O(4) C(18)C(1)	113.9(1.6)
O(4) C(4) C(5)	107.8(1.5)	O(7) C(2C)O(6)	121.1(2.0)
O(4) C(4) C(3)	109.0(1.4)	O(7) C(2C)C(21)	130.9(2.0)
C(5) C(4) C(3)	112.2(1.6)	O(6) C(2C)C(21)	107.7(1.8)
C(4) C(5) C(6)	108.3(1.4)	C(26)C(21)C(22)	118.5(1.9)
C(4) C(5) C(16)	108.2(1.5)	C(26)C(21)C(2C)	127.9(1.8)
C(6) C(5) C(16)	115.5(1.4)	C(22)C(21)C(2C)	113.3(1.9)

O(1) C(6) C(5)	111.5(1.3)	C(23)C(22)C(21)	115.0(2.1)
O(1) C(6) C(1)	100.4(1.2)	C(24)C(23)C(22)	125.4(2.2)
O(1) C(6) C(7)	108.2(1.3)	C(23)C(24)C(25)	119.4(2.2)
C(5) C(6) C(7)	112.8(1.3)	C(23)C(24)Br(1)	119.7(1.7)
C(5) C(6) C(1)	109.7(1.4)	C(25)C(24)Br(1)	120.9(1.8)
C(1) C(6) C(7)	113.6(1.3)	C(26)C(25)C(24)	118.2(2.1)
C(8) C(7) C(6)	115.3(1.4)	C(21)C(26)C(25)	123.4(1.9)
C(8) C(7) C(15)	108.0(1.4)		

(c) Some intramolecular non-bonded distances (Å).

Br(1)...C(23)	2.75	O(6)...C(7)	3.23
Br(1)...C(25)	2.85	O(6)...C(15)	3.08
O(1)...C(1)	2.30	O(6)...C(17)	3.44
O(1)...C(5)	2.45	C(1)...C(3)	2.54
O(1)...C(8)	2.82	C(1)...C(4)	2.53
O(1)...C(11)	2.37	C(1)...C(5)	2.52
O(1)...C(16)	2.76	C(2)...C(5)	3.05
O(1)...C(19)	2.80	C(2)...C(7)	3.39
O(2)...C(5)	3.19	C(2)...C(15)	3.59
O(2)...C(16)	3.32	C(3)...C(7)	3.79
O(4)...C(3)	2.47	C(3)...C(15)	3.60
O(4)...C(5)	2.42	C(5)...C(8)	3.43
O(4)...C(17)	3.04	C(5)...C(15)	3.06
O(5)...C(19)	2.79	C(6)...C(9)	3.01
O(6)...C(3)	2.48	C(7)...C(19)	3.15
O(6)...C(6)	3.21	C(10)...C(16)	3.23

(d) Intermolecular contacts ($< 3.8 \text{ \AA}$).

Br(1)...C(11)	I	3.64	O(5)...C(20)	III	3.72
Br(1)...C(14)	II	3.66	O(7)...C(11)	III	3.59
O(3)...C(23)	II	3.35	C(18)...C(19)	III	3.70
O(3)...C(22)	II	3.42	O(3)...C(4)	IV	3.33
O(5)...C(26)	III	3.05	O(3)...O(4)	IV	3.57
O(5)...C(19)	III	3.26	O(3)...C(16)	IV	3.78
O(5)...C(21)	III	3.46	O(4)...C(8)	V	3.49
O(5)...O(6)	III	3.64	O(4)...C(12)	V	3.52
O(5)...C(25)	III	3.65	O(4)...C(9)	V	3.74

The Roman numerals refer to the following transformations applied to the coordinates found in Table 3.3, the transformation is applied to the second atom of each pair.

I	$1/2 + x,$	$1/2 - y,$	$1 - z;$
II	$1/2 + x,$	$-1/2 - y,$	$1 - z;$
III	$-1/2 + x,$	$1/2 - y,$	$1 - z;$
IV	$1 + x,$	$y,$	$z;$
V	$-1 + x,$	$y,$	$z;$

Table 3.5

Mean molecular planes.

Plane no.	Displacements of atoms defining plane (Å)							
1	O(1)	C.C2	C(7)	-C.C2	C(8)	C.C2	C(1C)	-C.C2
2	C(4)	C.C3	O(4)	-C.C5	C(18)	C.C2	O(5)	C.C2
					C(1)	-C.C2		
3	O(4)	-C.C2	C(5)	C.C2	C(6)	-C.C2	C(18)	C.C2
4	O(4)	-C.C7	C(2)	-C.C7	C(3)	C.C6	C(18)	C.C8
5	C(1)	C.C7	C(2)	-C.11	C(3)	C.1C	C(4)	-C.C6
6	C(1)	C.CC	C(4)	C.CC	C(5)	C.CC	C(6)	C.CC
7	O(2)	-C.C3	C(3)	C.CC	C(8)	C.C2	C(13)	-C.C1
					C(14)	C.C2		
8	O(6)	C.C2	O(7)	C.C1	C(2)	-C.C1	C(2C)	-C.C2
					C(21)	C.CC		
9	Br(1)	-C.C1	C(21)	C.CC	C(22)	-C.C2		
	C(23)	C.C2	C(24)	C.C1	C(25)	C.CC		
					C(26)	C.CC		

Plane no. Displacements of out-of-plane atoms (Å)

1	C(6)	C.45	C(9)	-C.65
2	C(2)	-1.35	C(3)	-1.23
	C(5)	1.33	C(6)	1.3C
3	C(1)	-C.77	C(4)	-C.7C
4	C(1)	C.82	C(4)	C.67

Plane equations

Plane no.	P	Q	R	S	rms D
1	-0.4300	-0.6407	-0.6361	-11.6383	0.022
2	0.4681	0.2607	-0.8444	-6.0487	0.028
3	0.0043	0.6021	-0.7984	-7.8613	0.023
4	0.8011	-0.1031	-0.5895	-1.7730	0.069
5	0.8560	-0.4713	-0.2127	3.3806	0.087
6	-0.4079	0.7581	-0.5088	-8.1596	0.002
7	0.3852	0.7497	-0.5382	-0.4975	0.017
8	-0.1411	-0.9393	-0.3128	-5.4199	0.018
9	-0.0003	-0.9128	-0.4085	-5.6471	0.013

In this table P, Q, and R are the direction cosines of the plane normal, S is the plane to origin distance and rms D is the root mean square deviation in Å of the atoms defining the plane from the plane.

The plane equation is thus

$$PX + QY + RZ = S$$

where X, Y and Z are coordinates in Å, referred to the orthogonal axes a, b and c.

Figure 3.1

View of the molecule along the b axis, showing the numbering scheme adopted in the analysis.

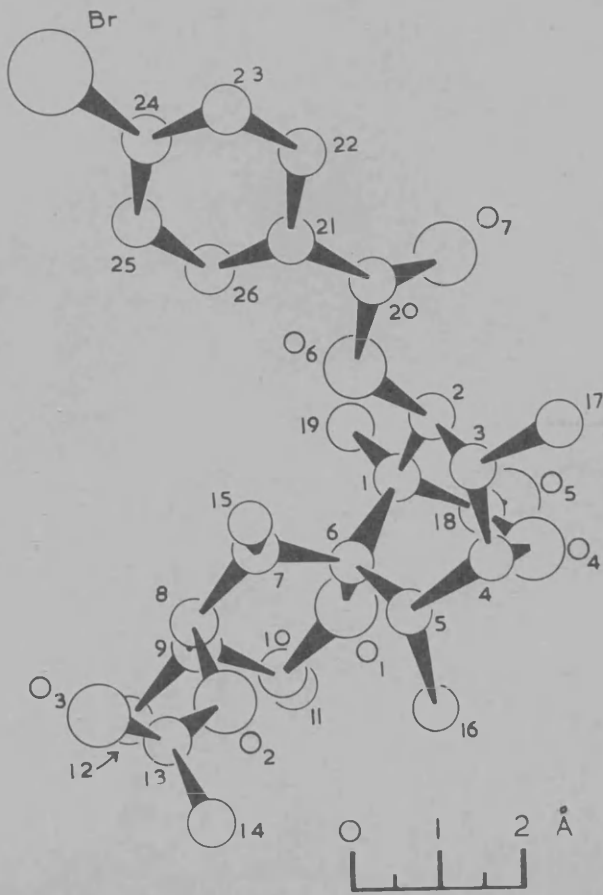


Figure 3.2

A molecular-packing diagram viewed along the a axis.

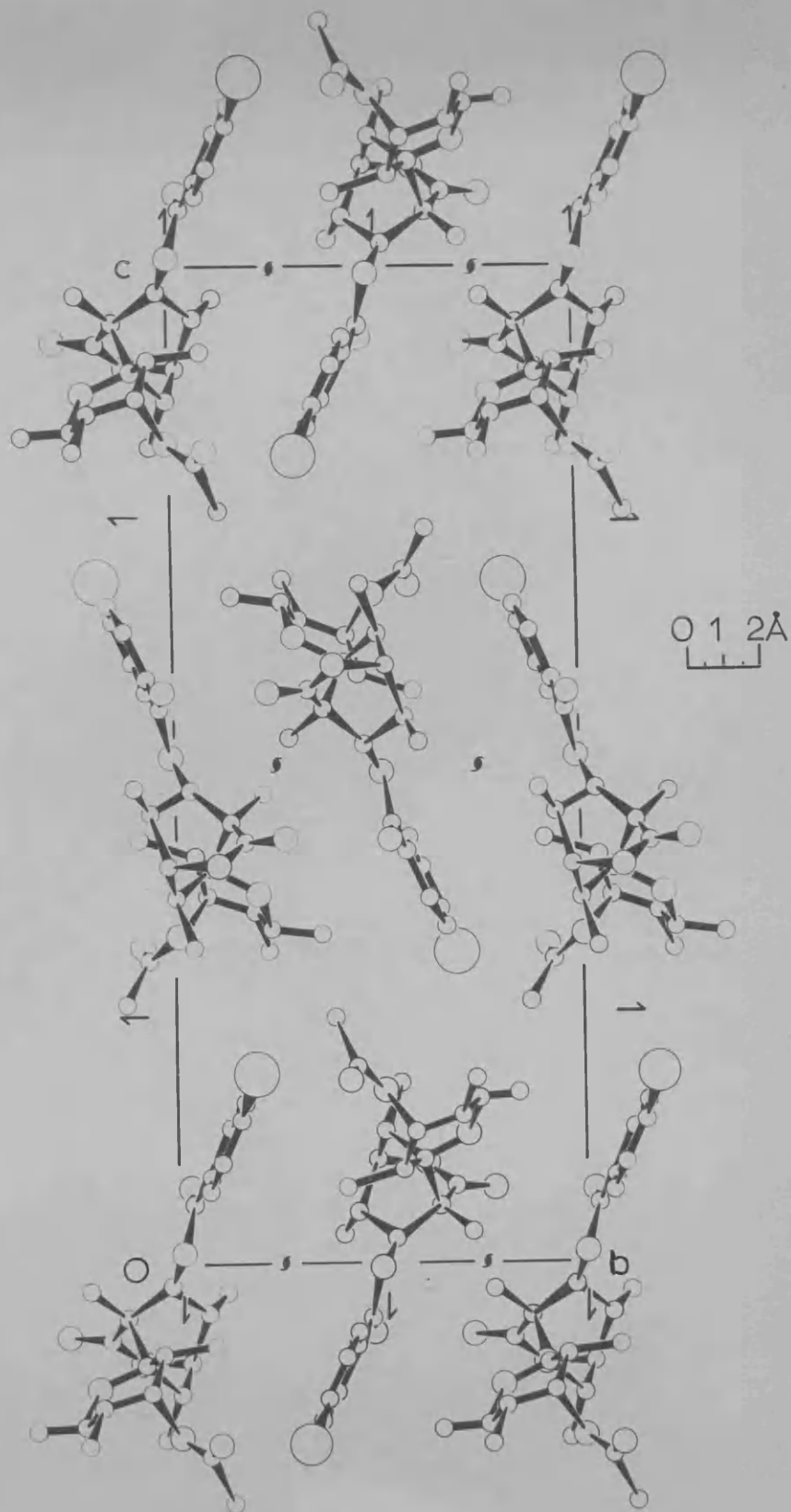


Figure 3.3

A stereoscopic view of the molecule, showing thermal ellipsoids of 50% probability.

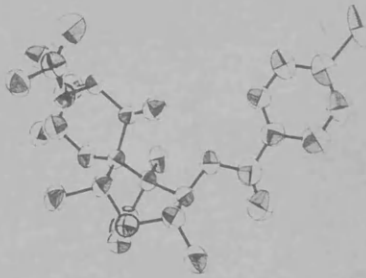
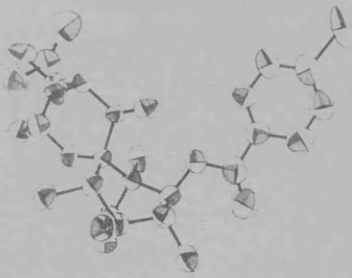
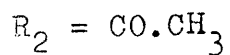
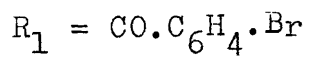
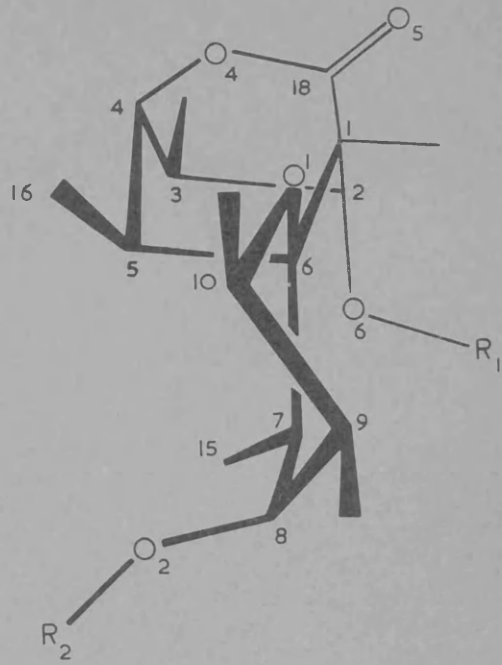


Figure 3.4

A representation of the molecule, showing the conformation adopted as a result of the steric interactions.





3.6 Discussion.

The X-ray analysis of the p-bromobenzoate derivative (IV) has confirmed the structure and absolute stereochemistry of the alcohol (II) and hence verifies the deduction of Aberhart, Overton and Huneck (1969, 1970) that the absolute configuration of portentol is that shown in (I).

Studies have been undertaken of the "in vivo" synthesis of portentol acetate and, whereas previous investigation of linear polypropionates showed that these were formed by incorporation of intact propionate units into the chain, it has now been established that portentol acetate is formed by uniform incorporation of acetate or malonate, both as starter and propagator units. With the structure of portentol unambiguously established, these results have been used to postulate a mechanism for its biosynthesis (Aberhart, Corbella and Overton, 1970).

The molecular framework of portentol consists of a tetrahydropyran ring joined at a spiro-centre to an oxabicyclo(2,2,2)octane system, where a δ -lactone group forms one of the bridges. However, the substituents attached to this skeleton, both in portentol itself and more particularly in the derivative used in the X-ray analysis, introduce a high degree of molecular overcrowding

and the conformation of the molecule is correspondingly adjusted to minimise these unfavourable non-bonded interactions (Fig 3.4).

In considering the derivative (IV), interactions between the substituents of the two rings are centred in two regions of the molecule, arising from compression between (i) O(6) and C(15), (ii) O(2) and C(5), and (iii) C(10) and C(16). These sets of interactions are minimised, firstly, by rotation of the tetrahydropyran ring about the C(5)-C(6) vector and a flattening of this ring at the spiro-carbon atom. O(1), C(7), C(8) and C(10) form the seat of the chair and C(6) is held close to the best plane through these four atoms (Table 3.5, equation 1), at a distance of 0.45 Å, as a result of its position at the junction of the tetrahydropyran and oxabicyclo(2,2,2)octane rings. C(9) is also forced closer to this plane, and lies at a distance of -0.65 Å from it. Lambert, Keske and Weary (1967) have found, from an analysis of vicinal coupling constants, that the conformation of tetrahydropyran should be very close to that of a perfect chair, and, for cyclohexane rings in the chair form and with tetrahedral valence angles, the distance of the out-of-plane atoms from the seat was shown to be 0.73 Å by Sim (1965).

In the same paper there is also established a mathematical relationship between the displacement of atoms from the mean plane of a regular six-membered ring in the chair conformation and the values of the corresponding bond angles, and it is of interest to compare these with the results of the present analysis. For a displacement of 0.64 Å the predicted average valence angle is 112° , and our values of 112.6 , 110.2 and 111.3° for angles C(9)-C(8)-C(7), C(8)-C(9)-C(10) and O(1)-C(10)-C(9) do not differ significantly from this. The O(1)-C(6)-C(7) and C(8)-C(7)-C(6) bond angles were found to be 108.2 and 115.3° respectively and the C(6)-O(1)-C(10) angle of 125.1° is significantly greater (seven e.s.d.s) than the values of 117.3 and 115.2° found for the corresponding angle in the two glucose residues of cellobiose (Jacobson, Wunderlich and Lipscomb, 1961).

Within the context of the tetrahydropyran ring alone, the valence angle at the spiro-carbon centre remains anomalously small. However, an examination of the orientation of the ring provides an explanation for this. In the undistorted molecule the O(6)...C(15) distance would be approximately 1.5 Å (as measured on a Dreiding model). The detected flattening of the tetrahydropyran ring and the twisting of the bridged

lactone ring would only increase the distance to 2.3 Å, whereas the actual separation was found to be 3.08 Å. This is achieved by a rotation of the tetrahydropyran ring around the C(5)-C(6) axis, resulting in values of 118.3, 113.6, 116.7 and 100.4° for the angles C(2)-C(1)-C(6), C(1)-C(6)-C(7), C(6)-C(7)-C(15) and C(1)-C(6)-O(1) respectively, and -10.9° for the torsion angle O(1)[C(6),C(5)]C(16). Therefore, as a consequence of this and of the constraints placed on C(6), the O(1)-C(6)-C(7) angle is reduced in order to minimise the resulting strain.

The unfavourable non-bonded interactions are also reduced, as mentioned earlier, by adjustment of the conformation of the bridged lactone system. Previous X-ray analyses (Mathieson, 1963, and references therein) have established that the lactone group is planar and the deviations from the best mean plane through C(4), O(4), O(5), C(18) and C(1) confirm this in the case of the portentol derivative (Table 3.5, equation 2). Values of 1.18, 1.35, and 1.47 Å for the O(5)-C(18), C(18)-O(4) and O(4)-C(4) bonds are in good agreement with previous results, both for esters and for lactones, showing the existence of an important contribution to the bonding from the resonance form $\begin{array}{c} \text{---} \text{C} = \text{O}^+ \text{---} \\ | \\ \text{O}^- \end{array}$ (for example, see Asher and Sim, 1965).

The δ -lactone is constrained to form a boat conformation with C(5) and C(6), and also with C(2) and C(3) and this was indicated by a carbonyl absorption frequency in the infrared (solution) of 1776 cm^{-1} (Cheung, Overton and Sim, 1965). The ring C(1)-C(18)-O(4)-C(4)-C(5)-C(6) forms an undistorted boat with C(4) and C(1) displaced 0.70 and 0.77 \AA respectively above the mean plane through C(6), C(5), O(4) and C(18); none of the latter atoms show a significant deviation from this plane, and C(5) and C(6) are displaced by 1.33 and 1.30 \AA from the lactone plane (Table 3.5, equations 2 and 3).

In order to alleviate the repulsion between O(6) and C(15), the C(2)-O(6) bond rotates in an exo-direction, causing the second δ -lactone ring, C(1)-C(18)-O(4)-C(4)-C(3)-C(2), to adopt a skew-boat conformation. This is shown in Table 3.5, equations 2 and 4. The mean plane through O(4), C(18), C(2) and C(3) is such that C(3) and C(18) have a significant displacement (0.06 and 0.08 \AA) above it, and O(4) and C(2) below (0.07 \AA). Furthermore, the displacement from the lactone plane is found, for C(3), to be 1.23 \AA and for C(2), 1.35 \AA . The best mean planes were calculated through atoms C(1), C(2), C(3), C(4) and through atoms C(1), C(5), C(6), C(4) (Table 3.5, equations 5 and 6) and, while it can be seen that there

is no significant deviation of atoms from the plane of the latter, those of the former confirm the twisting of the boat. This results in a value of $+18.5^\circ$ for the torsion angle $C(1)[C(2),C(3)]C(4)$ compared with the values of $+7.1$ and 0.3° found for the corresponding torsion angles $C(1)[C(18),O(4)]C(4)$ and $C(1)[C(6),C(5)]C(4)$.

The adjustments described above give rise to the solid-state conformation established by the X-ray analysis and this is further defined by the following intramolecular distances (Table 3.4(c)) : C(15) to (i) O(6), 3.08 Å (ii) C(2), 3.59 Å (iii) C(3), 3.60 Å (iv) C(5), 3.06 Å - and for C(16) to (i) O(1), 2.76 Å (ii) C(10), 3.23 Å and (iii) O(2), 3.32 Å.

In Table 3.5, equations 7, 8 and 9 show the two ester groups and the p-bromobenzene moiety to be planar, as would be expected. The bond lengths found in the analysis do not deviate significantly from accepted values (Sutton, 1965). All of the intermolecular contacts less than 3.8 Å are listed in Table 3.4(d). Two of the oxygen-carbon distances are significantly shorter than the corresponding van der Waals distance of 3.4 Å (Pauling, 1960) but it is very unlikely that any hydrogen bonding is involved in either case.

The structure of portentol differs mainly from that

of the derivative (IV) in the presence of the carbonyl oxygen at C(2) instead of the p-bromobenzoate group. Although the O(6)...C(15) interaction will be considerably reduced, it will still remain effective, and thus the conformational changes found in the derivative (IV) would also be expected, although to a lesser degree, in portentol (I).

CHAPTER 4THE EVALUATION OF ABSORPTION EFFECTS IN A DATA-REDUCTION PROGRAM.4.1 Introduction.

The object of this chapter is to describe a suite of programs which was developed to meet the growing requirements of the Glasgow crystallography group. These requirements were that, in view of the excellent data-collection equipment available, more effective use should be made of the diffraction data in order to allow the finer details of molecular structures to be investigated.

The effects of absorption and extinction of the X-ray beam were identified as being the two largest possible sources of error in the data and, as a result of this, data-reduction programs were written to apply corrections for the former effect and to provide parameters which would allow the latter effect to be dealt with at a later stage in the analysis.

In view of the nature of the structures studied by this group, and the facilities currently available to us, the Gaussian integration method was deemed to be the most suitable approach to absorption correction. A routine for the application of this procedure to

diffraction data has been detailed by Coppens (1965) and the crystallography group at Boston University kindly provided us with a FORTRAN IV listing of the version which they were developing for the IBM System/360.

This was translated into KDF9 ALGOL and subsequently modified to take advantage of the features available, both in the language and with the Glasgow University KDF9 computer, on which it was to be implemented. Data-reduction procedures were then designed around this routine to enable its integration with the Glasgow crystallography programs.

4.2 The Absorption Correction.

The absorption of X-radiation by crystalline material is due, mainly, to the photoelectron process and the classical absorption equation gives the relationship

$$I = I_0 \exp(-\mu t) \quad (1)$$

where I and I_0 are the intensities of the diffracted and incident beams respectively, t is the path length of the beam through the absorbing medium, and μ is the linear absorption coefficient. This latter term applies to a specific monochromatic radiation and material, and is calculated from the expression

$$\mu = G \sum_n P_n (\mu/\rho)_{\lambda, n}$$

where G is the density of the medium, P_n is the fraction by weight of element n , and $(\mu/\rho)_{\lambda,n}$ is the mass absorption coefficient of element n for radiation of wavelength λ . Thus the intensity of the diffracted beam is reduced, as a result of absorption, according to equation (1).

In considering diffraction by a crystal, it can be seen that the path lengths of the components of the incident beam will be unequal, so that (1) must be integrated over all of these paths in the volume of the crystal. If the transmission factor for a reflexion, A_{hkl} , is defined as the ratio of the observed diffracted intensity to the intensity which would be observed in the absence of absorption, then it can be shown (e.g. Buerger, 1960) that integration over the crystal volume, V , leads to the expression

$$A_{hkl} = \frac{\int_V e^{-\mu t} dV}{V} \quad . \quad (2)$$

In order to apply an absorption correction, therefore, the factor A_{hkl} must be computed and applied to the observed intensity, I_{obs} , to obtain the corrected diffraction intensity, I_{corr} ; so that

$$I_{corr} = I_{obs} / A_{hkl} \quad .$$

In practice it is sometimes found convenient to use the absorption factor, A_{hkl}^* , where $A_{hkl}^* = 1/A_{hkl}$, and hence

$$I_{\text{corr}} = A_{\text{hkl}}^* I_{\text{obs}} .$$

There are a number of methods for evaluating A_{hkl} and these vary in accuracy and generality of application.

(a) Correction for cylindrical crystals.

The integral (2) can be evaluated for the case of a perfect cylinder and tabulated values of the data required for this calculation are available in "International Tables for X-ray Crystallography", Vol. II. The use of this method requires accurate shaping of a suitable crystal and also a high length-to-diameter ratio in order to reduce the end-effect (where there is far less absorption).

(b) Correction for spherical crystals.

For a perfect sphere, A_{hkl} is a function of the Bragg angle, θ , only and thus the correction is comparatively simple. Tabulated values of A_{hkl}^* (ibid.) show, however, that there is a rapid variation in this factor with R (where R is the radius of the sphere), especially at low θ values, and it has been shown, as a result of this, that slight departures from ideal sphericity will lead to substantial errors in the absorption correction (Jeffery and Rose, 1964). There is also the major disadvantage that a small spherical crystal is extremely difficult to orientate crystallographically.

It should be remembered, in considering (a) and (b),

that accurate shaping of a crystal is extremely difficult and often undesirable, as in the case of very small crystals or crystals to be used in neutron diffraction work.

(c) The graphical method for a general correction.

In this approach (Albrecht, 1939; Evans, 1952; Rogers and Moffett, 1956) the crystal is divided into small volume elements and the exponential term (2) is evaluated, for each of these elements, by measurement of the path lengths on a scaled-up drawing. The required correction is thus the sum of all of these terms, divided by the number of volume elements. As this procedure must be repeated for each reflexion, it is obviously not well suited to three-dimensional analyses.

(d) Electronic computational methods for a general correction.

The preceding approximations were developed because, although the theory of absorption corrections has been exactly known for some considerable time, the tremendous number of calculations required has, until recently, been prohibitive in the direct evaluation of the absorption integral. Direct computation of the corrections for a crystal of arbitrary shape is obviously far more preferable and, with the increasing speed and storage capacity of electronic digital computers, this can now be readily achieved.

In order to evaluate the required corrections one must calculate the absorption for the actual path length travelled within the crystal by the incident beam, reflecting from each infinitesimal portion of the crystal. The result is then integrated over the entire volume of the crystal, and this requires a precise description of the crystal envelope.

Busing and Levy (1957) first described a program for the accurate high-speed computation of absorption corrections in which they used the Gaussian quadrature procedure, to be described later, to carry out the numerical evaluation of the absorption integral. Subsequently this method has been used by Coppens et al., (1965), Wuensch and Prewitt, (1965), and Ahmed and Singh, (1970).

A totally different approach is the analytical method first proposed for the relatively simple two-dimensional case by Howells (1950), and later extended to three dimensions by De Meulenaer and Tompa, (1966). This procedure (*ibid.*, see also Alcock, 1970) divides the crystal into a number of elementary polyhedra, within which the path length is a linear function of the coordinates of the volume element. For each of the polyhedra the contribution to the total transmission factor can be obtained, and the sum of these, divided by the crystal

volume, gives an analytical evaluation of the integral (2).

This method will always give an exact value for the absorption correction whereas the accuracy of the numerical approach is proportional to the number of grid points employed, and consequently converges towards the analytical result as the grid is made finer (Coppens et al., 1967). Furthermore, the computational time per reflexion in the analytical method is constant while with the numerical procedure the time, core storage requirements, and hence the expense, will increase in direct relation to the number of grid points.

The point at which the results of the two methods converge will obviously depend on the absorbing power of the crystal (i.e. the crystal dimensions and the value of the linear absorption coefficient) and, in cases of extreme absorption, the convergence has been reported to be very erratic and prohibitively expensive (Coppens et al., *ibid.*).

Thus, in considering the practical application of the two methods, it will be apparent that, while the analytical method is superior for heavily absorbing crystals, the numerical method produces results of satisfactory accuracy faster and cheaper for crystals showing generally high transmission factors. Coppens (1970)

has studied the performance of the two methods in the calculation of the corrections for a crystal of γ, γ' -dipyridyl dihydrate and has shown that the numerical method is the faster of the two in the calculation of transmission factors greater than 75%, where an accuracy greater than 1% is required, and greater than 56%, where an accuracy better than 2% is required.

The absorption effect in diffraction data is generally so large that even the use of a crude approximation is preferable to the complete omission of any correction (Buerger, 1960). Jeffery and Rose (1964) have discussed the tendency to underestimate errors due to absorption, and show that these are usually greater than the errors involved in the measurement of intensities, either by photographic or diffractometer techniques. This rule will apply, for example with Cu-K_{α} radiation, to organic crystals containing atoms heavier than oxygen and with dimensions greater than 0.1 mm. Absorption corrections can be ignored for crystals having dimensions less than 0.5 mm. when Mo-K_{α} radiation is used, but it is well worth noting that for organic bromides the errors appear to be almost as large as with Cu-K_{α} radiation.

The application of absorption corrections to diffraction data can be expected to affect the structural

model as follows -

- i) scale and thermal parameters should shift their values, depending on the size of the correction, since these have been compensating for the errors in the data
- ii) positional parameters should not alter significantly, unless the crystal has a non-centrosymmetric cross-section
- iii) the values of the estimated standard deviations should show a large reduction.

4.3 The Gaussian Integration Method of Absorption Correction.

The Gaussian method of numerical integration, applied to the evaluation of the integral (2), gives the approximation

$$A_{hkl} = \iiint_V \frac{1}{V} \exp(-\mu \bar{T}) dV \quad (3)$$

$$\sum_{i=1}^m \sum_{j=1}^m \sum_{k=1}^m (x_{\max} - x_{\min})(y_{\max}(x_i) - y_{\min}(x_i))$$

$$(z_{\max}(x_i, y_j) - z_{\min}(x_i, y_j)) R_i R_j R_k \left(\frac{1}{V} \exp(-\mu \bar{T}) \right).$$

where \bar{T} is the mean path length of the beam through the crystal. The other terms in the expression are explained in the corresponding expression for the triple integral in Appendix 1. The use of this approximation therefore reduces (2) to a form which can be evaluated by a computer. A number of different approaches have been used in the practical application of this method and the one to be

described in this section is that of Coppens (1965) which makes extensive use of vector and matrix algebra.

A three-dimensional grid is set up in the crystal along a set of axes, for example the crystallographic axes a, b and c, such that the position of the grid points will minimise the difference between the exact value of the absorption integral and the approximation (3) being used to evaluate it. The fractional coordinates of the grid points along the internal a axis, x_i , are then selected such that

$$x_i = x_{\min} + (x_{\max} - x_{\min})v_i \quad i = 1, \dots, m_a,$$

where m_a is the number of points along the a axis, and v_i is the Gaussian constant referred to in Appendix 1. The maximum and minimum x coordinates along the axis, x_{\max} and x_{\min} , are defined by the vertices of the crystal and hence are determined by solving the equations of the faces. The point of intersection of any three of the faces must either be a vertex or else lie outwith the crystal, and thus, by finding the coordinates of the true crystal vertices, the values of x_{\max} and x_{\min} can be established.

For each value of x_i , the values of y_{\max} and y_{\min} are found, and hence the fractional coordinates, y_j , of the grid points along the b axis are given by

$$y_j = y_{\min}(x_i) + (y_{\max}(x_i) - y_{\min}(x_i))v_j \quad j = 1, \dots, m_b$$

Finally, the upper and lower limits of the z coordinates, for given values of x_i and y_j , are used to determine the grid coordinates on the z axis, where

$$z_k = z_{\min}(x_i, y_j) + (z_{\max}(x_i, y_j) - z_{\min}(x_i, y_j)) v_k$$

$$k = 1, \dots, m_c$$

Thus it can be seen that the coordinates (x_i, y_j, z_k) will define a non-isometric grid with $(m_a \times m_b \times m_c)$ grid points which must, by definition, lie within the crystal. In practice it has been found that this method causes the grid points to accumulate near the surface of the crystal, where the change in absorption with path length is greatest. As a result of this, it has been shown (Lanczos, 1956) that, in order to achieve the same degree of accuracy in carrying out the integration over an isometric grid, one must use eight times as many grid points as with the Gaussian method. As the computation time of the correction factor is approximately proportional to the number of grid points employed, the use of a non-isometric grid represents not only a very considerable advantage but also, on most third-generation computers, the difference between practicality and impracticality.

A weighting factor is calculated for each grid point, which is proportional to the volume element represented by that point, and this has the value

$$R_i \times R_j \times R_k \times (z_{\max}(x_i, y_j) - z_{\min}(x_i, y_j)) \\ \times (y_{\max}(x_i) - y_{\min}(x_i)) \times (x_{\max} - x_{\min}).$$

Having determined the coordinates of the grid points and their associated weights, the value of the function

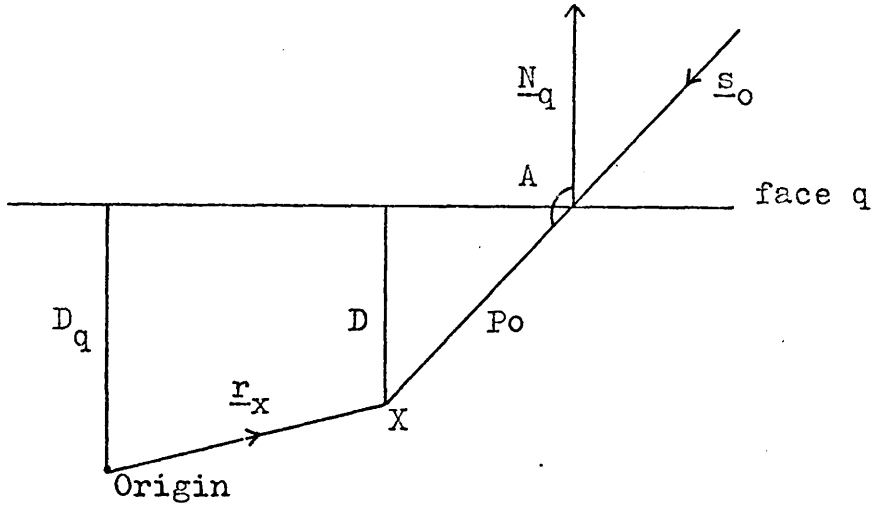
$$\frac{1}{V} \exp(-\mu \bar{T}) \quad (4)$$

must be calculated at each of these points. The direct-space components of the unit vectors \underline{s}_0 and \underline{s} , which correspond to the direction of the incident and diffracted beams respectively, are required for this and these can be obtained by a straightforward application of crystallographic vector theory. The details of this have been fully described by Coppens (1965) for the case of three-circle diffractometer, Weissenberg and precession camera geometry, and thus will not be repeated here. It should be noted in passing, however, with respect to this latter paper, that the components for the three-circle diffractometer case are derived, in part, from the expressions

$$\underline{T.b} = T_2 b^2 + T_3 b c \cos \alpha \\ \text{and} \quad \underline{T.c} = T_2 b c \cos \alpha + T_3 c^2,$$

without the negative sign which appeared in the paper.

The expression (4) involves the quantity \bar{T} and this is derived from the individual distances travelled by the components of the beam within the crystal, with respect to



If P_o is the distance which the beam, entering through face q , must travel to reach the grid point X , then

$$P_o = - \frac{D}{\cos A} = - \frac{D_q - \underline{r}_x \cdot \underline{N}_q}{\underline{s}_o \cdot \underline{N}_q},$$

where D is the perpendicular distance of the point X from the face q , and D_q is the perpendicular distance of the origin from the face q .

By analogy, if P is the distance which the beam travels from X to the face of exit, then

$$P = \frac{D}{\cos B}$$

Figure 4.1

each point on the Gaussian grid. Crystal faces, through which it is permissible for the beam to enter or exit, are first of all determined from the relationships

$$\underline{s}_o \cdot \underline{N}_q = \cos A \quad \text{and} \quad \underline{s} \cdot \underline{N}_q = \cos B ,$$

where \underline{N}_q is a unit vector, the face normal of the crystal face q , A is the angle between the incident beam vector and the face normal, and B is the angle between the diffracted beam vector and the face normal. Hence all crystal faces through which the beam can enter must have angle A obtuse and those through which the beam may leave will correspondingly have angle B acute. For a grid point X , defined by the radius vector \underline{r}_x , the distances P_o and P are easily derived (Fig. 4.1). Presented with a number of permissible faces of entry and exit, one therefore determines the corresponding values of P_o and P and chooses the smallest positive values of both to be the true distances travelled within the crystal by the beam, with respect to the grid point X .

For the volume element represented by this point on the grid, function (4) therefore has a value

$$\exp(-\mu(P_o + P))$$

and if R represents the associated weighting factor, then

$$R \exp(-\mu(P_o + P))$$

represents the contribution of the volume element to the

transmission factor. Hence if the value of this expression is calculated for each grid point, by repetition of this procedure, then the sum of these terms will be the required transmission factor, A_{hkl} , for a single reflection.

An average data set for a three-dimensional crystal structure analysis will contain somewhere between one thousand and six thousand data items and the procedure for the evaluation of (4) must be repeated for each one of these in order to obtain data which is fully corrected for the effects of absorption. At first appearances, therefore, the preceding method would not appear to be particularly practical. It is, however, ideally suited to the digital computer since, in essence, it consists of a series of iterative procedures which computers are very efficient in handling. The extremely large number of calculations involved for each reflection, and the fact that the Gaussian grid, once established, must be held in main memory, makes such a routine expensive in terms of computer time and core store usage. However this applies to all methods of absorption correction for three-dimensional data, and for accurate structure determinations there is no doubt that it is justified.

4.4 A Description of the Programs.

The data-reduction package which has been developed consists of four programs, which will be referred to as programs AT, A0, A1, and A2. Basic input to all of the programs consists of the cell dimensions and an orientation matrix, such that the axis of alignment of the crystal is either \underline{a} or \underline{a}^* . If absorption corrections are required then the linear absorption coefficient, the Miller indices of the crystal faces, and the perpendicular distances (in cm.) of these faces from an arbitrarily chosen origin must also be specified.

Program AT

The function of this program is to present the user, who wishes to correct for absorption, with information which will enable him to choose the optimum size of Gaussian grid for his requirements. This will obviously depend on a number of factors - the size and shape of the crystal, the extent of absorption, the degree of accuracy required and the computing time available.

Six reflections are chosen to represent the conditions which the user wishes to test, for example high and low-order axial reflections. The program will then set up a series of 64 Gaussian grids, with dimensions varying from $4 \times 4 \times 4$ to $16 \times 16 \times 16$, and, for each one in turn, will

calculate and print

- (a) the time taken to compute the grid coordinates and weights,
- (b) the transmission factor for each of the six reflections,
- (c) the time required to calculate (b).

During a data-reduction run on the computer, the time taken to calculate the transmission factors, using this set of programs, will account for approximately 90% of the total computing time and has been found to be proportional to the product of m_a , m_b and m_c . For an average size of grid, for example $8 \times 8 \times 8$, this is of the order of 8 seconds per reflection and thus it is obviously desirable to keep the grid size as small as is consistent with accurate results. The analysis presented by this program allows the selection of a grid size which represents the best compromise between a realistic time of computation and the point at which the transmission factors converge.

Program A0

This is a data-reduction program for use with the KDF9 computer, operating in a multiprogramming mode. Input consists of the data to be reduced and a series of flags which specify the various input, processing and output options required by the user. These are as follows :

- (a) Input options.

Input can be intensity data, i.e. h,k,l and Iobs,

obtained from a Weissenberg or precession camera, or from a three-circle diffractometer. In the latter case the standard deviations of the intensities and phi angles of the axial reflections should also be included. The data consists of single or multiple batches with corresponding scale factors. If absorption corrections are required the dimensions of the Gaussian grid must be given.

(b) Processing options.

These consist of

- i) calculation of transmission factors for the absorption correction (as detailed in section 4.3), with a maximum grid size of $8 \times 8 \times 8$,
- ii) calculation of spot-shape correction factors for upper-level Weissenberg data (after Phillips, 1954),
- iii) application of the specified batch scale factors,
- iv) calculation of the mean path length for the later correction of isotropic extinction,
- v) calculation of the components of the normalised vectors \underline{N} and \underline{D} for the later correction of anisotropic extinction in type 1 crystals,
- vi) calculation of the Lorentz, polarisation and rotation factors.

(c) Output options.

Currently, output is on two media. The line printer

lists full details of the corrections calculated for each reflection and a punched tape is produced which contains the output data in a suitable format for input to any program which may follow. As well as h, k, l and the structure amplitude this tape can carry

- i) the isotropic extinction parameter,
- ii) the anisotropic extinction parameters,
- iii) a batch number calculated to the user's specifications.

For three-circle diffractometer data the user may also specify the minimum acceptable value for a calculated structure amplitude, in terms of the standard deviation, below which the reflection will be treated as unobserved.

Programs A1 and A2

In the absorption correction routine the coordinates and weights of all of the grid points must be resident in main storage, and this represents a very heavy demand on even a large computer's storage capacity. The use of an $8 \times 8 \times 8$ grid, for example, means that 2Kwords must be reserved to store the grid alone, and with the additional storage required by the program, and for the program itself, it is just possible to fit program A0 into the extent of core allocated on KDF9 for multiprogramming.

This size of grid, however, would prove restrictive to the crystallographer with a heavily absorbing crystal.

A grid of dimensions $16 \times 16 \times 16$ requires 16Kwords of storage for its coordinates and represents the largest size of grid which the KDF9 could comfortably handle. To overcome these excessive storage requirements program A0 was divided into two parts - program A1 performs the calculation of the grid coordinates and weights and stores them on disk, and program A2 evaluates the various corrections involved in processing the intensity data.

The actual routines are identical to those in program A0 and since these two programs require the entire partition available to ALGOL users on KDF9 they should only be used in cases where a grid with more than 512 points is necessary.

A listing of programs A1 and A2 is given in Appendix 2.

The absorption correction routine in the programs was initially translated literally from FORTRAN IV to ALGOL to facilitate debugging and testing. Some considerable effort was then applied to optimising both the ALGOL coding and the procedural logic within some of the subroutines, notably the subroutine LENGTH which, as mentioned previously, accounts for a very large proportion of the computation time. This resulted in an approximately 35% decrease in

the calculation time of the transmission factors, making the application of the programs viable on KDF9 in the case of average-sized data sets.

Tests of the routine, carried out on data previously processed by the Boston University group, showed no significant deviations (less than 0.0002%) in the values of the transmission factors calculated by the two versions. Further comparative tests were then carried out with Busing and Levy's ORABS absorption correction program which also uses the Gaussian grid technique but evaluates the function (4) in a slightly different manner, employing the direction cosines of the X-ray beam rather than the vector technique described previously. Some discrepancies (of less than 1%) occurred between the values calculated by the two programs and after further testing these were attributed to the different methods employed to define the crystal envelope. In ORABS this is defined by determining the equations of the faces, whereas in the Coppens routine the indices of the faces and lengths of the face normals from an origin are used. Which of these methods is the more accurate has not yet been resolved.

REFERENCES.

- D.J.Aberhart, K.H.Overton and S.Huneck, (1969),
J.Chem.Soc. (D), 162.
- D.J.Aberhart, A.Corbella and K.H.Overton, (1970),
J.Chem.Soc. (D), 664.
- D.J.Aberhart, K.H.Overton and S.Huneck, (1970),
J.Chem.Soc. (C), 1612.
- F.R.Ahmed and P.Singh, (1970), "Crystallographic
Computing", ed. F.R.Ahmed, Munksgaard, Copenhagen.
- G.Albrecht, (1939), Rev.Sci.Instr., 8, 324.
- N.W.Alcock, (1970), "Crystallographic Computing",
ed. F.R.Ahmed, Munksgaard, Copenhagen.
- J.D.M.Asher and G.A.Sim, (1965), J.Chem.Soc., 1584.
- J.M.Bijvoet, (1949), Proc.Acad.Sci.Amst., 52, 313.
- W.R.Buckett, C.L.Hewett, F.A.Marwick and D.S.Savage, (1967),
Chim.Therap., 2, 186.
- M.J.Buerger, (1960), "Crystal Structure Analysis",
J.Wiley and Sons Inc., New York.
- W.R.Busing and H.A.Levy, (1957), Acta Cryst., 10, 180.
- F.G.Canepa, P.Pauling and H.Sorum, (1966), Nature, 210, 907.
- K.K.Cheung, K.H.Overton and G.A.Sim, (1965),
Chem.Comm., 634.
- C.Chothia and P.Pauling, (1968), Nature, 219, 1156.
- P.Coppens, L.Leiserowitz and D.Rabinovich, (1965),
Acta Cryst., 18, 1035.

- P.Coppens, J.DeMeulenaer and H.Tompa, (1967),
Acta Cryst., 22, 601.
- P.Coppens, (1970), "Crystallographic Computing",
ed. F.R.Ahmed, Munksgaard, Copenhagen.
- C.A.Coulson and C.W.Haigh, (1963), Tetrahedron, 19, 527.
- P.Davis and P.Rabinovich, (1956), J.Res.Nat.Bur.Stands.,
56, 35.
- J.DeMeulenaer and H.Tompa, (1965), Acta Cryst., 19, 1014.
- H.T.Evans, (1952), J.Appl.Phys., 23, 663.
- G.Ferguson and I.R.Mackay, (1970), J.Chem.Soc. (D), 665.
- D.D.Fitts and J.G.Kirkwood, (1955), J.Am.Chem.Soc., 77, 4940.
- V.T.Hahn, (1958), Acta Cryst., 11, 825.
- H.B.Henbest and B.J.Lovell, (1957), J.Chem.Soc., 1965.
- F.H.Herbstein and G.M.J.Schmidt, (1954), J.Chem.Soc., 3302.
- F.L.Hirschfeld, S.Sandler and G.M.J.Schmidt, (1963),
J.Chem.Soc., 2108.
- R.G.Howells, (1950), Acta Cryst., 3, 366.
- R.A.Jacobson, J.A.Wunderlich and W.N.Lipscomb, (1961),
Acta Cryst., 14, 598.
- J.W.Jeffery and K.M.Rose, (1964), Acta Cryst., 17, 343.
- J.A.D.Jeffreys, (1968), private communication.
- J.P.Jennings, W.Klyne and P.Scopes, (1965), J.Chem.Soc.,
7211.
- W.Klyne, (1965), "The Chemistry of Steroids", Methuen,
London.

- J.B.Lambert, R.G.Keske and D.K.Weary, (1967),
J. Am. Chem. Soc., 89, 5921.
- C.Lanczos, (1956), "Applied Analysis", Prentice Hall Inc.,
Englewood Cliffs, N.J.
- A.N.Lowan, N.Davids and A.Levenson, (1942),
Bull. Amer. Math. Soc., 48, 739.
- A.O.McIntosh, J.M.Robertson and V.Vand, (1952),
Nature, 169, 322.
- A.O.McIntosh, J.M.Robertson and V.Vand, (1954),
J. Chem. Soc., 1661.
- I.R.Mackay, J.M.Robertson and J.G.Sime, (1969),
J. Chem. Soc. (D), 1470.
- H.Margenau and G.M.Murphy, (1943), "The Mathematics of
Physics and Chemistry", Van Nostrand, New York.
- R.H.Martin and D.Bogaert-Verhoogen, (1967),
Tet. Letters, 3045.
- R.H.Martin, M.Flammang-Barbieux and J.Nasielski, (1967),
Tet. Letters, 743.
- R.H.Martin, (1968), private communication, see also -
R.H.Martin, M.Flammang-Barbieux, J.P.Cosyn and M.Gelbcke,
(1968), Tet. Letters, 3507.
- R.H.Martin and M.Deblecker, (1969), Tet. Letters, 3597.
- R.H.Martin, N.Defay, H.P.Figeys, M.Flammang-Barbieux,
J.P.Cosyn, M.Gelbcke and J.J.Schurter, (1969),

Tetrahedron, 4985.

R.H.Martin, G.Morren and J.J.Schurter, (1969),

Tet. Letters, 3683.

R.H.Martin and J.J.Schurter, (1969), Tet. Letters, 3679.

R.H.Martin, (1970), private communication.

A.McL.Mathieson, (1963), Tet. Letters, 81.

R.S.Mulliken, (1952), J.Am.Chem.Soc., 74, 811.

K.Nakamoto, (1952), J.Am.Chem.Soc., 74, 1739.

M.S.Newman, W.B.Lutz and D.Lednicer, (1955),

J.Am.Chem.Soc., 77, 3420, see also

O.E.Weigang, J.A.Turner and P.A.Trouard, (1966),

J.Chem.Phys., 45, 1126,

M.S.Newman, R.S.Darлак and L.Tsai, (1967),

J.Am.Chem.Soc., 89, 6191,

Fitts and Kirkwood, (1955),

Coulson and Haigh, (1963),

Herraez Zarza and Sanchez, (1965),

R.H.Martin, (1967 onwards),

and references therein.

M.S.Newman and D.Lednicer, (1956), J.Am.Chem.Soc., 78, 4765.

M.S.Newman and J.Blum, (1964), J.Am.Chem.Soc., 86, 5600.

L.Pauling, (1960), "The Nature of the Chemical Bond",

Cornell University Press, Ithaca, New York.

A.F.Peerdeeman and J.L.Bijvoet, (1956), Acta Cryst., 9, 1012.

- D.C.Phillips, (1954), Acta Cryst., 7, 746, see also
D.C.Phillips, (1956), Acta Cryst., 9, 819.
- D.R.Pollard, (1968), Ph.D. Thesis, University of Glasgow.
- C.K.Prout and J.D.Wright, (1968), Angew. Chem. Internat.
Edit., 7, 659.
- W.Rhodes and M.F.A.El-Sayed, (1962), J.Mol.Spec., 9, 42.
- J.M.Robertson, (1943), J.Sci.Instr., 20, 175.
- D.Rogers and R.H.Moffett, (1956), Acta Cryst., 9, 1037.
- D.S.Savage, A.F.Cameron, G.Ferguson, C.Hannaway and
I.R.Mackay, (1970), J.Chem.Soc. (C), in press.
- G.A.Sim, (1961), "Computing Methods and the Phase Problem",
eds. R.Pepinsky, J.M.Robertson and J.C.Speakman,
Pergamon Press, Oxford.
- G.A.Sim, (1965), J.Chem.Soc., 5974.
- G.Stulen and G.J.Visser, (1969), J.Chem.Soc. (D), 965.
- L.E.Sutton, (1965), "Tables of Interatomic Distances and
Configurations in Molecules and Ions", Special
Publication No. 18, The Chemical Society, London.
- J.Trotter, (1963), Acta Cryst., 16, 605.
- G.Tunell, (1939), Amer.Min., 24, 448.
- B.J.Wuensch and C.T.Prewitt, (1965), Z.Krist., 122, 24.
- H.Wynberg and M.B.Groen, (1968), J.Am.Chem.Soc., 90, 5338.
- M.A.Herraez Zarza and F.Sanchez, (1965),
Anales Real Soc. españ., Fis. Quim., 61B, 953.

APPENDIX 1.

The Gaussian Quadrature Method of Numerical Integration.

The method of approximate quadratures, applied to $\int_a^b f(x) dx$, replaces the function $f(x)$ with a function $g(x)$, where $g(x)$ can be evaluated in a simple way. If $f(x)$ is known to have $(n + 1)$ values, $y_0, y_1, y_2, \dots, y_n$, at $(n + 1)$ points within the interval a, b then the integral of $g(x)$ can be expressed as

$$\int_a^b g(x) dx = A_0 y_0 + A_1 y_1 + A_2 y_2 + \dots + A_n y_n,$$

where the A_i are constants, independent of y_i . Hence,

$$\int_a^b f(x) dx = \sum_{i=0}^{i=n} A_i y_i$$

and the values of A_i can be selected to minimise the approximation.

There are a number of ways of applying this method and that of Gauss is the most suitable with respect to the nature of the function involved in the absorption correction.

To carry this out, it is first of all convenient to change the limits of integration by making the substitution

$$x = a + (b - a)v,$$

thus $f(x) = f(a + (b - a)v)$

and $dx = (b - a) dv$.

$$\begin{aligned} \text{Therefore} \quad \int_a^b f(x) dx &= (b - a) \int_0^1 f(a + (b - a)v) dv \\ &\approx (b - a) \sum_{i=0}^{i=n} R_i f(x_i), \end{aligned}$$

where $f(x_i)$ is the numerical value of $f(a + (b - a)v_i)$ and hence the integral has been approximated to a weighted sum of n terms. The values of R_i are the relative weights of the terms of the sum, and the values of v_i determine the points, x_i , at which the integrand is evaluated. R_i and v_i are fractional constants, depending only on n , and their values are available for $n \leq 16$ (Lowan, Davids and Levenson, 1942) and for $n \geq 16$ (Davis and Rabinowitz, 1956).

For a triple integral the approximation becomes

$$\begin{aligned} \int_a^b dx \int_{c(x)}^{d(x)} dy \int_{e(x,y)}^{h(x,y)} f(x,y,z) dz \\ \approx \sum_{i=0}^n \sum_{j=0}^n \sum_{k=0}^n (b - a)(d(x_i) - c(x_i)) \\ (h(x_i, y_j) - e(x_i, y_j)) R_i R_j R_k f(x_i, y_j, z_k), \end{aligned}$$

$$\begin{aligned} \text{where} \quad x_i &= a + (b - a)v_i, \\ y_j &= c(x_i) + (d(x_i) - c(x_i))v_j, \\ z_k &= e(x_i, y_j) + (h(x_i, y_j) - e(x_i, y_j))v_k, \end{aligned}$$

and $a, b, c(x), d(x), e(x,y)$ and $h(x,y)$ are the limits of integration in the three dimensions.

For a more detailed discussion, see Largenau and
Murphy(1943).

APPENDIX 2.

KDF9 ALGOL Listing of the Data-reduction Programs A1 and A2.

DD318A100KP7+V030662-PST;

DATAB-DATA-REDUCTION-PROGRAM--PART-1.

Begin comment This program is a full data reduction program, given a set of intensity data it can correct for Lorentz, polarisation, spot-shape, and absorption effects and produce parameters suitable for use in extinction corrections. The absorption routine is that of P. Coppens from his DATAP program, using the method of Gaussian integration, and this program is based on the System/360 FORTRAN 4 version of DATAP in use at Boston University. Part 1 calculates the metric tensors and sets up the Gaussian grid;

library A0,A6,A2700,A2705;

real det,deltaz,gridpt,jj,pi,vol,xmin,xmax,ymin,ymax,
zmin,zmax,R1,R2;

integer outside,nrfaces,nopts,no,noapts,nobpts,nocpts,
absorb,i,j,k,k1,l,l1,lr,m,n1,n2;

array absorb,i,j,k,k1,l,l1,lr,m,n1,n2;

xyz,a,gausspts,temp,adres,dist3,S[1:3],

reclin,realclin[1:9],sum[1:16],

g,G,shufel,hkl,lkh[1:3,1:3],

faces[1:16,1:4],gaussV,gaussR[1:128],corner[1:50], 5];

prokl,lk[1:2,1:2],dist2[1:2],grid[1:4,1:4096],para1[1:5];

array x,y,z;

comment multiplies vector by matrix, $z(i) = x(i,j) \times y(j)$;

begin integer i,j;

for i := 1,2,3 do

begin z[i] := 0.0;

for j := 1,2,3 do z[i] := z[i] + x[i,j] × y[j];

end

end;

procedure MINMAX(a,aa,amin,amax);

value aa;

integer aa;

real amin,amax;

array a;

comment finds upper and lower limits in array a and
assigns them to amin and amax;

begin integer i;

amin := amax := a[1];

for i := 2 step 1 until aa do

begin if amax < a[i] then amax := a[i] else

if amin > a[i] then amin := a[i];

end

end;

procedure INSIDE(xyz,outside,nrfaces,faces);

value nrfaces;

array xyz,faces;


```

integer outside,nrfaces;
comment checks whether pt xyz is on surface of crystal,
      sets outside = 1 if outside;
begin real check,trouble;
integer i,j;
outside := 0;
for j := 1 step 1 until nrfaces do
begin check := 0.0;
for i := 1,2,3 do check := check + faces[j,i] × xyz[i];
trouble := faces[j,4] - check + 0.0000000001;
if trouble < 0.0 then begin outside := 1;
                        goto leave;
                        end
end;
leave:end;

open(20);
comment set up direct metric tensor G and invert to obtain
      recip tensor g;
pi := 3.1415926536/180.0;
for k := 1 step 1 until 3 do realdim[k] := read(20);
for k := 4 step 1 until 6 do realdim[k] := cos(pi × read(20));
for i := 1,2,3 do for j := 1 step 1 until i do
G[i,j] := G[j,i] := realdim[j] × realdim[i];
G[2,1] := G[1,2] := G[1,2] × realdim[6];
G[3,1] := G[1,3] := G[1,3] × realdim[5];
G[3,2] := G[2,3] := G[2,3] × realdim[4];
for j := 1,2,3 do
begin for i := 1 step 1 until j do
g[i,j] := g[j,i] := - G[i,j];
g[j,j] := 1 + g[j,j];
end;
for lr := 1,2,3 do
begin comment SMI3;
g[lr,lr] := 1/(1 - g[lr,lr]);
for j := 1,2,3 do
begin S[j] := g[lr,j];
if j ≠ lr then g[lr,j] := g[j,lr] := g[j,lr] × g[lr,lr];
end;
for j := 1,2,3 do
begin if j = lr then goto terminate;
for i := 1 step 1 until j do
if i ≠ lr then g[j,i] := g[i,j] := g[i,j] + g[i,lr] × S[j];
terminate:end
end of SMI3,calculate recip cell dimensions from tensor;
for k := 1 step 1 until 3 do recdim[k] := sqrt(g[k,k]);
recdim[4] := g[2,3] / (recdim[2] × recdim[3]);
recdim[5] := g[1,3] / (recdim[1] × recdim[3]);
recdim[6] := g[1,2] / (recdim[1] × recdim[2]);
for k := 7 step 1 until 9 do
begin realdim[k] := (if realdim[k - 3] > -e-5 then 90.00
else arctan(sqrt(1 - realdim[k - 3] ↑ 2)
/ realdim[k - 3])/ pi + 180.00);

```

```

recdim[k] := (if recdim[k - 3] < 10-5 then 90.00
else arctan(sqrt(1 - recdim[k - 3] ^ 2)
/ recdim[k - 3]) / pi);
end;
for i := 1,2,3 do for j := 1,2,3 do
begin comment SHUFFL-scans transformation matrix
to determine internal axial system;
shufel[i,j] := read(20);
if shufel[i,j] > 0 then a[i] := j;
end;
absorb := read(20);
if absorb = 0 then goto data;
for i := 1,2,3 do gausspts[i] := read(20);
nrfaces := read(20);
comment GRIT2--constructs Gaussian grid in crystal, grid axes
parallel to crystal axes;
for i := 1 step 1 until nrfaces do
for j := 1 step 1 until 4 do faces[i,j] := read(20);
comment load gaussian constants;
i := 1;
for jj := .211324866, .788675135, .069431844, .330009478,
.669990522,
.930568156, .033765243, .169395307, .380690407, .619309593,
.830604693, .966234757, .019855072, .101666761, .237233795,
.408282679, .591717321, .762766205, .898333239, .980144928,
.013046736, .067468317, .160295216, .283302303, .425562831,
.574437170, .716697697, .839704784, .932531683, .986953264,
.009219683, .047941372, .115048663, .206341023, .316084251,
.437333296, .562666704, .683915750, .793658977, .884951337,
.952058628, .990780317, .006858096, .035782558, .086399342,
.156353548, .242375682, .340443816, .445972526, .554027474,
.659556184, .757624318, .843646452, .913600658, .964217442,
.993141904, .005299533, .027712488, .067184399, .122297796,
.191061878, .270991611, .359198225, .452493745, .547506255,
.640801775, .729008389, .808938122, .877702204, .932815601,
.972287512, .994700468, .997593610, .987364278, .969137276,
.943207764, .910000993, .870062096, .824046826, .772710736,
.716896754, .657521340, .595559434, .532028447, .467971553,
.404440566, .342478660, .283103246, .227289264, .175953174,
.129937904, .089999007, .056792236, .030862724, .012635722,
.002406390, .998631931, .992805756, .982381128, .967453038,
.948160578, .924683807, .897241898, .866091060, .831522134,
.793857879, .753449955, .710675638, .665934301, .619643681,
.572235981, .524153833, .475846167, .427764019, .380356319,
.334065699, .289324362, .246550045, .206142121, .168477867,
.133908940, .102758102, .075316193, .051839422, .032546962,
.017618872, .007194244, .001368069 do
begin gaussV[i] := jj;
i := i + 1;
end;
i := 1;
for jj := .500000000, .500000000, .173927423, .326072578,

```

.326072578,	.085662246,	.180380787,	.233956967,	.233956967,
.173927423,	.085662246,	.050614268,	.111190517,	.156853323,
.180380787,	.181341892,	.156853323,	.111190517,	.050614268,
.181341892,	.074725675,	.109543181,	.134633360,	.147762112,
.033335672,	.134633360,	.109543181,	.074725675,	.033335672,
.147762112,	.053469663,	.080039164,	.101583713,	.116746268,
.023587668,	.124573523,	.116746268,	.101583713,	.080039164,
.124573523,	.023587668,	.017559730,	.040079044,	.060759285,
.053469663,	.092769199,	.102599232,	.107631927,	.107631927,
.078601584,	.092769199,	.078601584,	.060759285,	.040079044,
.102599232,	.013576230,	.031126762,	.047579256,	.062314486,
.017559730,	.084578260,	.091301708,	.094725305,	.094725305,
.074797994,	.084578260,	.074797994,	.062314486,	.047579256,
.091301708,	.013576230,	.006170615,	.014265694,	.022138719,
.031126762,	.036673241,	.043095081,	.048809326,	.053722135,
.029649292,	.060835236,	.062918728,	.063969098,	.063969098,
.057752834,	.060835236,	.057752834,	.053722135,	.048809326,
.062918728,	.036673241,	.029649292,	.022138719,	.014265694,
.043095081,	.003509305,	.008137197,	.012696033,	.017136932,
.006170615,	.025499030,	.029342047,	.032911111,	.036172897,
.021417949,	.041655962,	.043826047,	.045586939,	.046922199,
.039096948,	.048270044,	.048270044,	.047819360,	.046922200,
.047819360,	.043826047,	.041655962,	.039096948,	.036172897,
.045586939,	.029342047,	.025499030,	.021417949,	.017136932,
.032911111,	.008137197,	.003509305		

```

do
begin gaussR[i] := jj;
i := i + 1;
end;
comment calc lengths of recip vectors perpendicular to faces;
for i := 1 step 1 until nrfaces do
begin for j := 1,2,3 do
begin temp[j] := 0.0;
for k := 1,2,3 do temp[j] := temp[j] + faces[i,k] × g[k,j];
end;
sum[i] := 0.0;
for l := 1,2,3 do sum[i] := sum[i] + temp[l] × faces[i,l];
comment d* = sqrt([hkl][g][hkl]);
faces[i,4] := faces[i,4] × sqrt(sum[i]);
comment faces[i,4] = origin-face distance × recip vector
normal to face = Bd*;
end;
comment now find first address of Gaussian constants to be
used;
for i := 1,2,3 do
begin k := gausspts[i] / 2;
if k ≤ 8 then adres[i] := (k - 1) × k else adres[i] := 6 × k;
end;
no := nopts := 0;
vol := 0.0;
if gausspts[a[1]] ≠ 0 then goto threeD;

```

```

comment for 2D grid perpendicular to internal a axis fix
parameters referring to this axis;
R1 := 1.0;
xyz[a[1]] := 0.0;
n1 := nrfaces - 1;
goto xcoord;
comment for 3D case scan over all possible combinations of 3
faces to determine coords of corners of crystal;
threeD:n1 := nrfaces - 1;
n2 := nrfaces - 2;
for k := 1 step 1 until n2 do
begin for i := 1,2,3 do hkl[i,1] := faces[k,1];
k1 := k + 1;
for l := k1 step 1 until n1 do
begin for i := 1,2,3 do hkl[i,2] := faces[l,1];
l1 := l + 1;
for m := l1 step 1 until nrfaces do
begin for i := 1,2,3 do hkl[i,3] := faces[m,1];
comment AMI3-inverts hkl to lkh, matrix H(-1);
lkh[1,1] := hkl[2,2] × hkl[3,3] - hkl[3,2] × hkl[2,3];
lkh[2,1] := hkl[2,1] × hkl[3,3] - hkl[3,1] × hkl[2,3];
lkh[3,1] := hkl[2,1] × hkl[3,2] - hkl[3,1] × hkl[2,2];
det := hkl[1,1] × lkh[1,1] - hkl[1,2] × lkh[2,1]
      + hkl[1,3] × lkh[3,1];
if det = 0.0 then goto next3;
lkh[1,2] := hkl[1,2] × hkl[3,3] - hkl[3,2] × hkl[1,3];
lkh[2,2] := hkl[1,1] × hkl[3,3] - hkl[3,1] × hkl[1,3];
lkh[3,2] := hkl[1,1] × hkl[3,2] - hkl[3,1] × hkl[1,2];
lkh[1,3] := hkl[1,2] × hkl[2,3] - hkl[2,2] × hkl[1,3];
lkh[2,3] := hkl[1,1] × hkl[2,3] - hkl[2,1] × hkl[1,3];
lkh[3,3] := hkl[1,1] × hkl[2,2] - hkl[2,1] × hkl[1,2];
for i := 1,2,3 do for j := 1,2,3 do
lkh[i,j] := (-1)(i+j) × lkh[i,j] / det;
dist3[1] := faces[k,4];
dist3[2] := faces[l,4];
dist3[3] := faces[m,4];
comment vector Bd* multiplied by matrix H(-1) gives
vector whose components are coords satisfying eqns
of 3 faces in H;
MATVEC(lkh,dist3,xyz);
comment xyz are fractional coords of pt of intersection
of 3 planes since distances from origin to each of
faces given in cms, now check if pt is on crystal
surface, if outside reject;
INSIDE(xyz,outside,nrfaces,faces);
if outside ≠ 0 then goto next3;
no := no + 1;
corner[no] := xyz[a[1]];
comment store x coords of corners only;
next3:end
end

```

```

end;
comment find lower and upper limits in x;
MINMAX(corner,no,xmin,xmax);
xcoord:for nopts := 1 step 1 until gausspts[a[1]] do
begin if gausspts[a[1]] < 1 then goto nox;
comment xyz[a[1]] are fractional coords of grid pts along
internal a axis;
gridpt := adres[a[1]] + nopts;
xyz[a[1]] := xmin + (xmax - xmin) × gaussV[gridpt];
R1 := gaussR[gridpt] × (xmax - xmin);
comment R1 is gaussian weight corresponding to xyz[a[1]];
nox:no := 0;
for k := 1 step 1 until n1 do
begin comment scan over all possible combinations of two
faces to find coords of edges of crystal for a given x;
kl[1,1] := faces[k,a[2]];
kl[1,2] := faces[k,a[3]];
dist2[1] := faces[k,4] - faces[k,a[1]] × xyz[a[1]];
k1 := k + 1;
for l := k1 step 1 until nrfaces do
begin kl[2,1] := faces[l,a[2]];
kl[2,2] := faces[l,a[3]];
comment AMI2-inverts kl to lk,matrix K(-1);
det := kl[1,1] × kl[2,2] - kl[1,2] × kl[2,1];
if det = 0.0 then goto next2;
lk[1,1] := kl[2,2] / det;
lk[1,2] := -kl[1,2] / det;
lk[2,1] := -kl[2,1] / det;
lk[2,2] := kl[1,1] / det;
dist2[2] := faces[l,4] - faces[l,a[1]] × xyz[a[1]];
xyz[a[2]] := lk[1,1] × dist2[1] + lk[1,2] × dist2[2];
xyz[a[3]] := lk[2,1] × dist2[1] + lk[2,2] × dist2[2];
INSIDE(xyz,outside,nrfaces,faces);
if outside ≠ 0 then goto next2;
no := no + 1;
corner[no] := xyz[a[2]];
next2:end
end;
comment determine lower and upper limits in y for given x;
MINMAX(corner,no,ymin,ymax);
for nobpts := 1 step 1 until gausspts[a[2]] do
begin gridpt := adres[a[2]] + nobpts;
xyz[a[2]] := ymin + (ymax - ymin) × gaussV[gridpt];
R2 := gaussR[gridpt] × R1 × (ymax - ymin);
no := 0;
comment scan over all faces to find upper and lower
limits of z for given x,y;
for i := 1 step 1 until nrfaces do
begin if faces[i,a[3]] = 0.0 then goto next;
xyz[a[3]] := (faces[i,4]-xyz[a[1]]×faces[i,a[1]]
-xyz[a[2]]×faces[i,a[2]])/faces[i,a[3]];
INSIDE(xyz,outside,nrfaces,faces);

```

```

if outside  $\neq$  0 then goto next;
no := no + 1;
corner[no] := xyz[a[3]];
next:end;
MINMAX(corner,no,zmin,zmax);
deltaz := zmax - zmin;
for nocpts := 1 step 1 until gausspts[a[3]] do
begin nopts := nopts + 1;
comment store fractional coords of sampling pts and corres
weights;
gridpt := adres[a[3]] + nocpts;
grid[a[3],nopts] := zmin + deltaz  $\times$  gaussV[gridpt];
grid[a[2],nopts] := xyz[a[2]];
grid[a[1],nopts] := xyz[a[1]];
grid[4,nopts] := gaussR[gridpt]  $\times$  R2  $\times$  deltaz;
comment vol is equal to volume of crystal as a
fraction of volume of a parallelopiped whose
edges are parallel to a,b,c, and of length a,b,c cms;
vol := vol + grid[4,nopts];
end
end
end;
data:para1[1] := pi;
para1[2] := vol;
para1[3] := nrfaces;
para1[4] := nopts;
para1[5] := absorb;
disclaim;
discwrite(realdim,0);
discwrite(recdim,1);
discwrite(g,2);
discwrite(G,3);
discwrite(gausspts,4);
discwrite(faces,5);
discwrite(a,6);
discwrite(grid,7);
discwrite(para1,8);
discretain(1);
close(20);
ENTER([DD318A2-----]);
end->

```

DD318A2CCKP7+VC3C662-PST;

DATAB--DATA-REDUCTION-PROGRAM--PART-2.

begin

comment Part 2 carries out the data reduction routine,
correcting for absorption,Lp,scale,spot-shape, and
calculating extinction parameters,for Weissenberg,
precession,and 3-circle diffractometer data;

library AC,A6,A12,A14,A27C5;

real abx,abc,abxpc,cles,cone,cosmu,costh,cosphi,
eksisq,F,iobs,isigma,lambda,Lp,mu,meanpath,
phi,pi,p,r,sinsqth,sinphi,spo,sinmu,sinth,
sigmaF,scale,tempor,tamp,tilt,theta,vol,
volume,wt,zeta,zetasq,a1,a2,a3,b1,c1,e1,f1,
a11,b11,c11,dgd,ngn;

integer nrfaces,nopts,absorb,spot,exting,tech,
b,batchno,i,k,q,ipr,lr,
f,f2,f3,f4,f5,f6,f7,f1C,f11,f13,f14,f15,
bn,add;

array dee,Dee,n,N,sd,sod,s,so,d,t,x,a,gausspts[1:3],
recdim,readim[1:9],g,G,st,sot[1:3,1:3],
faces[1:16,1:4],grid[1:4,1:4C96],para1[1:5];

procedure QUARO(a,b,c,res1,res2);

value a,b,c;

real a,b,c,res1,res2;

comment finds roots of quadratic equation;

begin real temp;

temp := sqrt(b \uparrow 2 - 4 \times a \times c);

res1 := (- b + temp) / (2 \times a);

res2 := (- b - temp) / (2 \times a);

end;

procedure MATVEC(x,y,z);

array x,y,z;

comment multiplies vector by matrix, z(i) = x(i,j) \times y(j);

begin integer i,j;

for i := 1,2,3 do

begin z[i] := 0;

for j := 1,2,3 do

z[i] := z[i] + x[i,j] \times y[j];

end

end;

```

procedure VECMATVEC(x,y,z);
  array x,y;      real z;
  comment pre-multiplies matrix y by vector x and post-
            multiplies product by vector x,z = x(i)
            × y(i,j) × x(j);

  begin integer i,j;
        z := C.C;
        for i := 1,2,3 do for j := 1,2,3 do
          z := z + x[i] × x[j] × y[i,j];
  end;

procedure LENGTH(sd,sod,abx);
  array sd,sod;
  real abx;
  comment calculates path length of beam in crystal for
            each of the sampling points of the gaussian grid
            , and the absorption correction;
  begin real rdotn,Pok,Pk,ab,Po,P;
        integer in,out,i,k,ll;
        array cosin,cosout[1:16],inface,outface[1:16];
        abx := C.C;
        in := out := 1;
        comment calculate cosines of angles of incident
            and diffracted rays with all faces;
        for k := 1 step 1 until nrfaces do
          begin cosin[in] := cosout[out] := C.C;
            for i := 1,2,3 do
              begin cosin[in] := cosin[in] + sod[i]
                × faces[k,i];
                cosout[out] := cosout[out] + sd[i]
                × faces[k,i];
              end;
            comment reject face if angle between incident
            beam and face normal is acute;
            if cosin[in] > C.C then goto rej;
            inface[in] := k;
            in := in + 1;
            comment reject face if angle between diffracted
            ray and face normal is obtuse;
            rej: if cosout[out] < C.C then goto ect;
            outface[out] := k;
            out := out + 1;
          ect: end;
          in := in - 1;
          out := out - 1;
          comment calculate path length and absorption
            for each of the sampling points;
          for ll := 1 step 1 until nopts do
            begin Pok := Pk := 1012;
              for k := 1 step 1 until in do

```



```

begin rdotn := C.C;
  for i := 1,2,3 do
    rdotn := rdotn + grid[i,11] × faces
      [inface[k],i];
    Po := - (faces[inface[k],4] - rdotn)
      / cosin[k];
    if Pok > Po then Pok := Po;
  end;
for k := 1 step 1 until out do
  begin rdotn := C.C;
    for i := 1,2,3 do
      rdotn := rdotn + grid[i,11] × faces
        [outface[k],i];
      P := (faces[outface[k],4] - rdotn)
        / cosout[k];
      if Pk > P then Pk := P;
    end;
  comment calculate exponential function and
    multiply absorption for each grid pt by
    its gaussian wt;
  ab := exp(-((Pok + Pk) × mu )) × grid[4,11];
  comment sum absorption over all sampling pts;
  abx := abx + ab;
end;
abx := abx / vol;
end;

```

```

f := format([_nd.ddddd]);
  f2 := format([ss-nd.ddddd]);
f3 := format([12sndddc]);
f4 := format([s-ndds]);
f5 := format([ss-ndddd.dds]);
f6 := format([_ndd.dddds]);
f7 := format([s-ndd.dds]);
f10 := format([sssss-ndd.dd]);
f11 := format([ssss-nddd.ddsc]);
f13 := format([ss-n.ddddd;c]);
f14 := format([s-ndd.dds]);
f15 := format([sss-nd.ddd]);
open(1C); open(2C); open(3C);
writetext(3C,[[p1Cc5Cs]datab[cc42s]data*reduction*program
  [4c4s]]);
copytext(2C,3C,[;]);
gap(1C,2C);

```

```

discreclaim(C);
discread{realdim,C};
discread{recdim,1};
discread{g,2};
discread{G,3};
discread{gausspts,4};
discread{faces,5};
discread{a,6};

```

```

discread(grid,7);
discread(para1,8);
disclose;

pi := para1[1];
vol := para1[2];
nrfaces := para1[3];
nopts := para1[4];
absorb := para1[5];
q := 0;
spot := read(20);
exting := read(20);
tech := read(20);
lambda := read(20);
cone := read(20);
mu := read(20);
tilt := read(20);
batchno := read(20);
bn := read(20);
add := read(20);
writetext(30,[[4c4s]]);
if tech = 0 then writetext(30,[equi-inclination*weissenberg
*data]) else if tech = 2 then writetext(30,[4-circle*
diffractometer*data])
else writetext(30,[precession*data[ccssss]routine*for*
precession*data*established*but*not*tested]);
writetext(30,[[4c4s]corrected*for*Lp]);
if absorb = 1 then writetext(30,[,*absorption]);
if spot = 1 then writetext(30,[,*spot-shape]);
writetext(30,[,*and*scale]);
if absorb = 1 then begin writetext(30,[[ccssss]mu*=]);
write(30,f11,mu);
end;
if exting = 2 then writetext(30,[[4css]extinction*correction
*only*valid*for*isotropic*and*anisotropic*type-1*crystals
[ccss]anisotropic*extinction*parameters*output*on*
stream*1C])
else if exting = 1 then writetext(30,[[cccss]isotropic
extinction*parameter*output*on*stream*1C]);
writetext(30,[[p6css]DIRECT*CELL*DIMENSIONS[cc11s]A[9s]
B[9s]C[c5s]]);
for k := 1 step 1 until 3 do write(30,f15,realdim[k]);
writetext(30,[**ANGSTROMS[cc9s]ALPHA[8s]BETA[7s]GAMMA[css]]);
for k := 7 step 1 until 9 do write(30,f10,realdim[k]);
writetext(30,[* DEGREES[3c2s]RECIPROCAL*CELL*DIMENSIONS[2c7s]
A*STAR[6s]B*STAR[6s]C*STAR[css]]);
for k := 1 step 1 until 3 do write(30,f2,recdim[k]);
writetext(30,[**RECIPROCAL*ANGSTROMS[cc6s]ALPHA*STAR**BETA
*STAR**GAMMA*STAR[css]]);
for k := 7 step 1 until 9 do write(30,f10,recdim[k]);
writetext(30,[[4s]DEGREES]);

```

```

if absorb = C then goto data;
writetext(3C,[[5c2s]GAUSSIAN*GRID*DIMENSIONS[cc4s]
n(1)**n(2)**n(3,**no`ci`sampling*pts[ccs]]);
for i := 1,2,3 do write(3C,f4,gausspts[i]);
write(3C,f3,nopts);
cles := reldim[a[2]] × reldim[a[3]] × sqrt(1 - reldim[a[1]
+ 3]↑2);

if gausspts[a[1]] = C then goto out;
cles := cles / reldim[a[1]];
volume := vol × cles × 1000;
writetext(3C,[[4css]volume*of*crystal*is]);
write(3C,f,volume);
goto finish;
out:volume := vol × cles × 100;
writetext(3C,[[ccccss]cross*section*within*plane*of*internal
*b*and*c*axes*is*]);
write(3C,f,volume);
finish:writetext(3C,[[s]cmm[4c]]);
data:if tech = 1 then cosmu := cos(tilt / 57.29578);
if tech < 2 then writetext(3C,[[p6c4s]h*****k* * * 1*****
**iobs*****scale*****abs*** **spot*** theta* *****
*fobs])
else writetext(3C,[[p6c4s]h*****k* * * 1***** iobs*****sig*i*
**scale*****abs***** sig*f*****root*w*****theta*****
***fobs]);
comment input planes;
b := C;
nextbatch: b := b + 1;

lr := C;
if b > batchno then goto last;
writetext(3C,[[cc]]); gap(10,50);
scale := read(20);
nextplane:
x[1] := read(20);
if abs(x[1]) > 998 then begin writetext(3C,[[c]**no*of*
observed*reflexions*in*this*batch**]);
write(3C,f3,lr);
writetext(3C,[[c]**no*of*unobserved*reflexions*in*this
*batch**]);
write(3C,f3,q);
goto nextbatch;
end
else lr := lr + 1;

x[2] := read(20);
x[3] := read(20);
iobs := read(20);
if tech < 2 then goto omit;
isigma := read(20);
if (abs(x[a[2]]) + abs(x[a[3]])) = C then phi := read(20);
comment sin theta routine;
omit:VECMATVEC(x,g,sinsqth);
sinsqth := lambda × lambda × sinsqth × C.25;
if sinsqth ≥ 1.0 then begin lr := lr - 1;
for i := 1,2,3 do write(3C,f4,x[i]);

```

```

        writetext(3C, [* *sin*theta*greater*than*
        1.C** reflexion*omitted*from*processed
*data[c]]);
        goto nextplane;
    end;
costh := sqrt(1.C - sinsqth);
comment call absorption subroutine if absorption correction
    reqd;
abx := 1.C;
if absorb = C or iobs < C then goto spsh;
goto if tech < 1 then path1 else if tech = 1 then path3
    else path2;
comment determine components of incident and diffracted beams
    and then call LENGTH for calculation of absorption
    . sod and sd are the components of the incident and
    diffracted rays in direct space, so and s are the
    components in reciprocal space;
path1: abx := C.C;
comment jump here for Weissenberg data;
a1 := x[a[1]] × g[a[1],a[2]] + x[a[2]] × g[a[2],a[2]]
    + x[a[3]] × g[a[2],a[3]];
a2 := x[a[1]] × g[a[1],a[3]] + x[a[2]] × g[a[2],a[3]]
    + x[a[3]] × g[a[3],a[3]];
if a2 ≠ C.C then goto 16;
t[a[2]] := C;
t[a[3]] := 2.C × costh / recdim[a[3]];
goto 17;
16: a3 := a1 / a2;
t[a[2]] := 2.C × costh / sqrt(g[a[2],a[2]] + a3 × a3
    × g[a[3],a[3]] - 2.C × a3 × g[a[2],a[3]]);
t[a[3]] := - t[a[2]] × a3;
17: t[a[1]] := C.;
comment t are reciprocal space components of vector T, thus
    now find s and so using reciprocal components of D and
    hence sd and sod;
for i := 1,2,3 do begin s[i] := (t[i] + lambda × x[i]) × C.5;
    sc[i] := (t[i] - lambda × x[i]) × C.5;
    end;

MATVEC(g,so,sod);
MATVEC(g,s,sd);
LENGTH(sd,sod,abx);
goto excor;
path2: abx := C.C;
comment jump here for 3-circle diffractometer data;
t[a[1]] := C.C;
if (abs(x[a[2]]) + abs(x[a[3]])) ≠ C then goto 19;
cosphi := cos(phi / 57.29578);
sinphi := sin(phi / 57.29578);
t[a[2]] := 2.C × costh × sinphi × sqrt(1 - realdim[a[1]] + 3)↑2)
    / (realdim[a[2]] - realdim[a[2]] × realdim[a[1]] + 3) ↑ 2);
t[a[3]] := (-2.C × costh × cosphi - t[a[2]] × realdim[a[2]]

```

```

      × realdim[a[1] + 3]) / realdim[a[3]];
goto 110;
19:if x[a[3]] ≠ C then goto 111;
t[a[3]] := 2.C × cosh / realdim[a[3]];
t[a[2]] := C.C;
goto 110;
111:t[a[2]] := 2.C × cosh / sqrt(G[a[2],a[2]] + (x[a[2]] /
      x[a[3]]) ↑ 2 × G[a[3],a[3]] - 2.C × x[a[2]] × G[a[2],a[3]]
      / x[a[3]]);
t[a[3]] := - x[a[2]] × t[a[2]] / x[a[3]];
comment t are real space components of vector T,thus now
      find real components of D by transformation and then sd
      and sod;
110:MAI_VEC(g,x,d);
for i := 1,2,3 do begin d[i] := lambda × d[i];
      sd[i] := (d[i] + t[i]) × C.5;
      sod[i] := (t[i] - d[i]) × C.5;
      end;
LENGTH(sd,sod,abx);
goto excor;
path3:abx := C.C;
comment jump here for precession data,calc constants in first
      pass only;
if q > C then goto 116;
a1 := g[a[3],a[3]] / g[a[2],a[2]];
so[a[1]] := - realdim[a[1]] × cosmu;
b1 := 2.C × so[a[1]] × g[a[1],a[2]] / g[a[2],a[2]];
c1 := 2.C × g[a[2],a[3]] / g[a[2],a[2]];
e1 := 2.C × so[a[1]] × g[a[1],a[3]] / g[a[2],a[2]];
f1 := (1 - so[a[1]] ↑ 2 × g[a[1],a[1]]) / g[a[2],a[2]];
q := 1;
116:goto 112;
113:if d[a[3]] ≠ C.C then goto 114;
sot[1,a[2]] := -(2.C × sinsqth + so[a[1]] × d[a[1]]) /
      d[a[2]];
tempor := e1 + sot[1,a[2]] × c1;
tamp := sot[1,a[2]] ↑ 2 + sot[1,a[2]] × b1 - f1;
QUARO(a1,tempor,tamp,sot[1,a[3]],sot[2,a[3]]);
sot[2,a[2]] := sot[1,a[2]];
goto 115;
comment calculate quadratic eqn in so[a[2]],i.e. sot[a[2]]
;
114:p := -d[a[2]] / d[a[3]];
r := -(so[a[1]] × d[a[1]] + 2.C × sinsqth) / d[a[3]];
a11 := 1.C + p × p × a1 + p × c1;
b11 := 2.C × p × r × a1 + b1 + r × c1 + p × e1;
c11 := - f1 + r × e1 + r × r × a1;
comment find roots = so[a[2]];
QUARO(a11,b11,c11,sot[1,a[2]],sot[2,a[2]]);
for i := 1,2 do sot[i,a[3]] := p × sot[i,a[2]] + r;
comment components of s now found,= so + D(recip);
115:for i := 1,2 do begin st[i,a[2]] := sot[i,a[2]] +
      lambda × x[a[2]];

```

```

        st[i,a[3]] := sot[i,a[3]] + lambda × x[a[3]];
    end;
s[a[1]] := so[a[1]] + lambda × x[a[1]];
for ipr := 1,2 do begin so[a[2]] := sot[ipr,a[2]];
                        so[a[3]] := sot[ipr,a[3]];
                        s[a[2]] := st[ipr,a[2]];
                        s[a[3]] := st[ipr,a[3]];
                        MATVEC(g,so,sod);
                        MATVEC(g,s,sd);
                        LENGTH(sd,sod,abx);
                    end;
comment for precession camera data take average over two
        superimposed reflexions;
abx := abx / 2.C;
l12:MATVEC(g,x,d);
for i := 1,2,3 do d[i] := lambda × d[i];
if tech = 1 then goto l13;
for i := 1,2,3 do begin sd[i] := (d[i] + t[i]) × C.5;
                    sod[i] := (t[i] - d[i]) × C.5;
                end;
LENGTH(sd,sod,abx);

excor:if exting = 0 then goto spsh;
comment calculates parameters for input to extinction correction
        program,valid only for isotropic,and anisotropic in
        type 1 crystals;
meanpath := - ln (abx) / ( mu × 2.303 );
if exting = 1 then goto spsh;
comment calculate direct normalised components of vectors
        s D and N;
dee[1] := cles × ( sd[2] × sod[3] - sod[2] × sd[3] );
dee[2] := cles × ( sd[1] × sod[3] - sod[1] × sd[3] );
dee[3] := cles × ( sd[1] × sod[2] - sod[1] × sd[2] );
MATVEC(g,dee,Dee);
VECMATVEC(dee,g,dgd);
n[1] := cles × ( sod[2] × Dee[3] - Dee[2] × sod[3] );
n[2] := cles × ( sod[1] × Dee[3] - Dee[1] × sod[3] );
n[3] := cles × ( sod[1] × Dee[2] - Dee[1] × sod[2] );
MATVEC(g,n,N);
VECMATVEC(n,g,ngn);
for i := 1,2,3 do begin N[i] := N[a[i]] / sqrt(ngn);
                    Dee[i] := Dee[a[i]] / sqrt(dgd);
                end;

spsh:spo := 1.C;
        zeta := abs(x[a[1]]) × lambda / realdim[a[1]];
if spot = 0 or x[a[1]] = 0 then goto angle;
comment calculates Phillips spot-shape correction for
        upper level Weissenberg;

```

```

zetasq := zeta × zeta;
eksisq := 4 × sinsqth - zetasq;
abc := 1 - zetasq / 4;
spo := 1 + zeta × sqrt(4 × abc / eksisq - 1)
      / ((28.7 / sqrt(abc) + 75) × 4 × pi);

angle:sinmu := C.C;
sinh := sqrt(sinsqth);
theta := arctan(sinh / costh) / pi;
if tech = C then sinmu := zeta / 2.C;

comment calculate Lp factor;
Lp := 4 × costh × sqrt(sinsqth - sinmu ↑ 2) / (1 + (1 -
      2 × sinsqth) ↑ 2);
abxpc := abx × 100;
comment calculate Fobs;
if iobs ≥ C.C then F := sqrt(abs(scale × Lp × iobs × spo
      / abx));

for i := 1,2,3 do write(3C,f4,x[i]);
write(3C,f5,iobs);
if tech > 1 then goto diff;
write(3C,f7,scale);
write(3C,f6,abxpc);
write(3C,f7,spo);
write(3C,f14,theta);
write(3C,f11,F);
goto l unch;
comment calculate esd and wt for F and set those below
preset limit as unobserved, F = C;
diff:if iobs < C.C then F := sigmaF := wt := C.C else
      begin sigmaF := F × isigma / (2 × sqrt(iobs));
            if F < cone × sigmaF then begin
                F := C.C;
                lr := lr - 1;
                q := q + 1;
            end;

wt := sqrt(1 / sigmaF ↑ 2);
end;
write(3C,f4,isigma);
write(3C,f7,scale);
write(3C,f6,abxpc);
write(3C,f7,sigmaF);
write(3C,f6,wt);
write(3C,f14,theta);
write(3C,f11,F);

punch:for i := 1,2,3 do write(1C,format([s-nd;]),x[i]);
if bn > C.C then begin writetext(1C,[**1;]);
      write(1C,format([s-nd;]), x[bn] + add);
      end;
write(1C,format([ss-nddd.dd;c]),F);

```

```
if exting > C then write(1C,f13,meanpath);  
if exting = 2 then  
begin for i := 1,2,3 do write(1C,format([ss-d.ddd0+nd;])  
                                     ,Dee[i]);  
      for i := 1,2,3 do write(1C,format([ss-d.ddd0+nd;])  
                                     ,N[i]);  
      writetext(1C,[[c]]);  
end;  
goto nextplane;  
last:writetext(3C,[[p]]); gap(1C,2CC);  
close(1C); close(2C); close(3C);  
end→
```